Respiratory effort and other pathophysiological mechanisms of obstructive sleep apnoea

Laura Gell
MA (Cantab), MSci

A thesis submitted in total fulfillment of the requirements of
the degree of Doctor of Philosophy

College of Science and Engineering
Flinders University, Adelaide

December 19, 2019

Contents

List of Figures **ix**

List of Tables **xiii**

Abbreviations and symbols **xv**

Declaration **xvii**

Acknowledgements **xix**

Abstract **xxiii**

1 Introduction **1**

1.1 Motivation 2

1.2 Aims 4

1.3 Outline of Thesis 5

2 Literature Review **7**

2.1 Physiology 8

2.1.1 The Human Airway 8

2.1.2 Upper airway muscles 8

2.1.3 Airway collapse 9

2.1.4 Respiratory Pump Muscles 11

2.1.5 Neural control of respiratory muscles 12

2.2 Anatomical differences in OSA patients 13

2.3 Non-anatomical factors 14

2.3.1 Arousal threshold 14

2.3.2 Ventilatory instability (loop gain) 15

2.3.3 Dilator muscle responsiveness and effectiveness 16

2.3.4 Limitations of phenotype model 17

2.4 Compensatory Mechanisms 18

2.4.1 Respiratory effort and arousal 20

2.4.2 Role of arousal 21

2.4.3 Other airway recovery mechanisms 23

2.4.4 Relative Pump and UA muscle recruitment 24

2.4.5 Effort augmentation in OSA 25

2.4.6 Pressure sensitive mechanisms 26

2.5 Tools to measure respiratory effort 27

2.5.1 Oesophageal pressure 27

2.5.2 Epiglottic Pressure 28

2.5.3 Diaphragm electromyography 29

2.5.4 Non-invasive effort measures 29

2.5.5 Ongoing challenges 30

2.6 Summary 31

3 Developing reliable filtering methodologies to improve quality of oesophageal pressure and diaphragm EMG signals 33

3.1 Oesophageal Pressure 34
3.1.1 Introduction 34
3.1.2 Methods 39
3.1.3 Results 44
3.1.4 Discussion 49
3.2 Diaphragm EMG 51
3.2.1 Introduction 51
3.2.2 Methods 52
3.2.3 Results 53
3.3 Conclusions 55

4 The effect of occlusion on pressure measurements 57

4.1 Background 58
4.2 Theoretical considerations 60
4.3 Methods 62
4.3.1 Study sample 62
4.3.2 Study setup and protocol 62
4.3.3 Data analysis 64
4.3.4 Respiratory mechanics based analysis 64
4.3.5 Statistical analysis 65
4.4 Results 65
4.4.1 Participants 65
4.4.2 Effect of abdominal cuff 66
4.4.3 Effect of occlusion 66

4.5 Discussion 69
4.5.1 Study limitations 72
4.6 Conclusion 74

5 A novel method to quantify respiratory effort 75

5.1 Background 76
5.2 Theory 79
5.3 Methods 81
5.4 Results 83
5.5 Discussion 85

6 Physiological measures around occlusion 91

6.1 Background 92
6.2 Methods 94
6.2.1 Data analysis 94
6.2.2 Statistical analysis 95
6.3 Results 97
6.3.1 Arousal distribution 97
6.3.2 Breath-by-breath analysis 99
6.3.3 Respiratory effort and ventilation 99
6.3.4 Duty cycle 101
6.3.5 Muscle activity and ETCO2 101
6.4 Discussion 102
6.4.1 Methodological considerations 105

7 Airway recovery mechanisms **107**

7.1 Background . . . 108

7.2 Methods . . . 110

7.3 Results . . . 113

7.4 Discussion . . . 118

7.4.1 Potential Limitations . . . 121

8 Conclusion **125**

8.1 Thesis Objectives . . . 126

8.2 Key Findings . . . 127

8.3 Research Implications . . . 127

8.4 Limitations . . . 129

8.5 Future Recommendations . . . 130

References **131**

A Matlab GUI for analysis **147**

A.1 GUI Requirements . . . 147

A.2 User Interface . . . 148

A.3 Analysis Stages . . . 149

A.3.1 Data Import and Processing . . . 149

A.3.2 Modelling . . . 151

A.3.3 Event Analysis . . . 152

A.3.4 Breath-by-breath Analysis . . . 153

B Matlab code for method implementation **155**

B.1 Code to fit E and R 155

B.2 Code to implement method 156

C Additional figures for Chapter 6 **159**

D Additional figures for Chapter 7 **167**

List of Figures

2.1 Example of flow and pressure relationships in an open tube, a collapsed tube and a starling resistor 10

2.2 Compensatory mechanisms in OSA 19

2.3 Schematic showing measurement locations for epiglottic, oesophageal and gastric balloon catheters and multi-electrode array diaphragm EMG 28

3.1 Artefact segmentation and template averaging 40

3.2 Template changes over the course of the night 41

3.3 Block diagram of adaptive noise cancellation filters 42

3.4 Example ANC signal input and output for two methods 43

3.5 Example of frequency spectra from the three proposed filtering methods for oesophageal pressure cardiogenic artefact removal. 46

3.6 Examples of results from the three different filtering methods 47

3.7 Results of ANC filter and template subtraction filter for EMGdi 52

3.8 Filtered EMGdi using ICA decomposition and wavelet transform 54

4.1 Example occlusion trace 63

4.2 Group ensemble average plots of occluded and pre-occluded breaths 68

4.3 Mechanics corrections to the effect of occlusion on epiglottic and oesophageal pressure 70

5.1 Oesophageal pressure changes during an apnoea event 77

5.2 Attempted flow and volume derived from fits of Pmus and Poes during stable breathing 84

5.3 Attempted flow and volume derived from fits of Pmus and Poes over a period of obstruction 86

5.4 Ventilation and obstruction ratio derived from fits of Pmus and Poes over apnoea 87

5.5 Ventilation and obstruction ratio derived from fits of Pmus over less sever obstruction 88

6.1 Example of an event for detailed analysis. Measured flow (grey) and attempted flow (black), derived from oesophageal pressure and respiratory mechanics had the airway remained patent, oesophageal pressure, EMGdi and EMGgg plotted over the course of an obstructive apnoea event. 96

6.2 Distribution of arousal and re-obstruction relative to airflow recovery in OSA. 98

6.3 Distribution of arousal relative to airflow recovery in individual subjects . . 99

6.4 Breath-by-breath physiological measures with arousal (black) or no arousal (grey) 100

6.5 Example of augmented effort duty cycle at airflow recovery 102

7.1 An example airflow recovery event, with attempted flow (black line) and measured flow (grey line), oesophageal pressure and rectified, MTA EMGdi and EMGgg (100ms window) 111

7.2 Example arousal and non-arousal flow recovery responses from one participant 114

7.3 Example responses at all four averaging time-points from one participant (Baseline events N=100, A,B,C events N=174) 116

7.4 Group data distribution of flow onset relative to effort onset expressed as a fraction of inspiratory duration of the previous inspiratory effort. 118

7.5 Examples of multiple augmented duty cycle responses within one subject, highlighted in grey, including responses to within-breath obstruction suggesting the phenomena is common in OSA 122

A.1 Requirements for GUI analysis tool 148

A.2 Initial signal display screen on GUI 149

A.3 Calibration for flow channel. The user selects the region of calibration syringe manoeuvres, which are then detected and calibrated to a fixed volume 151

A.4 User interface for event review and scoring 152

C.1 Breath-by-breath physiological measures with arousal (black) or no arousal (grey) for Subject 1 160

C.2 Breath-by-breath physiological measures with arousal (black) or no arousal (grey) for Subject 2 161

C.3 Breath-by-breath physiological measures with arousal (black) or no arousal (grey) for Subject 3 162

C.4 Breath-by-breath physiological measures with arousal (black) or no arousal (grey) for Subject 4 163

C.5 Breath-by-breath physiological measures with arousal (black) or no arousal (grey) for Subject 5 164

C.6 Breath-by-breath physiological measures with arousal (black) or no arousal (grey) for Subject 6 165

C.7 EMGdi breath-by-breath group average results as scaled relative to pre event baseline value and by mean tonic activity during a period of stable wake 166

D.1 Responses at all four breath timing points from participant 2 (Baseline events N=100, A,B,C events N=121) 168

D.2 Responses at all four breath timing points from participant 3 (Baseline events N=100, A,B,C events N=252) 169

D.3 Responses at all four breath timing points from participant 4 (Baseline events N=100, A,B,C events N=133) 170

D.4 Responses at all four breath timing points from participant 5 (Baseline events N=100, A,B,C events N=23) 171

D.5 Responses at all four breath timing points from participant 6 (Baseline events N=100, A,B,C events N=14) 172

List of Tables

3.1 Elastance, resistance and goodness of fit obtained from the respiratory equation of motion for oesophageal pressure signals filtered by each of the three methodologies (Template subtraction, ANC with ECG input, ANC with template based input). 48

4.1 Patient characteristics (N=13) 66

4.2 Ventilatory parameters for occlusion and pre-occlusion breath. Values are mean ± SEM, N=13. 67

4.3 Individual subject model fits for epiglottic and pressure difference between occlusion and pre-occlusion breaths 69

5.1 Individual patient fits for E, R and r^2 83

7.1 Pressure and muscle activity at time zero for each breath and arousal condition. Values are group mean±SEM, N=6. 115

7.2 Breath parameters from attempted ventilation derived from oesophageal pressure, giving a measure of effort timings during obstruction 117

Abbreviations and symbols

AHI	Apnoea-hypopnoea index
ANC	Adaptive noise cancellation
BMI	Body mass index
CO_2	Carbon dioxide
COPD	Chronic obstructive pulmonary disorder
CPAP	Continuous positive airway pressure
CSA	Central sleep apnoea
E	Elastance
ECG	Electrocardiography
EEG	Electroencelography
EMG	Electromyography
EMGdi	Diaphragm electromyography
EMGgg	Genioglossus electromyography
ETCO2	End tidal carbon dioxide
FB	Breathing frequency
GG	Genioglossus
ICA	Independent component analysis
LMS	Least mean squares
MAS	Mandibular advancement splint
NREM	Non-rapid eye movement

OSA	Obstructive sleep apnoea
PEEPi	Intrinsic positive end expiratory pressure
Pcardiac	Cardiac pressure artefact
Pcw	Chest wall pressure
PIF	Peak inspiratory flow
Pepi	Epiglottic pressure
Pgas	Gastric pressure
Pmask	Mask pressure
Pmus	Muscle pressure
Poes	Oesophageal pressure
Ppl	Pleural pressure
PSG	Polysomnogram
R	Resistance
REM	Rapid-eye movement
UARS	Upper airway resistance syndrome
Ti	Inspiratory time
Te	Expiratory time
TP	Tensor palatini
Ttot	Total breath time
V	Volume
VI	Inspiratory minute ventilation
VE	Expiratory minute ventilation
Vti	Inspiratory tidal volume
Vte	Expiratory tidal volume
$\dot{\mathbf{V}}$	Flow
WOB	Work of breathing

Declaration

I certify that this thesis does not incorporate without acknowledgement any material previously submitted for a degree or diploma in any university; and that to the best of my knowledge and belief it does not contain any material previously published or written by another person except where due reference is made in the text.

Laura Gell

December 19, 2019

Acknowledgements

First and foremost, I would like to thank my supervisors, Peter and Karen, for their continued guidance and support. You have been wonderful mentors and I have learnt so much from you both.

Thanks to all those who participated in, or where involved in the original data collection for the studies presented in this thesis. You made this work possible. I would also like to thank my colleagues at both the Medical Device Research Institute and at the Adelaide Institute for Sleep Health for their assistance and friendship. Particular thanks must go to my fellow PhD students, I will miss you all immensely.

I must thank also my friends, in Adelaide and the UK, for keeping me sane. Dhara and Jess, thanks for making this place on the other side of the world home.

Finally, the deepest thanks are reserved for my family: Mum, Dad, Ben, Eleanor, Karen, Sandy, Ollie and Emily. I am endlessly grateful for your love, encouragement and understanding. I could not have done this without you.

For my grandmother, Frances Reynolds.
I know how proud you would be.

Abstract

Obstructive sleep apnoea (OSA) is a common respiratory disorder characterised by recurring upper airway collapse during sleep. OSA is associated with a number of serious negative effects on health and quality of life. Current main treatments include continuous positive airway pressure (CPAP), mandibular advancement devices, surgery and supine-avoidance, all of which focus on correcting anatomical abnormalities. However, low CPAP acceptance and variable efficacy with alternative treatments are such that the burden of untreated OSA is substantial. Furthermore, the pathogenesis of OSA is more complex than deficient anatomy alone, and a number of non-anatomical factors also contribute. All OSA patients can maintain airway patency during wake, but fail to successfully compensate for changes in muscle recruitment and respiratory drive following sleep onset. A fuller understanding of these fundamental compensatory mechanisms is needed to better guide potential therapeutic treatments for those for whom current options fail.

Respiratory effort plays a key role in modulating both upper airway and inspiratory pump muscle activity during sleep, and gradually augments following abrupt muscle relaxation at sleep onset. Brief cortical arousals from sleep to respiratory-related stimuli occur at a similar threshold of respiratory effort, suggesting that sensations arising from augmented inspiratory effort provide the primary stimulus for respiratory-related arousal. This may also explain the reduced OSA severity in deep sleep when effort increases and arousal frequency reduces. However, the more precise role of respiratory effort augmentation, either through central chemo-reflex drive, mechano-reflex responses or sleep stage related changes, in compensating for partial or complete airway collapse in OSA is not well understood. Nevertheless, respiratory effort and negative pressure effects are likely to be central to the sensitive balance between collapsing forces and muscle recruitment in the upper airway, which underpins pharyngeal patency.

The current 'gold standard' method of assessing respiratory effort in sleep is based on the inspiratory nadir in oesophageal pressure, usually recorded by a balloon catheter, to provide an estimate of pleural pressure swings. However, there are some limitations

with this technique. Pressure signals are susceptible to significant cardiogenic artefact; the effect of occlusion on pressure swings is not well understood; and absolute values are difficult to interpret and compare between individuals due to inherent inter-individual differences in respiratory mechanics. Furthermore, the relationship between neural drive to breathe, inspiratory muscle recruitment and oesophageal pressure swings is complex, particularly in the presence of abrupt changes in upper airway resistance and lung volume in OSA, and these effects have not previously been adequately considered.

The aim of this thesis was to apply signal filtering and respiratory system mechanics principles to provide a more thorough understanding of the role of respiratory effort in OSA pathophysiology. This work uses theoretical consideration of respiratory mechanics to inform the development of a new method for assessing respiratory effort. Novel tools and algorithms were created to facilitate detailed, breath-by-breath and within-breath analysis of respiratory effort and muscle activity changes over the course of airway collapse and recovery in OSA. Results provided new insights into mechanisms underpinning airway obstruction onset and recovery.

Firstly, new filtering techniques were developed and tested to minimise cardiogenic artefact in both oesophageal pressure and diaphragmatic electromyography signals, allowing for more detailed comparisons of respiratory activity isolated from cardiogenic effects.

Secondly, physiological recordings were used to investigate the effect of an externally applied occlusion on inspiratory oesophageal and airway pressure deflections in the context of classical respiratory system mechanics equations, suggesting that additional airway resistance would augment muscle loading and the resulting pressure deflections. This could be due to either distortion of the respiratory system altering elastance and resistance, intrinsic muscle compensation or reflex modulation of drive. The chest wall impedance term approaches zero with no flow and volume change, and should theoretically result in a more negative measured pressure for the same muscle pressure deflection. Oesophageal and epiglottic pressure swings were immediately more negative on the breath following occlusion onset, and these differences were remarkably well explained on the basis of increased 'effective' values of elastance and resistance in the classical respiratory equation of motion to account for chest wall effects. This approach enabled loading response to be separated from the underlying chemo-reflex drive component of oesophageal pressure. The combined effect was quantified, and then applied as a correction to oesophageal pressure to estimate total muscle pressure, a better measure of the underlying ventilatory drive, irrespective of occlusion.

A novel model of attempted ventilation was then derived from oesophageal pressure and

the respiratory system equation of motion, accounting for occlusion effects by using the experimental findings of the previous study. By a rearrangement of the classical respiratory system equation of motion, the method very usefully predicts the flow that would have been expected to have been achieved from the driving pressure had airway patency been maintained. Respiratory effort can then be expressed in units of ventilation directly comparable to achieved ventilation, thus providing comprehensive new metrics of both effort and obstruction on a breath-by-breath basis.

This model was used to explore respiratory effort augmentation over periods of airway collapse and airflow recovery in OSA, and for examining relationships between changes in diaphragm and upper airway muscle activity with and without arousal. Results showed elevated ventilatory drive rapidly falling below baseline levels leading into airway obstruction, followed by augmented drive associated with subsequent airflow recovery, which was more exaggerated preceding arousal. Events with an arousal were associated with greater respiratory effort, a greater ventilatory overshoot, and increased risk of further collapse in the post-recovery period. This supports the hypothesis that increased drive at end-obstruction promotes arousal and an increased ventilatory response, which may leave the airway more susceptible to ongoing cyclical airway collapse.

It was observed that airflow recovery did not always correspond to the start of a respiratory effort, which led to a secondary study into the timing of airway re-opening, and the effort and muscle activity at the point of airflow restoration. This analysis showed that flow often resumed near the nadir of oesophageal pressure or into the subsequent passive recoil phase of the respiratory cycle, in association with reflex-like modulation of respiratory pattern generator timing itself. Thus inspiratory activity resumed with substantial changes in the respiratory duty cycle. This new observation has not been previously reported and warrants further studies to determine if it reflects a reflex contributing to airflow recovery, or occurs in response to flow restoration.

The work of this thesis provides important new insights into the understanding of respiratory effort in OSA. The demonstration that abrupt airway occlusion influences oesophageal and epiglottic pressure deflections has important implications for the assessment of respiratory effort in future physiological studies of OSA. The analytical tools developed from this work show major potential for providing important insights into the mechanisms of airway collapse, flow limitation and obstruction compensation. Application of these tools to other data sets, and across a wider sample of OSA patients and event types, would further enhance our understanding of the physiological mechanisms of OSA.

Chapter 1

Introduction

1.1 Motivation

Obstructive sleep apnoea (OSA) is the most common pathological respiratory disorder in sleep, in which the upper airway frequently collapses. This results in cyclical periods of either severe airflow limitation (hypopnoea) or complete obstruction (apnoea), often accompanied by brief arousal from sleep, that repeats over the course of the night. OSA diagnosis and severity is assessed on the basis of the apnoea hypopnoea index (AHI), which is the number of apnoea and hypopnoea events per hour of sleep. OSA is a remarkably common and frequently undiagnosed condition. Epidemiological studies estimate that the prevalence of mild OSA (AHI>5 /hr) is around 1 in 5 adults, and moderate OSA (AHI>15 /hr) is at least 1 in 15, with up to 70% of cases undiagnosed (Young et al., 2002). Typically, population based studies show significant sex-based differences, with 2 to 3 times more cases of OSA in male than female populations (Punjabi, 2008). Risk factors include male gender, obesity, anatomy, alcohol consumption and smoking.

The impact of OSA on health and quality of life can be severe. OSA is linked to increased daytime sleepiness, increased risk of motor accidents (Tregear et al., 2009), reduced cognitive function and hypertension (Nieto et al., 2000). Longitudinal data have shown strong independent associations between OSA and increased risk of stroke and all-cause mortality (Marshall et al., 2008). Diagnosis of OSA is usually obtained through an overnight polysomnogram, in which multiple physiological signals are recorded. From these, respiratory events are identified by the following definitions: an apnoea is a $\geq$90% reduction in airflow for $\geq$10 seconds, while hypopnoeas is a reduction of airflow of $\geq$30% for $\geq$10 seconds, combined with either a $\geq$3% drop in oxygen saturation or cortical arousal (Berry et al., 2017).

The current first line treatment for OSA is continuous positive airway pressure (CPAP) applied via a nasal or full face mask (Sullivan et al., 1981). This is very successful in ensuring that pharyngeal airway patency is maintained, however, patient tolerance is low, with only around half of those prescribed CPAP using it enough to gain sufficient clinical benefit (Weaver and Grunstein, 2008). For those unable or unwilling to use CPAP, other secondary treatments are available. Mandibular advancement splints (MAS) lower AHI, particularly in patients with mild-moderate OSA and for whom upper airway size increases with MAS (Sutherland and Cistulli, 2011). Surgical intervention to remove excess tissue in the soft palate and tongue has positive results in some patients (Kezirian and Goldberg, 2006). Hypoglossal nerve stimulation has been shown to be successful in a subset of OSA patients, but the cost, invasive nature and requirement for pre-implantation drug induced sleep endoscopy limit its general uptake (Eastwood et al., 2011; Strollo Jr et al., 2014).

Weight loss (Newman et al., 2005) and controlling sleeping position to avoid supine sleep (Cartwright, 1984) result in an improvement in sleep apnoea, but often not sufficiently to treat it completely. Therefore, currently there are not suitable treatment options for all patients, resulting in a high burden of untreated OSA in the community.

OSA was long thought to be simply an anatomical problem, exacerbated by obesity and ageing which both increase airway collapsibility. However, it is now clear that the pathophysiology is much more complex. A number of additional non-anatomical physiological traits have been identified that can predispose a patient to OSA: unstable respiratory control or high loop-gain, an increased propensity to arouse to relatively modest airway obstruction events, and poor upper airway muscle compensation responsiveness (Eckert, 2018). Any given individual's OSA could be caused by one or more of these traits. Thus, optimal treatments are likely to vary according to underlying causal mechanisms. By identifying individual patient 'phenotypes', it is hoped that more personalised treatments can be prescribed to increase treatment acceptability, adherence and thus effectiveness.

There are clear benefits to such approaches in OSA. However, considering each trait in isolation risks ignoring the potentially complex effects of what are likely interrelated mechanisms. For example, the main CO_2 chemo-reflex drive to breathe is a major determinant of upper airway muscle recruitment, breathing effort and overall loop-gain. However, upper airway muscle activity is also modulated by mechano-receptor feedback mechanisms augmented by more negative airway pressures during obstructive breathing. Furthermore, breathing effort also appears to be the main factor triggering arousal, either through central drive pathways or directly via sensations arising from increased breathing drive or efferent-afferent mismatch. Thus, muscle recruitment responses, arousal and overall chemo-reflex feedback loop sensitivity (loop gain) are all inter-related, and dependent on either central drive or negative pressure, which can only increase through increased ventilator effort. High respiratory drive at the termination of obstructive events is also thought to lead to hyperventilation, which could lower chemo-reflex drive to breathe and promote ongoing respiratory instability. However, the role of augmenting effort, through either arousal or CO_2 drive in the period of increased ventilation following airway restabilisation, remains unclear.

A major hypothesis of this thesis is that changes in respiratory effort are a major determinant of airway collapse, when drive is too low, and are also central to the processes of airflow recovery and arousal from sleep, when the central drive to the upper airway and breathing is augmented. This is supported by several key pieces of evidence. Airway obstruction occurs abruptly when wake related inputs to upper airway muscle activity withdraw at sleep onset, and frequently recurs shortly after a brief period of recovery ven-

tilation following obstruction, often, but not always, in association with arousal. Arousal appears to occur at a threshold level of inspiratory effort, regardless of the respiratory stimulus (Gleeson et al., 1990). Airflow recovery can often occur without arousal, meaning compensatory mechanisms can recruit pharyngeal dilators sufficiently to re-establish patency (Younes, 2004). The only known pathways for dilator stimulation during sleep are central chemo-reflex drive or negative pressure, meaning good measures of these are vital for improved understanding of the physiological processes that govern OSA (Younes, 2003). Furthermore, OSA severity reduces in deep sleep, when respiratory effort is increased (Ratnavadivel et al., 2009). Therefore, respiratory effort appears to be one of the central factors underpinning OSA.

Understanding these observations in OSA is very challenging because current methods available for measuring and quantifying respiratory effort are limited and problematic to interpret. Oesophageal pressure is the gold standard measure, and is a surrogate for pleural pressure. However, measurement is invasive, absolute values vary significantly between patients, and signals are often significantly distorted by cardiogenic artefact. Additionally, the mechanical influence of occlusion on pressure values is often ignored in sleep research despite the fact it is potentially significant. To combat and investigate these limitations, this thesis presents a novel method for better quantifying respiratory effort in units of ventilation, that can be directly compared to achieved ventilation. New techniques for cardiogenic filtering and estimation of chest wall effects are also discussed. These methods are then applied to detailed physiologic sleep study data to investigate the physiological mechanisms operating in OSA.

1.2 Aims

The central aims of this thesis are as follows:

Aim 1: To develop new filtering techniques required for short time scale reliable analysis and model fitting for physiological analysis of oesophageal pressure and diaphragm electromyography (EMG) signals.

Aim 2: To determine relative effects to an applied external occlusion on the current gold standard measures of respiratory effort in sleep (oesophageal and epiglottic pressure). The magnitude of mechanical and configurational effects is currently unknown, but these are important to separate from effort augmentation for the interpretation of oesophageal pressure as a measure of the underlying central respiratory drive.

Aim 3: To implement and test a novel method to quantify respiratory effort and obstruction breath-by-breath in OSA using the classic respiratory equation of motion.

Aim 4: To use the new tools developed to investigate the underlying role of inspiratory drive and negative pressure during obstruction and in compensation mechanisms for dilator muscle recruitment and flow recovery, with and without arousal.

1.3 Outline of Thesis

To address the goals outlined, the thesis is structured as follows:

Chapter 1 is an introduction to the thesis and lays out the motivation and aims of the work presented.

Chapter 2 describes the current literature on ventilatory effort, airway collapse and compensatory mechanisms for stability in OSA.

Chapter 3 covers the development of custom signal filtering methods required for in-depth analysis of oesophageal pressure and diaphragm EMG as measures of ventilatory effort.

Chapter 4 examines the magnitude of chest wall effects on pleural pressure and estimated ventilatory effort by exploring the effect of abrupt occlusion on oesophageal and epiglottic pressure.

Chapter 5 outlines a novel quantitative method for estimating ventilatory effort in "attempted" units of ventilation derived from trans-thoracic pressure in both theory and application to sleep data in OSA.

Chapter 6 applies the new measure of ventilatory effort to explore the role of drive augmentation over the course of airway obstruction and flow recovery in OSA, and how it relates to muscle recruitment and arousal.

Chapter 7 examines more closely the mechanism behind flow recovery in OSA. Novel observations into the temporal relationship between effort and flow onset are presented and explored in more detail.

Chapter 8 discusses the contribution of this thesis to the field of sleep research, the limitations of the work and finally highlights areas for future research.

Chapter 2

Literature Review

2.1 Physiology

2.1.1 The Human Airway

The upper airway is comprised of five sections: the nasal cavity; the nasopharynx, extending from behind the nose to above the soft palate; the oropharynx, the region from the soft palate to above the epiglottis; the hypopharynx, the area from the epiglottis to the cricoid cartilage behind larynx; and the larynx itself (White and Younes, 2012). Muscles surround much of the upper airway with no rigid support from bone or cartilage; the soft palate and the tongue lie at the anterior whilst the pharyngeal constrictor muscles lie at the posterior and lateral walls of the pharyngeal airway. This enables the pharynx to behave as a collapsible tube, which is an essential adaptation for speech and swallowing. However, it also leaves the airway vulnerable to collapse if muscle activity is not sufficient to maintain patency, as occurs during sleep in OSA. Airway collapse most commonly occurs in the oropharynx, though this can extend to the hypopharynx (Rama et al., 2002).

2.1.2 Upper airway muscles

There are a number of different muscles in the human upper airway (UA) that are involved in the breathing process. These muscles can be divided into two main groups; the pharyngeal dilators and pharyngeal constrictors. The dilator muscles are the primary control muscles involved in airway patency. These can be further separated into those that control tongue position (genioglossus, hyoglossus and styloglossus), those that control the soft palate shape and position (levator palatini, tensor palatini, palatoglossus, palatopharyngeus and musculus uvula) and those that influence hyoid bone position (geniohyoid, mylohyoid, digastric, stylohyoid, omohyoid, sternohyoid and thyrohyoid) (White and Younes, 2012).

The genioglossus (GG) is the largest extrinsic muscle of the tongue and is the most commonly studied UA dilator muscle in respiratory sleep research, due in part to its large size and accessibility, as well as its observed role in maintaining airway patency (Remmers et al., 1978). The GG connects the mandible to the base of the tongue and is innervated by the hypoglossal nerve. When stimulated, GG contracts and pulls the tongue forward, increasing the retrolingual space in the upper airway. This is a highly complex process and involves many types of phasic and tonic motor units (Cori et al., 2018). The GG muscle exhibits both phasic inspiratory activity and tonic expiratory activity and is stimulated by negative pressure, chemo-reflex drive and wakefulness related drive inputs to the GG

and other skeletal muscles more generally (Loewen et al., 2011; Trinder and Jordan, 2011; Wheatley et al., 1993).

The tensor palatini has been the subject of several studies. Unlike the genioglossus, it typically shows constant tonic activity across the breathing cycle under normal resting conditions (Nicholas et al., 2012). The tensor palatini (TP) has been shown to exhibit short-latency reflex activation response to negative pressure applied during wakefulness, but no subsequent suppression, unlike the combination of brief activation and then suppression response observed in GG (Eckert et al., 2010). This suggests there are fundamental differences between the UA dilator muscles in their responses to airway pressure and possibly other stimuli, and that this additional suppression observed in GG likely occurs via inhibition of respiratory active neurons, much like the diaphragm (Jeffery et al., 2006*a*). The TP negative pressure reflex is markedly reduced during non-rapid eye movement (NREM) sleep, which may contribute to retropalatal collapse (Wheatley et al., 1993).

The pharyngeal constrictors are primarily responsible for airway closure during swallowing, and are thought to be minimally active in sleep. Kuna et al observed limited resting respiratory activity, and any activity tended to be expiratory and to increase with an additional respiratory stimulus, e.g. hypercapnia or hypoxia (Kuna and Smickley, 1997). There is some evidence to suggest that constrictor activity reduces airway size at normal lung volumes, however Kuna et al showed that at low lung volume in cats (below functional residual capacity), constrictor stimulation could decrease UA compliance, stiffening the airway and even dilating the airway in some cases (Kuna, 2000). Therefore, it is possible these muscles could be involved in mechanisms promoting airway patency. In human studies, the superior pharyngeal constrictors exhibited no activity during stable NREM sleep or during obstruction. However, activation patterns during airway reopening following apnoea were similar to that of the UA dilator muscles, with recruitment occurring during inspiration (Kuna et al., 1997). This suggests constrictors play a minimal role in precipitating collapse during sleep, but does not exclude them from playing a role in airway reopening.

2.1.3 Airway collapse

At sleep onset, ventilation falls due to increases in upper airway resistance and lower drive to respiratory muscles (Hudgel et al., 1984; Morrell et al., 1995; Wiegand et al., 1989). Upper airway dilator muscle activity reduces significantly with the cessation of wake stimulus in both OSA subjects and controls (Wheatley et al., 1993). These changes are substantially greater in OSA patients (Mezzanotte et al., 1992), suggestive of neuromuscular compensa-

tion for poorer airway function during wake that is impaired during sleep, exposing OSA patients to increased UA collapse risk. In healthy individuals, compensatory mechanisms including augmented inspiratory muscle activity and upper airway protective reflexes are thought to help maintain airway patency (Henke et al., 1992). In OSA pathogenesis however, these compensatory mechanisms are clearly insufficient to adequately successfully oppose upper airway collapsing forces.

It is clear then, that during sleep, particularly in OSA patients, the upper airway can behave like a floppy tube with a propensity for partial or complete collapse. Unlike a rigid tube where flow is directly proportional to the driving pressure across the segment, in a collapsible tube, increased negative intraluminal pressures, associated with downstream driving pressures, reduce lumen dimension to dynamically increase airflow resistance with correspondingly reduced airflow. This behaviour is analogous to a Starling resistor, where a 'choke point' develops that dynamically limits airflow irrespective of increases in driving pressure (Conrad, 1969).

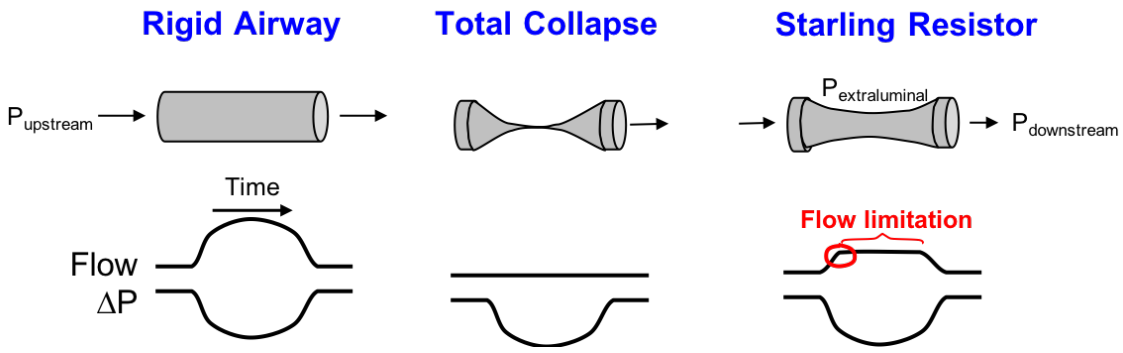

Figure 2.1: Example of flow and pressure relationships in an open tube, a collapsed tube and a starling resistor. Note the choke point in the starling flow, where despite increasingly negative downstream pressure, flow values remain constant.

To stiffen the airway and end Starling-like behaviour, an increase in UA dilator activity is required. However, UA activity is mediated by increased chemical drive which also inevitably increases negative intraluminal and driving pressures, which may worsen rather than improve collapse. These phenomena likely explain why upper airway collapse is difficult to reverse once established and why arousal often arises from augmented ventilatory effort associated with airway obstruction events.

It is important to note that the Starling model of upper airway behaviour during sleep

has some important limitations that fail to account for several observations from this complex anatomical system. Whilst often Starling-like, anatomical differences along the length of the pharynx result in more complex changes in pressure-area and -flow relations. Negative effort dependence is often observed in OSA, where flow in fact decreases with increased effort unlike the flow truncation and limitation predicted by the Starling model (Owens et al., 2014). This could be caused by mechanical independence along the length of the pharynx such that initial sites of collapse may be precipitated at sites initially most vulnerable to collapse and then propagate along the airway. Thus dynamic changes in upstream resistance may differentially increase the pressure drop and transluminal pressure across the choke point (Wellman et al., 2014). These studies suggest pharyngeal collapse is not a simple behaviour easily modelled by classical systems. Nasal versus oral airflow pathways, partly divided by the compliant soft palate, partly influenced by tongue position, also likely contribute to more complex behaviours than predicted from Starling-like behaviour alone. Given complex and highly dynamic airflow interactions with upper airway anatomy, muscle activation and longitudinal traction effects; the sites and mechanism of collapse likely vary considerably along among patients.

2.1.4 Respiratory Pump Muscles

The human respiratory system is driven by inspiratory and expiratory skeletal muscles. During quiet breathing at normal levels of ventilatory drive, inspiration is active whilst expiration generally reflects passive system recoil back to resting end-expiratory lung volume. The diaphragm is the principal driving muscle of ventilation, and works in combination with the intercostal muscles and accessory muscles to increase lung volume. The diaphragm contracts and moves downwards while the intercostal muscles draw the ribs upward and out to expand the chest wall. This induces a negative pressure difference across the respiratory system, from the airway opening to the alveoli, via more negative intrathoracic and pleural pressure, which ultimately drives flow and lung volume changes. During passive expiration, the pump muscles relax and the elastic nature of the lung and chest wall initiates recoil, increasing pressure and expelling air from the lung via the pressure gradient relative to atmosphere. At high ventilatory drive (e.g. during exercise or under stress), additional recruitment of abdominal and accessory muscles can invoke forced expiration by actively reducing thoracic volumes to create increased expiratory pressure gradients.

2.1.5 Neural control of respiratory muscles

There are two main neural pathways that can independently control the respiratory muscles. During passive breathing, control is automatic and centrally co-ordinated by the medulla and driven largely by two coupled oscillators, one inspiratory and one expiratory (for more detail, see Feldman and Del Negro (2006)). The inspiratory rhythm generator is dominant and located in the pre-Bötzinger complex. It is controlled by inputs from central and peripheral chemo-receptors responding mainly to arterial CO_2 changes and mechano-receptors in the lungs and upper airway via reflex pathways (for review, see Ramirez et al. (2013)). Breathing can also be voluntary, as readily observed during breath holds, and in daily activities like eating and speaking. Thus, respiratory muscles can be controlled by more direct pathways from the motor cortex.

Neural drive is then distributed to respiratory motoneurones, with strong evidence to support differential distribution according to neuromechanical matching, where motoneuronal output is controlled according to mechanical advantage (Butler and Gandevia, 2008). Studies in both animals and humans suggest that in the intercostal muscles this differentiation happens within an individual motoneurone pool to a specific muscle, suggesting fine-tuned adaptation to optimise efficiency (De Troyer et al., 2003; Legrand and De Troyer, 1999). There is also strong evidence to support that individual respiratory pump muscles are recruited at different times and for different durations. Saboisky et al. showed in single motor unit recordings that the diaphragm is recruited prior to other respiratory pump muscles, with a gradient of drive to different motoneurone pools (Saboisky et al., 2007). This may reflect an optimisation of respiratory work in relation to mechanical advantage, but would need to be adaptable to changes in mechanics, either through volume or positional changes or functional changes relating to disease. For further details on the distribution of drive to the respiratory muscles by automatic and voluntary pathways, see Butler (2007).

The upper airway dilator muscles are also activated by underlying neural drive from lower brainstem circuits (Akahoshi et al., 2001; Pillar et al., 2001), as well as by reflex responses to pressure changes in the upper airway (Horner et al., 1991; Malhotra et al., 2002; Wheatley et al., 1993). Genioglossus recruitment occurs approximately 100ms prior to inspiratory pump muscle activation and airflow, via central pathways (Strohl et al., 1980). Applied negative pressure has been shown to increase pre-activation of the upper airway muscles relative to diaphragm (van Lunteren et al., 1984). Animal studies into transmission pathways of drive to hypoglossal motoneurones suggest there is a separate pathway than to phrenic motoneurones, which allows for independent recruitment of upper airway and pump muscles (Peever et al., 2002). This could be highly beneficial mecha-

nistically for controlling airway patency and managing the balance between inspiratory collapsing pressures and upper airway activity. However, it is not yet clear if similar separate pathways also exist in humans and many details regarding neuromuscular control mechanisms relevant to maintaining human upper airway patency during sleep remain largely unknown.

2.2 Anatomical differences in OSA patients

Many studies have assessed airway anatomy of OSA patients compared with controls and found those with OSA have a narrower and more collapsible airway. Obesity and increased neck circumference are key risk factors for OSA relevant to these findings (Pinto et al., 2011). Studies during wake show OSA patients in general have a narrower pharyngeal airway than healthy subjects, as measured across a range of imaging modalities (computer tomography, magnetic resonance imaging and endoscopy) (Haponik et al., 1983; Isono et al., 1997; Schwab et al., 1995). There is also more soft tissue surrounding the airway in apnoeic patients than controls. Schwab et al. also reported increased pharyngeal wall thickness and volume in OSA patients (Schwab et al., 1995). Studies consistently show increased tongue size and volume in apnoeic patients as compared to controls, as well as increased soft palate dimensions (Schwab et al., 1995, 2003). There is also evidence to support that OSA patients have more fat deposits in the area around the oropharynx than weight-matched controls (Horner et al., 1989).

Not only is the pharynx narrower in OSA populations, it is also mechanically more collapsible when compared with healthy controls. By examining airflow responses at different upper airway holding pressures, spanning both positive and negative pressures relative to atmospheric pressure, Isono et al found increased critical closing pressure of pharyngeal collapse during sleep (Pcrit) in OSA over control participants while under general anaesthesia (Isono et al., 1997). Other studies have also shown correlations between collapsibility and reduced upper airway calibre, suggesting collapse itself may be modulated by mechanical properties (Schwartz et al., 1998; Sforza et al., 2000). On the other hand, Pcrit measurements are typically "passive" and based on a sudden drop in airway pressure from a positive holding pressure where upper airway resistance and upper airway muscle activity during sleep is artificially low. "Active" Pcrit measurements, using more gradual drops in pressure with higher airway resistance and upper airway muscle activity are typically much higher, supporting the importance of neuromuscular drive influences (Azarbarzin et al., 2017).

There is, however, clear overlap between the OSA and control groups, both in terms of

Pcrit and airway size. Some patients have OSA despite seemingly normal anatomy, and some people can maintain upper airway patency during sleep despite a narrow and more collapsible airway. In addition, OSA severity as measured by polysomnography and AHI is not directly correlated to airway size or collapsibility either during wakefulness or sleep (Kirkness et al., 2003; Younes, 2003). This suggests other non-anatomical deficits are also important in the pathogenesis of OSA and that a single anatomical or functional measurement cannot accurately predict who will have OSA, or who will respond to a particular treatment option.

2.3 Non-anatomical factors

In addition to anatomical differences that can predispose patients to OSA, there are a number of non-anatomical traits that play an important role in sleep apnoea pathogenesis (Eckert, 2018). Current standard treatment options focus on resolving upper airway anatomical deficits, by splinting the airway open with CPAP or increasing pharyngeal space either through mandibular advancement or surgery. A relatively recent concept that OSA reflects interactive effects between a number of key pathophysiological traits has gained widespread acceptance. This concept of phenotyping, perhaps more accurately termed endotyping, recognises that underlying causal mechanisms are likely to vary considerably between individual patients. A better understanding of causes on an individual patient basis is clearly needed to support more targeted "precision medicine" approaches to treatment to replace the current "one size fits all" approach of CPAP use, which ultimately fails to successfully treat many patients. The main non-anatomic traits in OSA are thought to include reduced upper airway dilator muscle effectiveness, a reduced arousal threshold (more easily aroused) and oversensitive respiratory control. These non-anatomical factors generally correspond to failures in the compensatory mechanisms that can successfully mitigate airflow obstruction and ventilatory instability in patients without OSA.

2.3.1 Arousal threshold

Arousal often occurs at the end of an obstructive event, and provides an additional wake stimulus to upper airway muscles such that airway patency can rapidly be restored even in the presence of total airway occlusion. Arousal was long thought to be essential for airflow recovery in OSA, until it was shown that arousal is sometimes absent and often occurs after airflow recovery. The ventilatory increase associated with arousal may in fact be detrimental to ongoing ventilatory and upper airway stability, by promoting a

subsequent reduction in chemo-reflex drive to upper airway muscles that may perpetuate future cyclical UA collapse (Younes, 2004).

An individual's propensity to arouse is variable. A patient who wakes up at a lower level of a ventilatory stimulus (earlier in an obstruction event) is expected to show more arousals and greater disturbance to their sleep, but shorter events with less desaturation. On the other hand, a patient able to tolerate more severe obstruction with greater oxygen desaturation and ventilatory drive before awakening would be expected to exhibit a quite different OSA presentation, with potentially fewer but more severe events. Thus, arousal threshold is now considered to be an important factor in OSA (Eckert and Younes, 2014).

Given that arousal is not necessary for airflow recovery, and is possibly associated with negative effects on ventilatory and upper airway stability (Eckert and Younes, 2014), an individual with a low arousal threshold may benefit from treatments designed to prevent or postpone arousal, to enable airway recovery without arousal and with less sleep disturbance. Sedative-based treatments have been proposed for these patients, and studies have explored the efficacy of a number of agents. Jordan et al summarised results from these studies (Jordan et al., 2017). Agents include antidepressants, e.g trazadone (Eckert et al., 2014; Smales et al., 2015) and non-myorelaxant sedatives Zopiclone (Carter et al., 2016) and its stereo-isomer Eszopiclone (Eckert et al., 2011). Overall, group data from sedative trials have shown mixed effects on the severity of OSA, as measured by AHI. In studies that assess phenotypic traits of responders and non-responders, there is evidence that the arousal threshold can be increased and AHI reduced in patients with a demonstrably low ventilatory arousal threshold, though effect sizes are modest. Sedative therapy is therefore likely useful in a sub-set of carefully selected patients, but the ongoing challenge is in identifying those that will benefit most.

2.3.2 Ventilatory instability (loop gain)

In the context of OSA, ventilatory instability and loop gain is very useful for describing the ventilatory control response to chemical blood gas disturbances caused by airway obstruction. Arterial CO_2 is the main chemical stimulus to the central neural controller drive to breathe. Obstruction, arousal and hyperventilation all cause substantial fluctuations in CO_2 away from a stable set-point which central ventilatory control usually serves to maintain. The gain or sensitivity of the respiratory control system to these changes will affect the ongoing stability of the ventilatory system. This stability is usefully quantified by the loop gain of the system, which is defined as the ratio of the magnitude of the ventilatory response to disturbance relative to the magnitude of initial disturbance, which is a

function of the overall gain of the feedback loop associated with ventilatory control (Eckert et al., 2013). There are several factors affecting loop gain: the plant gain (change in CO_2 per unit change in ventilation, which is a function of the respiratory response to neural drive), the circulation delay (time for arterial CO_2 changes to be detected by central and peripheral chemoreceptors) and controller gain (change in ventilation per unit change in CO_2, which is a function of chemo-sensitivity of the neural drive response). High loop gain indicates a system that tends to overcompensate for rising CO_2 levels by excessively increasing ventilation, promoting larger subsequent CO_2 level drops below stable breathing levels and ongoing instability. A low loop gain represents a more stable control system, where responses are more appropriate to any given level of ventilatory disturbance. Loop gain can be estimated algorithmically from breathing responses to experimental ventilatory disturbances such as with CPAP manipulations (Wellman et al., 2013) or naturally occurring disturbances as recorded by standard polysomnography (Terrill et al., 2015). Proposed treatments for patients with high loop gain include supplemental oxygen (Edwards, Andara, Landry, Sands, Joosten, Owens, White, Hamilton and Wellman, 2016) or drug therapies to dampen ventilatory control responses. Acetazolomide has been shown to reduce loop gain by 40%, and to help improve AHI (Edwards et al., 2012).

2.3.3 Dilator muscle responsiveness and effectiveness

Upper airway dilator muscles are integral to pharyngeal patency and overcoming dynamic collapsing forces that vary over the course of inspiration and expiration. Reduced dilator muscle activity during sleep contributes to flow limitation and collapse, even if the airway is anatomically normal. Upper airway muscle activity is abruptly reduced at sleep onset compared to wake, but then typically rapidly increases over several breaths to above wake levels via compensatory mechanisms that augment upper airway muscle activity in response to increased UA resistance, flow limitation and the associated hypoventilation (Wilkinson et al., 2008). Whether this is successful at maintaining airway patency depends on two main factors: the muscle responsiveness, or sensitivity of electromyographic (EMG) responses to ventilatory disturbance; and the effectiveness of augmented EMG activity to re-open the airway. Muscle responsiveness reflects how successfully EMG activity increases in response to increased stimuli from chemo-reflexes and negative pharyngeal pressure changes. This can be measured by assessing the breath by breath relative changes in upper airway EMG muscle activity compared to changes in the nadir or pharyngeal or oesophageal pressure. A patient with poor muscle responsiveness will exhibit little to no augmentation of muscle activity during airway obstruction, despite increasing chemical and negative pressure stimuli. Approximately one third of OSA patients studied showed

such behaviour (Eckert et al., 2013). Enhanced muscle responsiveness is seen in obese subjects without OSA (Sands et al., 2014), suggestive of an important protective trait in these individuals and that poor muscle responsiveness likely plays a pathogenic role in OSA.

Muscle effectiveness describes how well increased muscle activity translates to increased upper airway dilation and airflow. Airway dilation itself is difficult to assess quantitatively without direct visualisation with an endoscope. However, airflow changes during gradual CPAP reductions provide a useful marker of how well muscle recruitment translates into airflow. Patients with OSA have been found to have poor muscle effectiveness when compared with healthy controls (Jordan et al., 2007). Unlike for the arousal threshold and loop gain traits, there are not yet any practical clinical tests or measurements of muscle responsiveness that can be applied to a standard polysomnogram (PSG). This is an important limitation for which new standardised measurements will be an important addition to support the utility of clinic based OSA phenotyping. However, given the importance of UA dilators for protecting the UA, this is likely to represent an important area for potential therapeutic targets. Recent studies of pharmacological interventions targeting UA muscle responses using atomoxetine and oxybutynin have shown promising results across a broad range of phenotypes, significantly reducing AHI, supporting the potential value of this approach (Taranto-Montemurro et al., 2019).

2.3.4 Limitations of phenotype model

There is no doubt that phenotyping, and identifying these non-anatomical traits in OSA has greatly enhanced our understanding of OSA pathogenesis, and the different presentations of such a heterogeneous condition. This approach is designed to identify patients most suited to certain treatment options. However, considering each as a separate trait in isolation also risks ignoring the links between what are clearly interdependent phenomena. Wellman and colleagues do make attempts to combine some of the 'steady state' versions of these phenotypic traits in a model to predict the presence of OSA with the goal of providing a diagnostic aid (Wellman et al., 2013).

However, airway collapse and reopening are dynamic processes which change with sleep stage and depth. Thus, particularly for understanding the physiological mechanisms, it is important to also consider the system as a whole. There are two main pathways to stimulate respiratory system activity during sleep: mechanoreceptor feedback from negative pressure and/or stretch in the lung and upper airway; and peripheral and central chemoreceptor feedback, to augment neural drive. Changes from wake to sleep and sleep

stage transitions also augment these physiological responses. Each of the non-anatomical traits is mediated by some or all of these stimuli. Interventions to quantify individual traits by a value at the beginning of night study is unlikely to reflect the true complexity and variation in a patients sleep apnoea over the course of a whole night, or indeed multiple nights. It is possible such methods are oversimplifying the underlying physiology, meaning individualised therapies to target specific traits cannot successfully reduce AHI to acceptable levels. Work into combination therapies (treating multiple traits together) shows more promising results, and may be a way to address this limitation (Edwards, Sands, Owens, Eckert, Landry, White, Malhotra and Wellman, 2016).

Furthermore, currently, the phenotyping model relies on intervention and CPAP manipulations to define characteristics like Pcrit and muscle responsiveness. Inherently, such manoeuvres introduce unnatural pressure and volume changes to the system, which can influence how the upper airway behaves. This is a significant limitation to the work discussed above. Clearly, there is a difficult challenge between using intervention to extract more detailed information about different aspects of the respiratory system in sleep, and not allowing such intervention to influence how the system responds. These intervenstions are also very labour intensive, and require specialist training, so are unlikely to be widely applicable clinically in routine diagnostic polysomnography. Due to the analysis challenges of extracting similar data from naturally occurring events in sleep, there is currently a lack of studies that explore this. A careful examination of these underlying changes over the course of events in OSA is required for a better understanding of mechanisms in OSA.

2.4 Compensatory Mechanisms

The human airway is able to recover from collapse through a combination of compensatory responses. These include arousal, increased muscle recruitment to stiffen the airway, increased breathing effort and duty cycle changes. Mechanisms are complex, undoubtedly interact and are likely to vary on an individual basis. A key observation in OSA is that most patients demonstrate periods of stable breathing during the night, most often in deep sleep, but potentially also in other stages of sleep (Ratnavadivel et al., 2009; Younes, 2003). These periods are associated with increased dilator muscle activity (Jordan et al., 2009). From this it is clear that under favourable conditions, pharyngeal dilators can maintain airway patency during sleep in most patients. Closer analysis of arousal prevalence and timing revealed patency can be established prior to or entirely without arousal, indicating other non-arousal mechanisms must be capable of opening the airway (Younes, 2004).

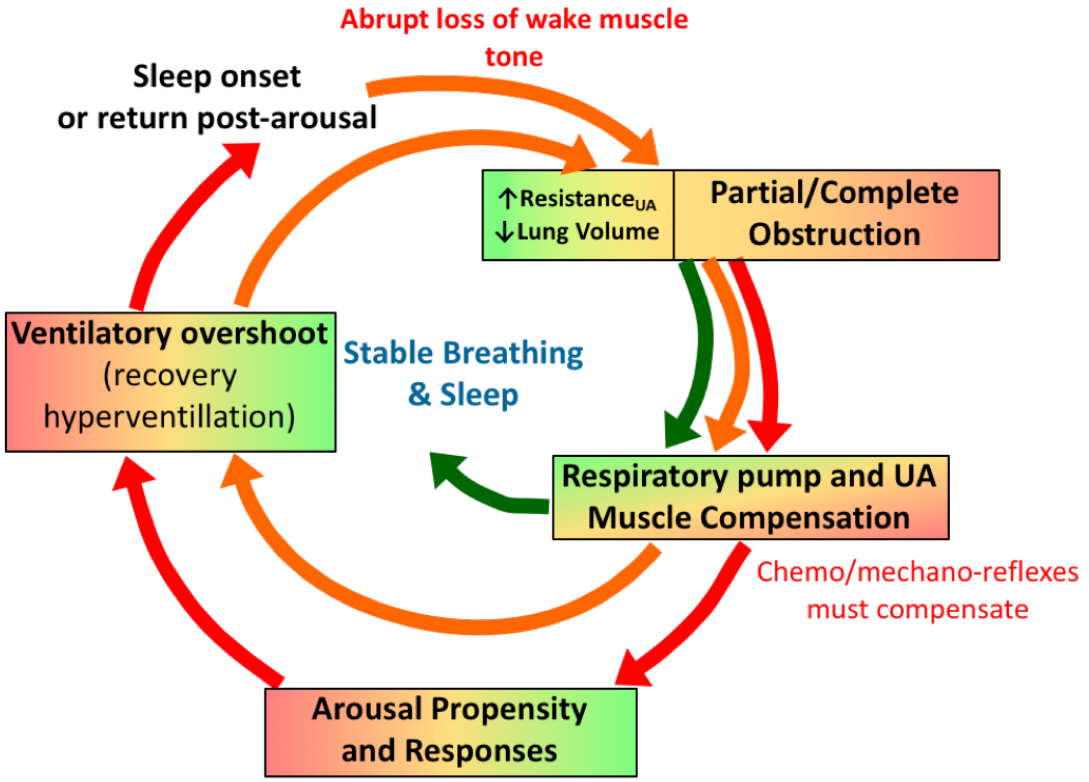

Figure 2.2: Illustration of the role of compensatory mechanisms and arousal in cyclic obstruction and stable sleep in OSA. In order to achieve periods of stable breathing, compensation must be adequate to counter airway collapsing forces but not induce ventilatory overshoot which can further disrupt chemoreflex balance

2.4.1 Respiratory effort and arousal

Arousal is often observed around the time airflow is re-established following collapse in OSA, which led to the long-accepted idea that arousal was an essential airflow recovery mechanism. Remmers et al proposed a theoretical 'balance of forces' model in which increasing recruitment of both the upper airway muscles and inspiratory pump muscles during obstruction worked to oppose the other, such that dilator activity was insufficient to overcome the increasing negative pressure without additional stimulus from arousal (Remmers et al., 1978). They theorised that it is only with this additional wake stimulus that the mechanics of the system become favourable and patency can be re-established. To examine the mechanisms underlying arousal at the end of a respiratory event, Vincken et al performed breath by breath analysis of diaphragm EMG in four OSA patients (Vincken et al., 1987). A progressively increasing time under tension was observed for the diaphragm over the course of obstruction until the airway reopened at a time closely related to arousal. The inspiratory muscle force at the time of arousal was found to approximate the fatigue threshold. This was suggested as evidence of a reflex mechanism stimulated by either UA or inspiratory pump muscle mechano-receptors when driving effort forced them to a certain degree of contraction.

Gleeson et al. sought evidence to support the hypothesis that arousal results from increasing ventilatory effort by examining oesophageal pressure during respiratory events induced by resistive, hypoxic and hypercapnic stimuli in eight healthy participants (Gleeson et al., 1990). This showed that within each individual, a consistent threshold level of ventilatory effort occurred on the breath prior to arousal regardless of the ventilatory stimulus, but with considerably more variability in threshold levels between subjects. These results support the hypothesis that sensations arising from increased respiratory effort provide the common ventilatory stimulus for respiratory related arousal, which can be measured on an individual basis by assessing oesophageal or airway pressure deflections associated with respiratory related arousal. Gleeson et al. proposed that mechano-receptors in the upper airway may primarily mediate the arousal response as a result of increased negative pressure, but did not rule out the possibility of intrathoracic receptor involvement. A further possibility is that sensations arising from outgoing motor command itself, or a mismatch between outgoing motor command and sensory afferent feedback, may ultimately underpin respiratory related arousal. Human experiments showing that disrupting sensory feedback during volitional motor tasks substantially alters perceptions of motor task outcomes strongly support central integration of proprioceptive sensorimotor feedback related to outgoing motor drive to skeletal muscles (Gandevia et al., 2006). Thus, whilst the precise nature of arousal mechanisms inevitably remains somewhat speculative,

sensations arising from the level of outgoing motor command to inspiratory muscles are clearly of central importance.

2.4.2 Role of arousal

Later studies made it clear that cortical arousal is not essential to restoring airway patency. Younes showed most patients can achieve stable breathing during sleep without arousal (Younes, 2003). Furthermore, after airway collapse, three quarters of OSA patients were able reopen their airway prior to or without arousal at least some of the time (Younes, 2004). When accompanied by arousal, ventilation at airway reopening was increased relative to events without arousal but was more than sufficient to rapidly restore ventilation and CO_2 to eucapnic levels regardless of the presence or absence of arousal. These findings challenged the traditional concept of arousal being an important airway protective mechanism and raised the possibility that exaggerated hyperventilation and subsequent hypocapnia following arousal could promote further airway collapse and ongoing cyclical ventilatory instability and arousal. Airflow recovery without arousal is proportionally less frequent with more severe respiratory events (Jordan et al., 2007; Younes, 2004), consistent with the concept of competing inspiratory effort-related arousal and muscle recruitment thresholds.

Since Younes' landmark findings, several further studies have investigated arousal timing more closely, with the aim of understanding how these observations relate to the arousal threshold concept of Gleeson and others. Amatoury et al carefully examined the within-breath timing of respiratory-induced cortical arousals (Amatoury et al., 2018), hypothesising that if negative airway pressure was the primary stimulus for arousal, then arousal should occur consistently around the nadir pressure swing during inspiration. Instead they found that 35% of arousals occurred during the expiratory phase of the respiratory cycle, and that arousals during inspiratory efforts were distributed relatively evenly throughout the inspiratory phase. Flow had returned to baseline levels on the breath prior to arousal in the expiratory arousal group but remained reduced for inspiratory arousals, suggesting airflow recovery preceded expiratory but not inspiratory arousals, though this was not directly measured. The magnitude of epiglottic pressure swing preceding arousal was not different between inspiratory and expiratory cases, however the effect of airflow onset on pressure values was not accounted for. This is highly problematic given that epiglottic pressure is thought to reflect pleural pressure swing only under the assumption the airway is occluded, and flow will invariably alter the pressure signal. The authors appear to define inspiratory and expiratory phases from the flow signal alone, however in the presence of obstruction it is difficult to know at which point in the breathing effort cycle airflow

recovery is actually occurring. As effort relates more directly to neural drive and compensatory mechanisms, the relative epiglottic pressure phase would be a useful addition to the results. Nevertheless, the study highlights the complexity of arousal mechanisms, and the close link to the airflow recovery process.

Two studies have since re-evaluated arousal threshold in OSA populations with contrasting findings. Xiao et al analysed oesophageal pressure and diaphragm EMG at the end of hypopnoea and apnoea events terminating with and without arousal in 17 untreated OSA subjects to more closely assess relationships between arousal and airflow restoration responses (Xiao et al., 2015). They found a wide range in both Poes and EMGdi at event termination, with no systematic differences between events with and without arousal. Other important observations included that in a proportion of arousal events (11% of apnoeas, 33% of hypopnoeas), neural drive exceeded the end-event levels earlier during the obstruction without triggering arousal. EMGdi at the end of hypopnoeas was slightly but significantly larger than at the end of apnoeas, but there were no similar differences in Poes.

Li et al investigated whether they could determine threshold epiglottic pressure values that trigger arousal in 31 OSA patients (Li et al., 2019). Like Xiao et al., they found variable levels of pressure preceding arousal within and between individuals. However, their results did show that events terminating with an arousal were associated with a more negative level of epiglottic pressure than those that occurred without arousal. There was considerable overlap in negative epiglottic pressure values between the two cases and in four subjects, events without arousal were in fact associated with more negative epiglottic pressure. To mitigate potential sleep stage effects, in a secondary analysis, events were only selected for analysis if an arousal event could be paired with a non-arousal event occurring within three minutes of each other and in the same sleep stage. Here, all subjects showed more negative nadir epiglottic pressure during arousal events than compared to non-arousal events. In the study of Li et al, arousal events were excluded if nadir epiglottic pressure occurred in the middle part of the respiratory event as opposed to immediately prior to arousal. Given Xiao et al reported this happened quite frequently, particularly with hypopnoeas, this may have introduced a potential bias and ignored physiologically important data. Consistent with previous studies, Li et al found that approximately a third of events occurred without an arousal. Respiratory events associated with arousal were generally more severe than those occurring without arousal, exhibiting a greater proportion of apnoeas compared to hypopnoeas, longer duration and a greater oxygen desaturation associated with events.

The reasons behind the different findings of Xiao et al and Li et al is not clear. Methodology

for measuring respiratory effort is challenging, and the current gold standards, Poes and EMGdi, have limitations. Changes in flow and volume are known to effect pressure values and muscle recruitment. The nature of relationships between ventilatory drive itself and oesophageal pressure, epiglottic pressure and diaphragm EMG during hypopnoea and apnoea are not well understood. Epiglottic pressure is accepted as a proxy to pleural pressure only under conditions of a collapsed airway, such that pressure at the epiglottis is approximately equal to that at the oesophagus. Worryingly, Li et al use epiglottic pressure measures in both apnoea and hypopnoea, where continued airflow will undoubtedly affect pressure values. There is no discussion of these potentially problematic effects in their paper. Consequently, the interpretation of these study findings remains difficult. It is worth noting that although negative oesophageal pressure values preceding arousal were more consistent within-subjects compared to between subjects in the original study of Gleeson et al, within-subject responses remained quite variable. Two patients in particular exhibited large pressure ranges in arousal threshold across stimuli (ranges 9-18 cmH_2O and 21-30 cmH_2O) so the work of Xiao et al. and Li et al. are not entirely contradictory to earlier findings. However, the concept of a threshold level of negative pressure that itself elicits arousal is perhaps overly simplistic and not entirely supported by the available evidence. Given known changes in arousal propensity across different stages in sleep, it appears unlikely that a single threshold value of pressure divides arousal from non-arousal events across the whole night. More likely is that a range of pressures, with some overlap, helps to explain within- and between-subject variability in arousal responses where airflow recovery with or without arousal is clearly possible, potentially influenced by positional and sleep depth effects. Whether an arousal occurs before the airway opens is likely governed by a number of mechanisms driven by underlying neural drive to upper airway dilator muscles and other reflex responses. Clearly, there are still important questions to be addressed concerning what sensory processes are primarily responsible for triggering arousal.

2.4.3 Other airway recovery mechanisms

Given airflow recovery can occur without arousal, there must be other non-arousal physiological mechanisms underlying this process. There is evidence to support that increased GG muscle activity and increased respiratory time are involved in airflow recovery (Jordan et al., 2007). However, OSA patients appear to show an impaired ability to recover ventilation without arousal compared to control subjects (Younes et al., 2012). Younes et al found that when the airway opened without arousal, the GG activation required was 10.4±9.5% GGmax compared to 5.4±4.6% GGmax when airway opening was also asso-

ciated with arousal (Younes et al., 2012). These findings suggest that relatively modest increases in upper airway dilator activity, but potentially on a background of differing arousal propensity and airway collapse severities, may largely determine whether arousal or sufficient muscle recruitment to re-open the airway occurs first.

If arousal is not necessary for airflow recovery, it may instead predispose the airway to further instability through arousal-induced hyperventilation and a corresponding subsequent decrease in chemical drive to breathe. However, available evidence does not support reduced dilator activity after events ending in arousal vs non arousal (Jordan et al., 2011), or reduced GG activity in healthy subjects following arousal both with and without prior resistive loading in the ten breaths following arousal (Cori et al., 2012; Jordan et al., 2015). Arousals have also been shown to induce hypocapnia, which is consistent with the theory that arousal could negatively affect airway and ventilatory stability by reducing ongoing drive to breathing and upper airway muscles (Cori et al., 2017), but the same study found GG activity did not fall below pre-arousal occlusion levels. This was thought to be due to a protective after-discharge response of the UA dilator muscles, maintaining activity despite reducing ventilatory drive. However, pre-arousal occlusion levels may not be the most relevant baseline for comparisons. Analysis was limited to five breaths following the return to sleep, such that the effect of hypocapnia may not yet have influenced central control of respiratory muscles due to circulatory delay of the arterial CO_2 system likely exceeding this time period. It was argued it is unlikely central drive remained unaffected in this time period as reduced nadir epiglottic pressure swing was observed over the recorded period, which was taken to be a sign of reduced neural drive. However this reduction in epiglottic pressure swings could be due to resistance changes in the UA, which were not measured. A previous study into GG activity following induced hypocapnia in stable sleep did show reduced airway dilator activity (Hudgel et al., 1987). However, this involved healthy subjects and hypocapnia induced by continuous hypoxia as opposed to an immediate response to arousal, which may mechanistically be quite different. Understanding the role of neural drive augmentation and respiratory effort in the mechanisms responsible for airflow recovery with and without arousal is clearly important.

2.4.4 Relative Pump and UA muscle recruitment

Key early studies set out to define the relationship between the chemoreceptor control of upper airway and respiratory muscle function in OSA patients. In animals, there is evidence to support that hypercapnia results in somewhat greater increases in GG recruitment relative to that of the diaphragm (Brouillette and Thach, 1980), which could be an important airway compensatory mechanism. However, studies in humans found a

linear response of GG and diaphragm EMG to both hypoxia (Önal et al., 1981) and hypercapnia (Onal et al., 1981), suggesting similar control mechanisms for both muscle groups. A further study examined diaphragm, GG and alae nasi responses to both chemical stimuli and respiratory loading (Patrick et al., 1982). The relationship between peak EMGdi and EMGgg was in most cases proportional, increasing with chemical and resistive stimuli. However, several subjects showed minimal increase in GG activity despite significant diaphragm recruitment. These findings suggest that upper airway and respiratory muscles share related drive inputs, but likely with somewhat different recruitment thresholds and subsequent sensitivities. Consequently, GG activity may be differentially suppressed by hypocapnia relative to the diaphragm. Increased respiratory muscle recruitment with inspiratory load alone could reflect stimulation of muscle spindles, negative pressure receptors in the upper airway or a conscious response to the load given that these studies were performed in healthy subjects during wake. During airway occlusion in sleep, EMGdi and EMGgg were shown to increase in parallel, and in a linear fashion with oxygen desaturation where airflow recovery did not occur until GG recruitment increased out of proportion with diaphragm. This was hypothesised to reflect a reflex mechanism, possibly from stretch receptors in the upper airway (Önal et al., 1982). Applied continuous negative airway pressure (CNAP) induces immediate increases in EMGdi and EMGgg in wake but not during sleep in healthy subjects (Aronson et al., 1989). Subsequent gradual augmentation in EMGdi and EMGgg activity corresponded with arterial oxygen desaturation, but did not appear to be sufficient to restore airway patency until arousal occurred. These data support that wake and sleep muscle responses are intrinsically different, and this may help partly explain the pathogenesis of airway collapse in OSA.

2.4.5 Effort augmentation in OSA

There is strong evidence to support that augmenting respiratory effort is a key mechanism employed to compensate for airway collapse. Mild obstruction can be counteracted by increasing effort such that peak inspiratory flow increases. It has also been shown that inspiratory time increases and expiratory time decreases with continued flow limitation, such that duty cycle increases (Jordan et al., 2007; Onal and Lopata, 1986; Younes, 2003). These mechanisms can help to increase ventilation to compensate for reduced flow, such that with mild-to-moderate flow limitation, ventilation can often remain sufficient to maintain blood gas homeostasis, without necessarily the need for augmented UA muscle recruitment or arousal. Unlike arousal, it appears that duty cycle changes are gradual and likely derive from the pattern generator response to chemoreflex stimulation of the central neural control of ventilation. However, the severity of obstruction will clearly de-

termine how effective these mechanisms are in compensating for flow limitation or total airway occlusion. These mechanisms are likely to be most effective with less severe flow limitation. In contrast, during an obstructive apnoea, where maximum inspiratory flow is zero, duty cycle changes themselves will have no effect on ventilation until the airway begins to re-open.

2.4.6 Pressure sensitive mechanisms

Even if the airflow restoration and arousal events are not causally related, it remains clear that arousal and airway reopening often occur at a similar time after obstruction, following a period of increasing respiratory drive and negative intrathoracic pressure. UA muscle activity increases intensely at this point (Younes et al., 2012). There are several mechanisms that may explain this phenomenon. Firstly, it is possible that central respiratory drive itself translates directly into sufficient upper airway dilator muscle activity to reopen the airway, such that temporal coincidence with augmenting negative inspiratory pressure reflects directly related events. Whether this occurs before or after arousal would then depend on the relative levels of drive needed to trigger arousal and/or re-open the airway, both of which are likely to be a function of sleep stage and depth. This is discussed in detail by Younes (Younes, 2008). Alternatively, it is possible that more peripheral upper airway dilator mechano-receptor responses themselves play a role in triggering arousals via reflex responses. There is strong evidence for negative pressure reflex responses in the upper airway in both wake and sleep (Eckert et al., 2007; Horner et al., 1991). Topical anaesthesia applied to the UA increases apnoea duration and maximum oesophageal pressure deflection before arousal, suggesting some mechano-receptor involvement in airway reopening (Berry et al., 1995). In addition, phasic GG activity for a given level of negative oesophageal pressure deflection decreased significantly with application of anaesthesia (Berry et al., 1997). This suggests mechanoreceptors in the UA do play a significant role in dilator recruitment in response to pressure changes. However, in both studies, a component of UA muscle activity was still observed after anaesthesia, implying a central ventilatory drive component is also important, and/or involvement by deeper sensory muscle afferents, such as from muscle spindles and potentially some Golgi tendon organs not influenced by topical anaesthesia.

2.5 Tools to measure respiratory effort

Respiratory effort is clearly integral to the pathophysiology of OSA, particularly in arousal and airway reopening mechanisms, but potentially also in determining if there is sufficient upper airway dilator muscle activity to maintain an open airway. Respiratory effort is also clearly a major feature that distinguishes obstructive from central respiratory events.

Respiratory effort can be quantified in terms of the electrical activity of the driving muscles (diaphragm, intercostal and accessory muscle EMG), expansion of the thorax and/or abdominal motion (respiratory bands) or from related pressure changes (oesophageal or epiglottic pressure). Oesophageal pressure and diaphragm EMG are regarded as gold–standard measures, as both can provide quantitative measures of inspiratory effort. However both these measures have significant limitations as neither is directly reflecting neural drive. Both are difficult to interpret as they do not have units meaningfully comparable between individuals and exhibit high inter-subject variability. As a result, values are often quoted relative to those during wake, a period of stable sleep or expressed as a percentage of maximal inspiratory effort manoeuvres, with no consensus as to the most meaningful approach. Anatomical factors and flow/volume changes are known to alter values, and signal processing challenges mean analysis is generally limited to peak inspiratory values, which are not necessarily representative of overall inspiratory effort where changes in breathing timing are also important.

2.5.1 Oesophageal pressure

Oesophageal pressure gives a reliable estimate of pleural pressure changes generated by muscle force expanding the thoracic cavity (Flemale et al., 1988). According to American Academy of Sleep Medicine (AASM) guidelines, oesophageal pressure is the reference standard for respiratory effort measurement (Berry et al., 2012) for use in detecting central events, Cheyne-Stokes breathing and respiratory effort-related arousals (RERAs). However, oesophageal pressure is rarely recorded in standard diagnostic polysomnography due to its invasive nature. Some small changes in sleep architecture have been found with oesophageal pressure manometry, but these are relatively minimal (Chervin and Aldrich, 1997), with little to no reduction in sleep efficiency (Hutter et al., 2004; Skatvedt et al., 1996) and no change in arousal index (Chervin and Aldrich, 1997; Hutter et al., 2004; Skatvedt et al., 1996; Skiba et al., 2015). Furthermore, no systematic differences in AHI have been observed with versus without an oesophageal catheter (Hutter et al., 2004; Skatvedt et al., 1996; Skiba et al., 2015). Oesophageal pressure changes can be monitored by air-filled oesophageal balloon catheters, fluid-filled catheters or catheter-tip pressure

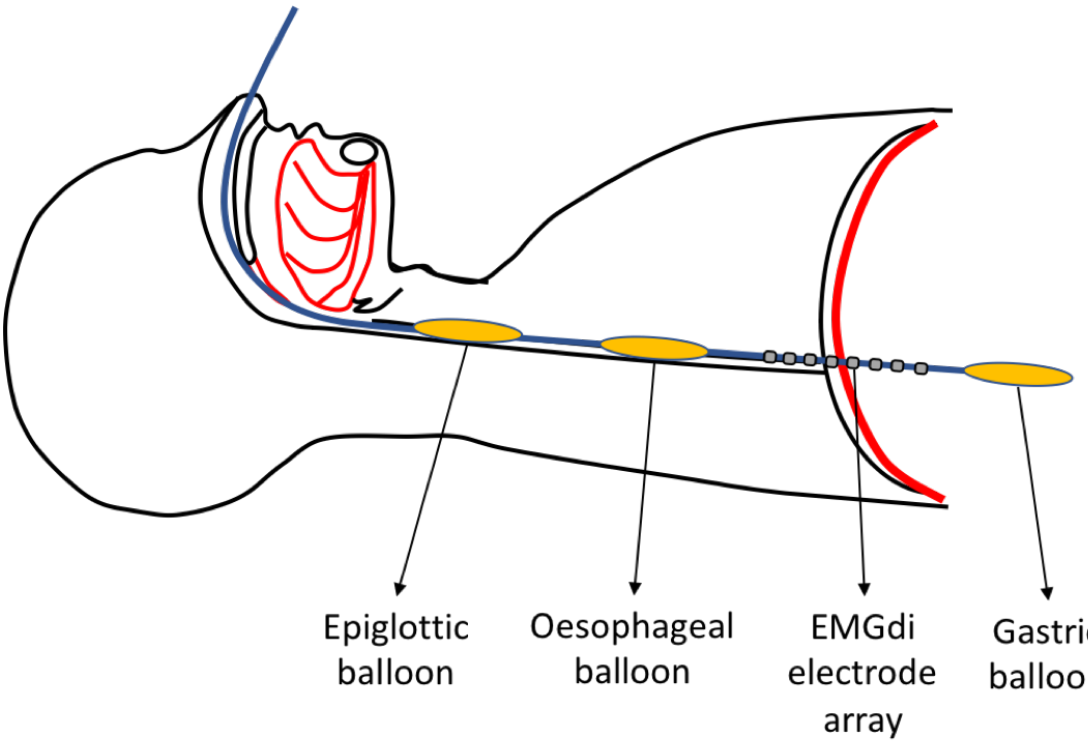

Figure 2.3: Schematic showing measurement locations for epiglottic, oesophageal and gastric balloon catheters and multi-electrode array diaphragm EMG.

transducer systems (German and Vaughn, 1996). Recording oesophageal pressure by both air- and liquid- filled catheters follows similar protocol, details of which can be found in a review by Kushida et al. (2002). Catheter-tip pressure transducer systems are more expensive, and less commonly used in sleep research or diagnostics. Whilst absolute values of Poes can be influenced by catheter position, mode of measurement, posture, lung volume and respiratory mechanics, changes in pressure associated with ventilation are likely to remain relatively immune to these effects.

2.5.2 Epiglottic Pressure

Airway pressure changes at the level of the epiglottis can also be measured as a marker of respiratory effort. During occlusion, these values correspond closely to pleural and oesophageal pressure. This technique is most commonly used in a research setting, and can also be used to provide a measure of upper airway resistance. In a study comparing a physiology sleep study with epiglottic catheters to standard polysomnography, there was no effect on sleep quality, arousal index or the apnoea-hypopnoea index, though there were some small effects on sleep stage distribution towards lighter sleep (Carter et al., 2018).

Epiglottic manometry is often used to define key non-anatomical traits for phenotyping studies, including measures of upper airway collapsibility (Pcrit) and the arousal threshold (nadir pressure on the breath prior to arousal) (Eckert, 2018). Epiglottic pressure is more affected by changes in upper airway resistance than oesophageal pressure, so is less often used as a continuous marker of respiratory effort.

2.5.3 Diaphragm electromyography

Diaphragm electromyography (EMGdi) provides a measure of the electrical activity of the primary inspiratory muscle. EMGdi can be recorded from surface electrodes positioned in the right anterior axillary line in the seventh and eighth intercostal space, though such measures are prone to significant artefacts from intercostal muscles, cardiac activity, underlying diaphragm movement and positional effects. Calibration towards meaningful inter-subject comparisons of EMGdi activity are inherently difficult, and typically restricted to expression as a percentage of either maximal inspiratory manoeuvre, usually a Mueller manoeuvre, or baseline activity. Increased thoraco-abdominal adiposity with obesity can also make obtaining meaningful EMGdi recordings difficult. A study comparing oesophageal pressure to surface EMGdi found that EMGdi could usefully help to distinguish central from obstructive events, but only recommended clinical use when oesophageal pressure was not available (Stoohs et al., 2005).

Intra-oesophageal EMGdi monitoring via a catheter provides a more robust measure of diaphragm muscle activity. Single pair electrode recordings can be subject to positional changes so more commonly multi-pair electrodes spanning the diaphragm are used along with analysis protocols that focus on the electrode pair showing the largest signal for each breath (Luo et al., 2008). Direct intramuscular recordings are also possible (e.g. (De Troyer et al., 1997; McKenzie et al., 2009)), and provide very high quality signals largely immune to most artefacts except ECG. However, these studies carry a pneumothorax risk so are used only in highly specialised research contexts .

2.5.4 Non-invasive effort measures

For clinical use, non-invasive measures of respiratory effort are substantially more practical than catheter manometry in routine sleep studies. Non-invasive alternatives include respiratory inductance plethysmography (RIP), pulse transit time, snore analysis, jaw movement analysis, suprasternal pressure monitoring and forehead venous pressure. These methods were recently reviewed by Vandenbussche et al. (2015). However, few of these

methods have been adequately tested and validated against oesophageal pressure monitoring to support routine use. Most studies have focused on RIP, which is currently used clinically to assess respiratory effort non-invasively. Bands with embedded inductance sensors are placed around the thorax and abdomen, and changes in the cross-sectional area of these anatomical regions stretch the band and alter the impedance across the sensors. These signals, when summated with appropriate calibration factors derived using short-term pneumotachograph based tidal volume measurements or fixed bag volume breathing manoeuvres, can be used to estimate tidal volume and ventilation with moderate precision, although RIP calibration factors are sensitive to body movements. Much more commonly RIP signals remain uncalibrated and simply used as qualitative respiratory signals of thoraco-abdominal motion. Currently, RIP is recommended by the AASM for qualitatively monitoring respiratory effort during clinical polysomnography (Berry et al., 2012). RIP is very useful for distinguishing between central and obstructive events, and detecting increased effort. However, RIP only measures volume expansion at two levels, rather than pressure changes or muscle activity, so remain only an indirect marker of muscle force. Furthermore, these signals can change considerably with a change in band position, and calibration remains technically quite difficult in a clinical setting. RIP bands have not been validated to assess a quantitative measure of the degree of inspiratory effort as can be obtained from Poes or EMGdi. Thus, currently there are no non-invasive measures that have been validated for such purposes.

2.5.5 Ongoing challenges

Despite the in-depth physiological insight that measures of respiratory effort like oesophageal pressure and diaphragm EMG can provide, important technical and practical limitations have limited their widespread use. Both signals are highly susceptible to cardiogenic artefact distortion, because of the close proximity of the heart and high power of electrical and pressure signals it produces. Physiological and recording (e.g. catheter placement, intervening tissue properties) differences between individuals and arbitrary units of measurement makes interpretation and direct comparison of values between individuals very challenging. The inter-relationships between augmented respiratory drive itself, induced negative pressure and control mechanisms in OSA are not yet clear. More research is needed to better understand the respiratory and pathophysiological mechanism related information content of these signals, and what they could reveal about variable phenotypes in OSA, mechanisms of airway collapse and arousal and possible novel therapeutic targets designed around a greater understanding of pathogenic mechanisms.

2.6 Summary

In OSA, airway collapse occurring during sleep appears to reflect complex interactions between an abrupt loss of wake inputs to upper airway and respiratory muscles, an anatomically vulnerable airway, compensatory mechanisms including ventilatory and upper airway dilator muscle recruitment and arousal, and respiratory control factors. Arousal is often associated with airflow recovery but is clearly not always essential for airway opening as airway recovery can occur without and frequently precedes arousal. Other compensatory mechanisms must therefore be vital to this process. These are likely to include negative airway and intra-thoracic pressure mediated compensatory mechanisms, chemoreflex responses and underlying co-ordinated neural drive changes to muscles involved in breathing. A greater understanding of the relationship between underlying neural drive to breathe and negative pressure remains an important research target to better understand the complex pathophysiological mechanisms underpinning OSA.

Chapter 3

Developing reliable filtering methodologies to improve quality of oesophageal pressure and diaphragm EMG signals

Respiratory effort is currently best assessed either from oesophageal pressure (Poes) or diaphragm electromyography (EMGdi) signals recorded using custom intra-oesophageal catheters. However, due to the close proximity of the heart to the positioned catheter, both signals are highly susceptible to cardiogenic noise which is high in power and substantially overlaps the frequency ranges relevant to respiratory activity. Therefore, extracting useful respiratory information from these noisy signals remains a significant analysis challenge. Physiological responses of interest during upper airway obstruction and recovery in OSA include short latency reflexes, therefore tools must preserve such details with minimal signal loss. In this chapter, existing cardiogenic artefact filtering methods for Poes and EMGdi described in the literature are reviewed and refined for use on OSA signals, and a methodology is proposed for use in future studies.

This aligns with Aim 1 of the thesis: To develop new filtering techniques required for reliable short time scale analysis and model fitting for physiological analysis of oesophageal pressure and diaphragm EMG signals.

3.1 Oesophageal Pressure

3.1.1 Introduction

Pressure swings in the oesophagus, as measured by an oesophageal balloon, are accepted as a reliable surrogate for pleural pressure changes in respiratory medicine (Baydur et al., 1982; Dechman et al., 1992; Gillespie et al., 1973). Poes has been used to estimate the mechanics of the lung and chest wall (Guerin et al., 1993) and to estimate clinically important variables such as work of breathing (WOB) and dynamic intrinsic positive end expiratory pressure (PEEPi) (Akoumianaki et al., 2014; Gottfried et al., 1986). In sleep, strong evidence supports that pleural pressure changes are key to major mechanisms of OSA pathogenesis, providing a direct marker of dynamic changes in underlying central respiratory drive and pharyngeal collapsing pressures. This includes the observation respiratory-related arousal is now understood to occur around a threshold level of negative oesophageal pressure swings associated with augmented breathing effort, independent of the respiratory stimulus (Gleeson et al., 1990). In addition, to re-establish patency following partial or complete airway collapse requires substantial upper airway dilator muscle recruitment, where the only two known non-arousal pathways are through increasing chemical drive to breath and through negative airway pressure related mechano-reflexes (Younes, 2003). Thus, oesophageal pressure swings provide one of the most important direct markers of the two non-arousal stimuli needed for pharyngeal muscle recruitment,

and the respiratory related arousal threshold during sleep. Therefore, accurate measures of the respiratory component of oesophageal pressure are important and could provide great insight into the fundamental pathophysiology of OSA.

To measure oesophageal pressure, typically a 5-10 cm long thin-walled latex balloon catheter is inserted nasally and positioned in the mid-thoracic region of the oesophagus. This is fully deflated, then inflated with a minimal volume of air (typically 0.5-1 ml) to ensure that catheter pressure changes faithfully reflect intrathoracic pressure changes, indicative of pleural pressure changes, over the flat portion of the balloon pressure-volume curve. However, the close proximity of the oesophageal balloon to the heart means that the pressure signal is often contaminated by cardiogenic oscillations. Careful placement of the oesophageal catheter can reduce the relative size of these oscillations but not remove them entirely, and residual artefact can still alter the respiratory signal of interest (Schuessler et al., 1998). This degrades the fits of the models of respiratory mechanics and can distort values of PEEPi, WOB and peak inspiratory negative pressure swings from baseline, which is often used as a measure of inspiratory effort. As a result, reliable analysis of Poes requires prior filtering to remove cardiogenic artefact and to isolate the respiratory component. This is not trivial due to the close frequency ranges of the heart rate (0.8-2.5Hz) and respiratory rate (0.17-0.67Hz) (Cheng et al., 2001). While the fundamental respiratory frequency is below cardiac frequency, spectral densities of the two signals substantially overlap, meaning simple filtering techniques with frequency based cut-offs (e.g. low pass filter) will also distort the respiratory component (Cheng et al., 1999). In addition, it is known that upper airway dilator muscles can produce short latency reflex responses to induced negative pressure drops (Eckert et al., 2007), so accurate measures of abrupt pressure changes are likely important. This means moving average based filtering techniques with a large degree of smoothing are also not appropriate. Accurate identification of start and end times of active inspiratory effort are also vital for analysis of duty cycle and effort augmentation, and therefore preserving the sharp initial deflection points in the oesophageal pressure signal, reflecting the onset of inspiratory muscle recruitment, is important. As a result, a filtering solution must account for these requirements.

Theory

An oesophageal pressure signal can be thought of as composed of two independent components, a cardiac (Pcardiac) and a respiratory (Presp) pressure term, such that

$$P_{oes} = P_{cardiac} + P_{resp} \tag{3.1}$$

In biomedical signal processing, separating unknown components from a noisy signal is a

recurring problem due to the number of physiological processes that occur in close proximity. Differences between subjects can make signals difficult to predict, although using additional physiological data can aid filtering methods. The electrocardiogram (ECG) signal is a relatively stable signal strongly dominated by cardiac power with a distinctive QRS complex that can be readily identified through peak detection algorithms. Generally, ECG noise is low compared to signal power, and can be minimised with a band pass filter such that the ECG can be used to provide reliable R-wave detection for timing information relevant to the heart rhythm and thus cardiogenic artefact in Poes.

Literature Review

Adaptive filtering has been proposed as a suitable method for similar biological filtering problems where noise and signal spectra overlap. It uses a reference signal thought be a close approximation to either the desired signal or the noise component, and an algorithm such as least mean squares (LMS) to continuously adapt filter weights to output a close fit to the desired input signal. For oesophageal pressure artefact removal, it is challenging to record directly a less contaminated respiratory or cardiac pressure signal non-invasively to use as a reference signal. Instead, an adaptive filter requires another channel derived from other physiologic signals. There are several possibilities in this regard. Schuessler and Bates proposed a custom adaptive filter designed to remove these unwanted cardiogenic oscillations with algorithmic determination of a Pcardiac signal (here after referred to as the Schuessler-Bates method) (Schuessler et al., 1998). Their complex model used cross-correlation to recursively estimate a response function that relates cardiogenic pressure to an impulse function derived from ECG R-wave intervals. Theoretically, their method required computationally expensive deconvolution to estimate a transfer function to calculate cardiogenic pressure from oesophageal input. However, they made the assumption that, with a sufficiently short delay between a cardiac event and its appearance in Poes, this response corresponds to the Poes segment during the R-R time interval between peaks of the QRS complex in ECG. Pcardiac is estimated recursively by averaging these segments using a forgetting factor based on the heart rate and respiratory rate to change the memory depending on the estimated variation in the signal. Pcardiac is then subtracted from oesophageal pressure to obtain an estimated respiratory pressure signal. This method allows for recursive adaptation of input waveform changes over time. However, short latency heart rate variability is not well accounted for in a recursive ensemble-averaged scheme.

There have been several proposed modifications to the Schuessler-Bates method. Cheng et al proposed two methods for filtering oesophageal pressure; an adaptive finite impulse response (AFIR) filter, and a modified adaptive noise cancellation (MANC) method with

an airflow reference signal (Cheng et al., 2001). The MANC method was also based on an LMS adaptive algorithm, which is advantageous because it is simple and computationally efficient. Cheng et al found MANC to be more successful at eliminating cardiac noise than AFIR methods, particularly when there was any overlap between cardiac and respiratory frequency or their harmonics (Cheng et al., 2001). Results showed reduced power at heart rate frequencies in the fast Fourier transform of filtered signals, and improved fits of airway resistance. However, MANC uses the airflow trace as the reference respiratory input signal. This is a key limitation to the method, likely to be problematic in the context of mechanical ventilation or airway obstruction in OSA, where oesophageal pressure swings will not translate directly to airflow at the mask. Therefore, for this application, such a reference signal was not considered to be appropriate.

Seppa et al adapted the Schuessler-Bates method for impedance pneumography and replaced the recursive averaged cardiogenic waveform with a lung-volume dependent parametric model, separating waveforms into four lung-volume dependent bins (Seppä et al., 2011). Their method did not include any template adaptation over time, and they acknowledged that including this step would be slower and more computationally demanding than in the original Schussler-Bates method due to the need to adapt each of the four cardiac templates individually. If such adaptation is required, they recognised the original Schussler-Bates method may be advantageous. Lung volume information is required for this scheme, but absolute lung volume is not easily measured from sleep recordings. Relative volume can be calculated from the integrated flow signal, but mask leak, as well as configurational changes and total lung volume changes, during obstruction are difficult to track over the course of the night meaning this step was not considered to be useful for the applications in this thesis.

Other methods of filtering oesophageal pressure include template subtraction via multiple regression and scaling. Graßhoff et al proposed a block-wise non-recursive template subtraction method of removing cardiogenic artefact from oesophageal pressure (Graßhoff et al., n.d.). Waveforms were normalised in length with R-R interval before ensemble averaging over a specified number of waveforms to create a template. Any slope was then removed from the template by linear interpolation de-trending from end points. Preliminary tests on short (30sec) segments showed consistent waveform shape, and template subtraction reduced power at heart rate frequency in the Fourier transform. The authors hypothesised this method is superior to the Schuessler-Bates method due to the waveform time scaling being able to better account for heart rate variability in template averaging, and its block-wise structure, equally weighting waveforms from a buffer period as opposed to favouring more recent templates with a recursive forgetting factor. However, no comparison of results were available from the two methods or discussion of the application

of either to longer periods of data, where greater variability in cardiac waveforms may become more problematic.

Filter Design Specification

The studies discussed above have all focussed on application of oesophageal pressure filtering to respiratory mechanics in critical care. The purpose of the work in this thesis is to better understand continuous respiratory effort from pleural pressure swings in sleep, meaning there are several important additional considerations to those outlined above. Data analysis for whole night sleep recordings require a much longer timeframe than considered in previous studies. Dynamic changes in both respiratory effort and its translation into airflow are known to occur over both long and short time-scales across sleep stages and partial or complete airway obstruction events, so the ability for an algorithm to adapt and account for these effects is particularly important. OSA can induce alternating sequences of bradycardia and tachycardia in response to ventilation changes (Penzel et al., 2003). Arousals are very common in OSA and are associated with increased sympathetic neural activity and accelerated heart rate (Azarbarzin et al., 2014), which will likely alter cardiogenic artefact. Any positional changes during sleep could also affect relative pleural and cardiac pressure swings. Unlike applications in mechanical ventilation, patients are all spontaneously breathing and hence prone to swallows and other artefacts in Poes that could impair algorithm performance, particularly of adaptive algorithms, if not carefully monitored for and excluded. Another requirement for this project was that filtering methods should be suitable for future application in real time (or near to real time) scenarios. As part of the wider project scope, it was important that tools developed could be adapted for this purpose. This requirement could be met by either adaptive filters or template subtraction as they can run with only a short delay time.

In light of previous literature, three solutions to this problem were investigated:

1. A cardiogenic waveform ensemble-averaged template subtraction method.
2. An adaptive filter based on an LMS-algorithm using the cardiogenic waveform ensemble-averaged template as a reference signal.
3. An adaptive filter based on an LMS-algorithm using the ECG as a reference signal Each method is presented below and compared in the following section.

Each filter will be developed and tested on samples of oesophageal pressure patient data. The challenge in developing and implement a methodology to adequately remove cardio-

genic oscillations is that the precise interaction between cardiogenic and respiratory is complex (it is common to assume interdependence but in reality, both thoracic pressure changes due to respiration will influence the cardiogenic waveform and vice versa). Therefore, filtering aims to separate two unknown physiological signals, which is not readily simulated for testing. Instead, filter performance is assessed by comparing power spectra signal output of real data to determine how much of the power over the cardiac frequency and respiratory frequency bands remain after filtering with each method. There is no 'gold standard' respiratory drive signal to validate the cleaned oesophageal pressure against, so instead, we propose fitting the filtered data to the respiratory equation of motion (Campbell, 1958). It is expected that successfully removing cardiogenic oscillations will improve data fit to this linear model of respiratory motion. This provides an objective criteria by which to compare the performance of the three filtering methods. Schuessler et al use a similar model validation method in their study (Schuessler et al., 1998). The results will determine which filter is most appropriate for further use in this thesis.

3.1.2 Methods

Cardiogenic Template Method

A low pass filter with cut-off frequency of 0.6 times the heart rate frequency was applied to Poes to isolate respiratory components below the heart rate frequency, accounting for known heart rate variability in sleep (Bonnet and Arand, 1997). This respiratory baseline was subtracted from the original Poes signal. The ECG signal was pre-processed with a band pass filter 0.5-40Hz and R-waves were identified using peak detection at 1.7 times the rms value of the ECG signal (Schuessler et al., 1998). The R-wave timing was used to separate individual cardiac pressure waveforms from the filtered Poes signal. These waveforms were normalised in length using interpolation and any slope between start and end points was removed. Then, artefacts were ensemble averaged to create a template for continuous updating over the course of the night using a fixed length buffer (here set at 120 waveforms) as shown in Figure 3.1.

To apply template subtraction across a night of sleep, it was important to consider how much the cardiogenic pressure waveform might change over time and how long a buffer for the averaged waveform would be required. Figure 3.2 shows ensemble average waveforms from 60 second windows taken every 30 minutes across a full-night (around 8 hours) of sleep recording from one example patient. There is some variation in amplitude, but this appeared to fluctuate randomly across the periods measured with no overall temporal trend. Generally, waveform and features remained largely consistent over time. Therefore,

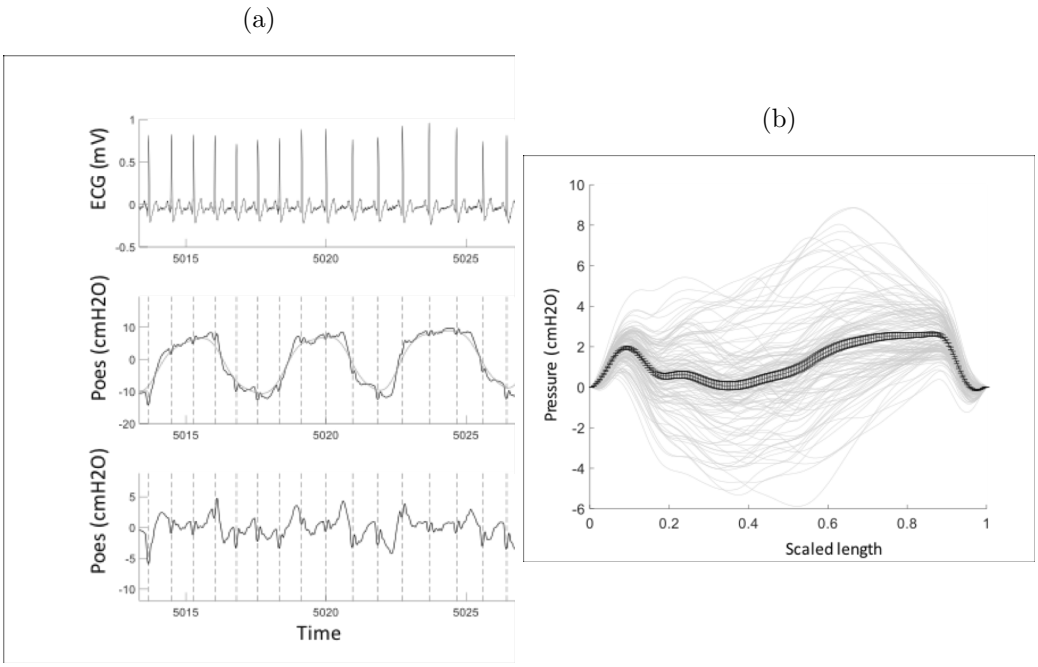

Figure 3.1: a) ECG is used to define HR intervals (marked by dotted lines on Poes plots). Unfiltered Poes (black line) and the low pass filter output respiratory baseline (grey line) are shown in the second figure. Individual artefact waveforms are extracted from the Poes signal with the respiratory baseline subtracted, as shown in the third plot. b) Artefacts are normalised in time then ensemble averaged to produce a template waveform. For the length of the template buffer (120 waveforms), each individual artefact waveform is plotted (grey) as well as the ensemble average (black)

it was felt best to ensure the template updated as a moving average from a defined buffer length, normalising the length of each artefact to account for heart rate changes as they occur.

Given previous studies did not report the optimised artefact buffer length to produce a cardiac pressure template, the method required determination of a reasonable choice of window to apply for block averaging templates for oesophageal pressure. During sleep in OSA, artefacts like swallows are relatively common and often result in extreme pressure values and signal clipping which would significantly distort ensemble averages of the artefact waveform. A minimum threshold of variance was used to remove intervals containing clipped artefacts, where the signal flatlined. Amplitude thresholds were also implemented to exclude regions of extreme values. To help guide an appropriate choice of window length for the template average, tests were performed to investigate the standard deviation (SD) over the ensemble averaged waveform with different numbers of artefacts in the buffer. After around 100 waveforms, the mean SD stabilised, and further increases in the artefact buffer length did not change the standard deviation over the averaged template. Informed by this, a window length of 100 artefacts was selected for ensemble averaging. The template was stretched to fit each HR interval then subtracted from the original signal. Baseline removal ensures overlap between individual templates is smooth with no discontinuities in the signal.

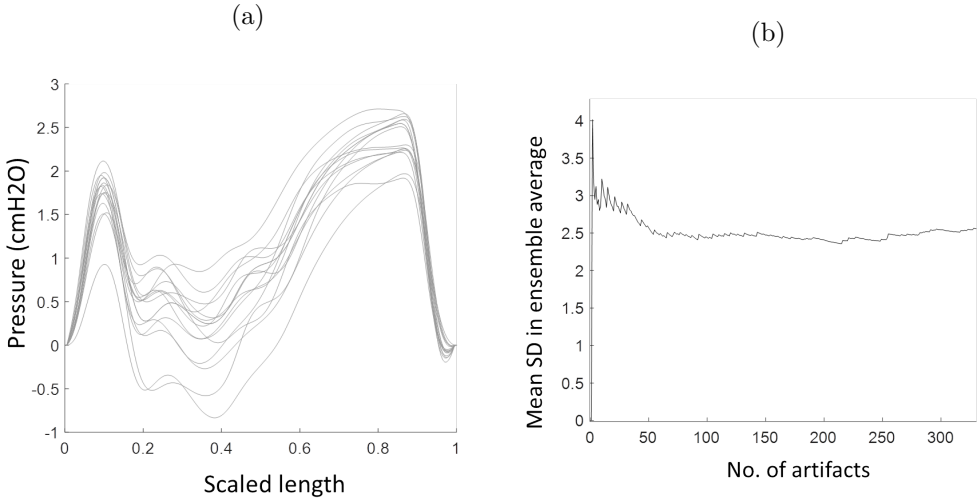

Figure 3.2: a) Template changes over the course of the night. Ensemble averages of artefacts from a 60 second window were calculated every 30 minutes across the data set. The timing and shape of the main waveform features remain relatively consistent over time, but with some changes in amplitude. b) Mean standard deviation for ensemble average as a function of the number of individual artefacts used to create the template.

Adaptive Filter Method

Any adaptive noise cancellation (ANC) algorithm requires two main inputs. The primary input d is composed of the original signal s and an additional noise source z so that $d = s + z$. The second input is a reference noise signal x which is correlated with the noise from the primary input but uncorrelated with the original signal. The reference noise signal x passes through an adaptive filter to produce an output y designed to match to the noise in the original signal z by minimising the error term, $e = d - y$, the difference between the primary input and the estimated noise signal (Widrow et al., 1975).

The LMS algorithm is proposed as the adaptation method, which minimises a weighted linear least squares cost function. Here, the original signal is the raw Poes, composed of a desired respiratory signal and cardiogenic noise. The two reference noise sources proposed are the ECG signal directly, or the cardiogenic template derived noise signal as described in the previous section. The two schemes are shown in Figure 3.3. Examples of signal inputs for the noise source channel of the two schemes are shown in Figure 3.4.

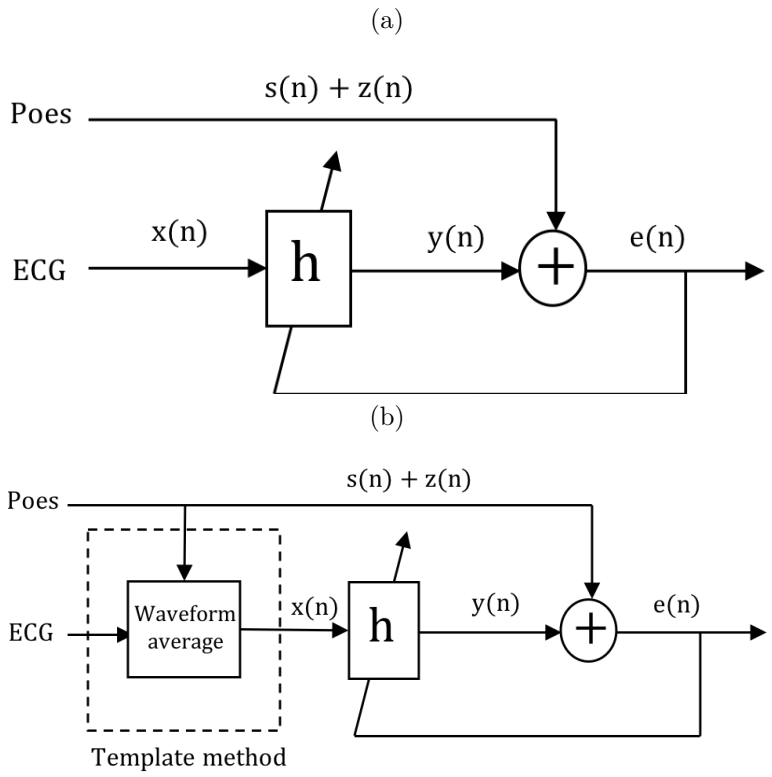

Figure 3.3: Block diagram of adaptive noise cancellation using reference signal of either a) ECG or b) cardiogenic waveform signal created using the template method above.

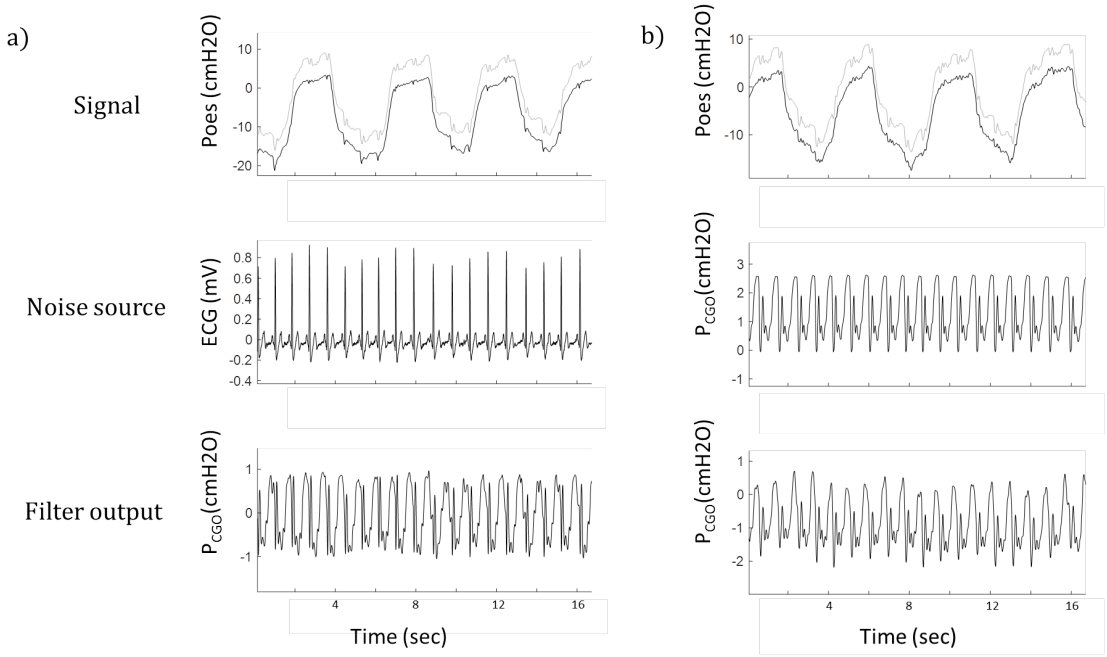

Figure 3.4: Example ANC signal input and output for the two methods. a) ECG based noise source ANC filter. b) cardiogenic pressure template based noise source ANC filter. Raw Poes signal (grey) and filtered Poes (black) are shown on top plots. The noise input to LMS adaptive noise canceller and output are shown below for each method.

Adaptive Filter Parameters

The adaptive filter parameters include filter length n, which is the number of weighting coefficients, w_n, and step size μ, which governs how much filter coefficients can change in each iteration.

Filter length is the number of samples analysed at one time. To account for any residual respiratory changes in the cardiogenic artefact, a minimum filter length was proposed by Cheng et al that depends on the frequency of the respiratory signal and the sample rate (Cheng et al., 2001). This can be calculated by the equation

$$L = \frac{1}{2}\frac{T_{max}}{T_s} \tag{3.2}$$

where Tmax is the maximum period of the signal and Ts the time interval between samples. For oesophageal pressure signals, Tmax is approximately 5 s, the usual maximum length of a respiratory cycle, and Ts is 0.005 s for a sample frequency of 200 Hz. Therefore, filter length was set at 500.

In developing an LMS algorithm, selection of μ is important because it determines whether convergence occurs. As μ gets increasingly large, filter weights will oscillate with large variance about optimal conditions and may diverge. If μ is too small, convergence will be very slow and filtering results deteriorate. The choice of μ is difficult and highly dependent on the power of the input signal. In practice, μ is chosen through trial and error, somewhat limiting the practical application and reproducibility of this approach. In trials during filter development, it was found that a choice of $\mu = 1x10^{-6}$ appeared to most reliably achieve convergence and optimal filtering for oesophageal pressure sampled at 200 Hz. This reflected a balance between enabling timely convergence and maintaining stability in the presence of artefacts, which would distort the filter coefficients if μ was too large.

3.1.3 Results

Patients and Data

The three filtering methods were tested on pre-recorded data from eight patients with moderate-to-severe sleep apnoea (body mass index (BMI) 30-40 kg/m^2, apnoea-hypopnoea index (AHI) $>$ 30 events/h). Flow and volume were recorded via a nasal mask and pneumotachograph. Poes was measured using a custom catheter with a 5-cm latex balloon. All analysis was performed in MATLAB (The MathWorks, Natick, 2017). Filters were

applied to whole night data recording. Results were tested on 10 minute stable data segments and the waveforms and power spectra of signals pre- and post- filtering from each of the three methods discussed are illustrated in Figure 3.5.

Filter Performance

Visual inspection shows a clear reduction in the cardiac component of the Poes signal at the HR frequency using all methods. This is confirmed in the power spectra which show reduced power in the band ±10% about the cardiac frequency. There is some frequency spread in the cardiac frequency, but this is expected given recordings are across sleep disordered breathing, where there are known changes in heart rate associated with obstructive events (Bonnet and Arand, 1997; Penzel et al., 2003).

Examples of the output from each filter is given in Figure 3.6 relative to the unfiltered oesophageal pressure for comparison. Additional smoothing could be applied prior to analysis. These segments show an example where filtering is successful, an example where filters respond to an unusual respiratory event and an example where cardiogenic power is reduced, but there is still some underlying noise. The results from the ECG-based ANC filter show signs of distortion, particularly when cardiogenic noise is strong.

Model Fitting

In order to test the physiological application of the proposed filter approaches, both filtered and unfiltered Poes were fit to the linear respiratory equation of motion to derive values of airway resistance and elastance:

$$P = E.V + R.\dot{V} \tag{3.3}$$

where P is the pressure applied across the respiratory system, V is the volume and $\dot{V}$ is the flow at any point in time and R and E are the resistance and elastance of the respiratory system. This well-established classic respiratory mechanics model is known to provide good fits to experimental data (Mead and Agostoni, 1964). If filtering successfully reduces cardiogenic noise, then respiratory model fits should improve. This also provides a quantitative and objective measure to assess which of the three filtering methodologies performs best.

Oesophageal pressure and pneumotachograph flow data from eight subjects recorded dur-

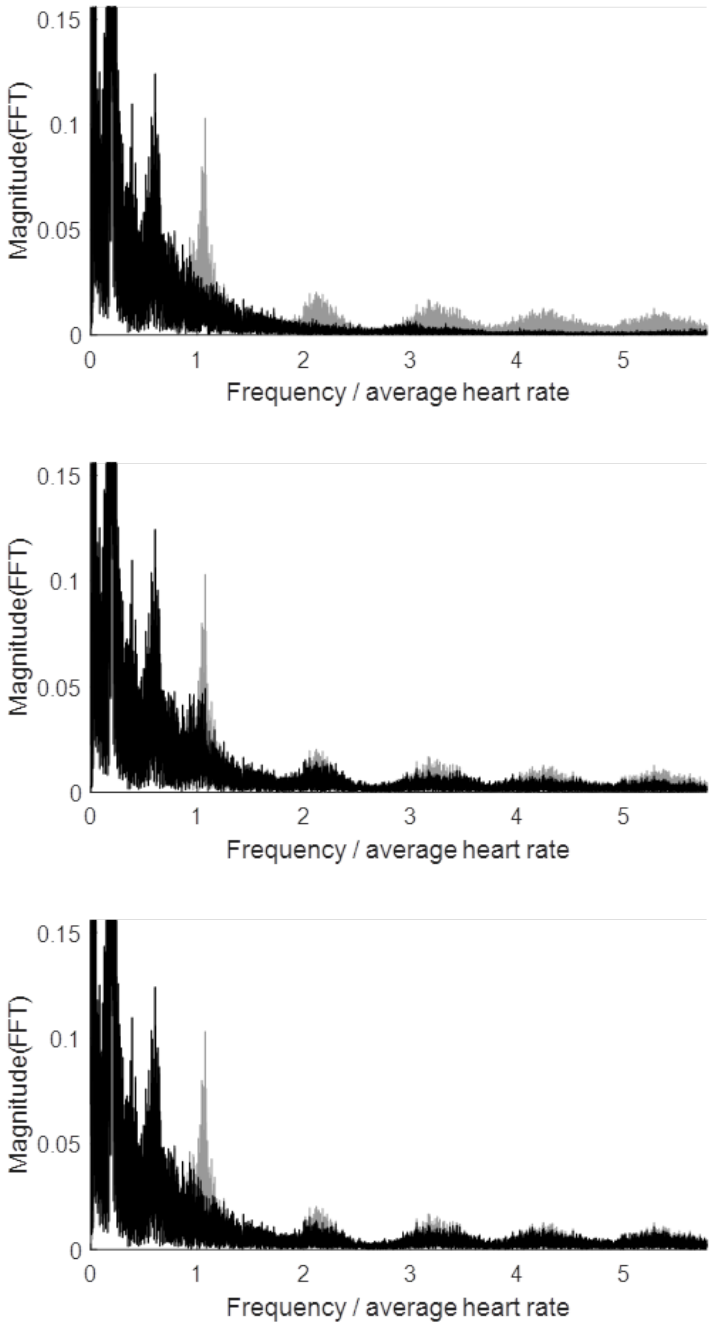

Figure 3.5: The three frequency spectra are given, for unfiltered (grey line) and filtered Poes (black line) by template subtraction (top spectrum), middle figure adaptive filter with ECG input (middle spectrum) and adaptive filter with template input (bottom spectrum)

(a)

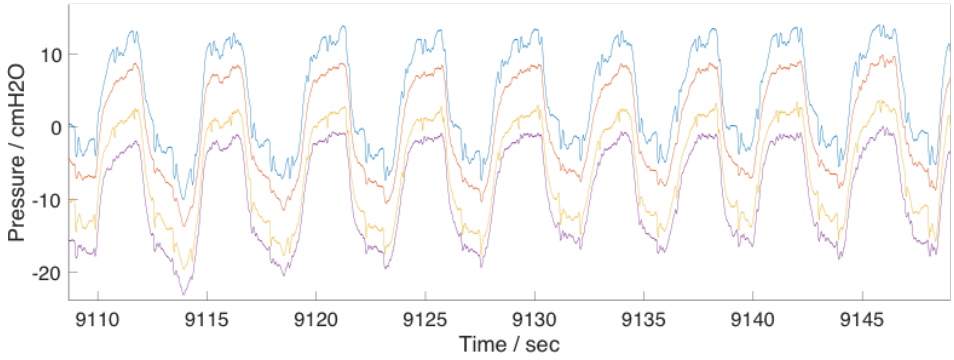

(b)

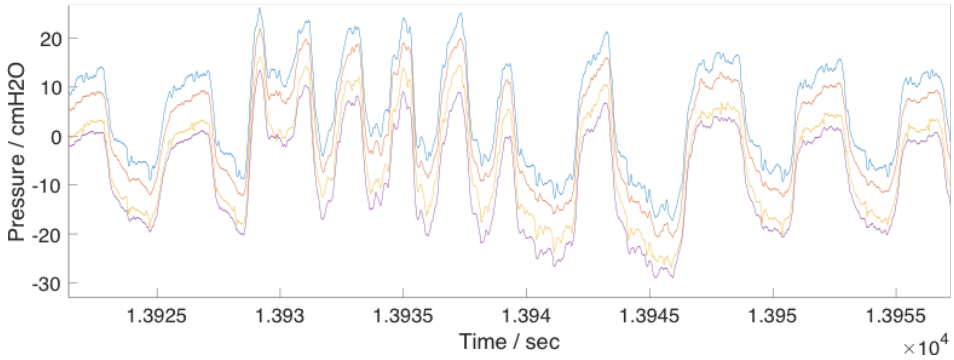

(c)

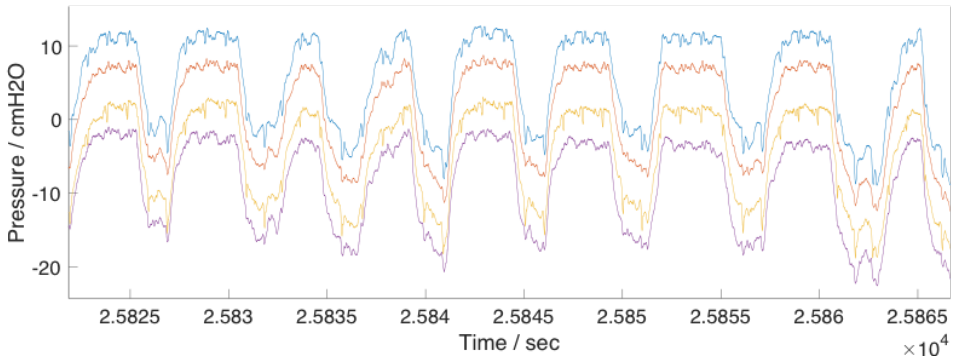

Figure 3.6: Examples of results from the three different filtering methods. Unfiltered Poes (blue line) is plotted along side the filtered signal from Template Subtraction (red line), ANC with ECG input (yellow line) and ANC with template based input (purple line). Pressure signals have been offset by 3 cmH_2O. a) Filters work well under normal conditions b) Unusual respiratory behaviour does not significantly distort filter output c) An example where filtering is less successful and some residual noise remains.

Table 3.1: Elastance, resistance and goodness of fit obtained from the respiratory equation of motion for oesophageal pressure signals filtered by each of the three methodologies (Template subtraction, ANC with ECG input, ANC with template based input). Values are shown as mean ± SD

Study	No. Breaths	Unfiltered Poes			Template Subtraction			ANC with ECG input			ANC with Template input		
		E (cmH2O/l/s)	R (cmH2O/l/s2)	r^2	E (cmH2O/l/s)	R (cmH2O/l/s2)	r^2	E (cmH2O/l/s)	R (cmH2O/l/s2)	r^2	E (cmH2O/l/s)	R (cmH2O/l/s2)	r^2
1	100	-13±29.3	-30.8±14.9	0.94±0.05	-12.6±27.9	-30.6±15	0.96±0.04	-12.58±28.29	-30.58±14.82	0.95±0.04	-12.65±27.55	-30.56±14.88	0.96±0.05
2	100	-15.1±13.1	-14±9	0.75±0.1	-15.5±13.3	-14.8±8.9	0.89±0.07	-15.13±12.91	-14.18±8.82	0.8±0.09	-15.13±12.91	-14.18±8.82	0.8±0.09
3	100	-5.4±0.7	-6.1±1	0.94±0.03	-5.4±0.6	-6.1±0.8	0.98±0.02	-5.77±0.87	-5.97±0.87	0.97±0.02	-5.41±0.56	-6.1±0.74	0.98±0.02
4	100	-14.3±9.7	-9.7±7.1	0.89±0.07	-14.1±9.9	-10.2±6.5	0.93±0.05	-14.06±10.08	-10.36±6.41	0.88±0.09	-13.71±10.03	-10.56±6.51	0.93±0.05
5	100	-15.9±2.7	-10.3±2.2	0.93±0.02	-15.9±2.7	-10.5±1.7	0.97±0.01	-15.46±2.7	-9.98±1.11	0.99±0.01	-15.89±2.7	-10.57±1.19	0.99±0.01
6	100	-5.9±3.9	-6.4±2.2	0.81±0.09	-5.9±3.9	-6.4±2.2	0.95±0.06	-20.24±57.43	3.85±27.02	0.76±0.14	-5.34±4	-6.46±2.32	0.92±0.05
7	100	-10.2±17.3	-19.1±8.6	0.92±0.07	-10.2±17.3	-19.2±8.7	0.91±0.07	-10.21±17.28	-19.03±8.49	0.93±0.06	-9.54±16.94	-19.41±8.45	0.93±0.06
8	100	-6.7±1.1	-21.5±3.5	0.81±0.05	-6.6±0.8	-21.4±2.7	0.96±0.02	-6.49±0.77	-21.26±2.68	0.94±0.03	-5.2±0.72	-21.67±2.68	0.94±0.02
Group	100	-10.8±9.7	-14.8±6.1	0.87±0.06	-10.8±9.5	-14.9±5.8	0.94±0.04	-12.49±16.29	-13.44±8.78	0.9±0.06	-10.36±9.43	-14.94±5.7	0.93±0.04

ing an overnight sleep study were examined. In order to test model fits on data from periods of stable breathing with an open airway, a five minute period of stable breathing was selected, and 100 breaths were identified for each subject that met a minimum criterion of at least 75% of the mean minute ventilation measured at baseline. Linear regression was used to fit pressure, flow and flow derived volume to Equation 3.3 for filtered and unfiltered oesophageal pressure, to determine constants E and R on a breath-by-breath basis. Goodness of fit was assessed for each breath using the co-efficient of determination, r^2, and mean values assessed for each subject. Table 3.1 provides values for E, R and r^2 fit parameters for unfiltered Poes and filtered signals from each of the three methods presented above (template subtraction, ANC with ECG signal input, ANC with a template-waveform based signal input). Values are given as mean $\pm$ standard deviation (SD) for each subject over the 100 breath period, and as a group average.

Absolute values of elastance and resistance were very consistent across filtered and unfiltered models, with the exception of the ECG based adaptive filter for subject 6. Inspection of these signals revealed a poor quality ECG signal, meaning the adaptation algorithm did not converge successfully. The template subtraction method produced the highest value of r^2. A Student's t-test performed on r^2 values demonstrated significantly improved r^2 for the filtered pressure signal vs. unfiltered (0.94 ± 0.01 vs 0.87 ± 0.06, P=0.01).

3.1.4 Discussion

Figure 3.5 suggests that the template subtraction method performed better at removing higher frequency harmonics in the Poes signal than the two adaptive filter methods. The results of the respiratory mechanics model fit also showed the template subtraction method provided the best results by most improving model fit and r^2 value. This was somewhat surprising, as the additional adaptation was thought likely to improve fits to the cardiogenic template. However, it may be that by allowing continuous adaptation, any artefacts such as swallows distort filter weights and reduce fits, whilst a simple template subtraction with updating history and exclusion criteria minimises these effects. These results indicate that template subtraction is a better filtering strategy for ongoing analysis over long periods of sleep recording, in which artefacts are not excluded first. A secondary benefit of this approach is that the template method is computationally more efficient, removing the adaptation step entirely. For the purpose of the remaining analyses described in this thesis, these results were considered sufficient to support ongoing application of the template subtraction method for reducing the cardiogenic noise in oesophageal pressure signals whilst preserving respiratory related signal content. The ECG based ANC filter failed in subject 6, where poor signal quality meant the filter weights did not success-

fully converge. This method is more susceptible to distortion from artifact as there is no template averaging, which will be a problem with noisy data sets.

A template-based filter has been proposed to remove cardiac noise from the oesophageal pressure signal while preserving respiratory information content. This appeared to perform better than two adaptive filter methods based on an LMS algorithm. The validity of the method for separating respiratory components of oesophageal pressure was demonstrated through improved model fits to a well validated model of respiratory system mechanics.

Once a template has been created, the filter runs with a delay of one heart rate interval to fit the cardiogenic waveform to the given R-R interval. This is sufficiently fast for future near real time applications envisaged. The alternative adaptive filter approach proposed was based on the LMS algorithm, which is simple and computationally efficient. Selecting step size for an adaptive filter is very important as it governs convergence. For the ECG noise source, a small step size resulted in a long time to reach optimum filter weights. However, increasing the step size left the system susceptible to artefact disruption to weights, potentially impacting filter performance with a risk of introducing drift into the output noise. For these reasons, this approach is likely best suited to preselected regions of artefact-free Poes.

In this chapter, and for the remainder of this thesis, it has been assumed that respiratory and cardiac components of pleural pressure are largely independent. However, it should be noted that there is likely to be some degree of coupling given that cardiac volume changes will partly depend on pleural pressure influences on cardiac filling pressures. Nevertheless these effects should be relatively small compared to direct transmission of heart movements to balloon pressure changes, so this assumption of independence was considered to be reasonable, and necessary for the purpose of practical full-night cardiogenic artefact filtering.

These results support that the cardiac filtering methods presented are very useful for diminishing cardiogenic artefacts on Poes, prior to deriving a modelled attempted ventilation using the respiratory system equation of motion. The excellent fits of filtered signals to the model suggest the cleaned signal provides a more reliable representation of respiratory driving pressure, and can therefore be used as a measure of respiratory effort. It remains to be seen if having multiple templates gated at points in the breathing cycle or lung volume could improve fits, in line with the work by Seppä et al. (2011). More sophisticated methods of weighted-averages or gain adaptation to optimise template fit could further improve filtering performance. Results may also be improved by including additional adaptive amplitude criteria or iteration fits for the subtraction of waveforms, so

that the template is optimised on a waveform-by-waveform basis. However, these would increase computational time for improvements that may only be marginal. Although results obtained with the template filtering method were considered sufficient for the remaining thesis work, further work to advance filtering methods would likely improve results.

3.2 Diaphragm EMG

3.2.1 Introduction

Diaphragm electromyography (EMGdi) signals also provide insight into respiratory effort by measuring electrical activity of the primary inspiratory muscle, and will be used later in the thesis to investigate inspiratory pump muscle activity during airway collapse. However, these signals also contain significant cardiogenic artefact from the electrocardiographic (ECG) signals from the heart, which can greatly reduce signal quality. The ECG frequency range is mostly found within 1-50Hz while the EMGdi signal is mostly within 0.5 to 150Hz (Schweitzer et al., 1979). High-pass filter techniques have been shown to be ineffective, due to substantial spectral overlap (Akkiraju and Reddy, 1992). Therefore, cardiac filtering methods for EMGdi signals are also required.

Gating techniques, in which periods of the EMGdi signal with ECG artefact are discarded, are widely used but result in significant signal loss (Levine et al., 1986). Template subtraction has been shown in some cases to remove artefact while preserving the respiratory activity in EMGdi, but methods required careful manual selection of multiple templates, due to variation in waveform shape (Levine et al., 1986). Adaptive filters have been used to remove noise, but results have been mixed, achieving reported ECG activity removal of up to 85% (Akkiraju and Reddy, 1992). Simulated results were excellent, but real data showed some remaining ECG artefact (Chen et al., 1994). This is not surprising given that there will be some inherent temporal variation in real data, and the high power of the ECG component means any residual artefact will dominate the signal. An adapted method of event-synchronous interference cancellation, using adaptive gain-amplification of an artefact template to remove noise, has also been proposed (Deng et al., 2000). This is similar to methods discussed above for oesophageal pressure removal through subtraction using an artefact template. Results showed promise, but were only examined using surface EMGdi recordings, which have substantial further problems of poor signal-noise, contamination from inter-costal muscle activity and motion artefacts arising from diaphragm and chest wall motion. To circumvent these problems and to obtain measurements of EMGdi more directly comparable to Poes, intra-oesophageal EMGdi was recorded via an intra-

oesophageal catheter for the remaining work described in this thesis. Consequently, as with Poes, further work was undertaken to help select the most practical and appropriate cardiogenic artefact filtering methods for application to full-night EMGdi recordings.

3.2.2 Methods

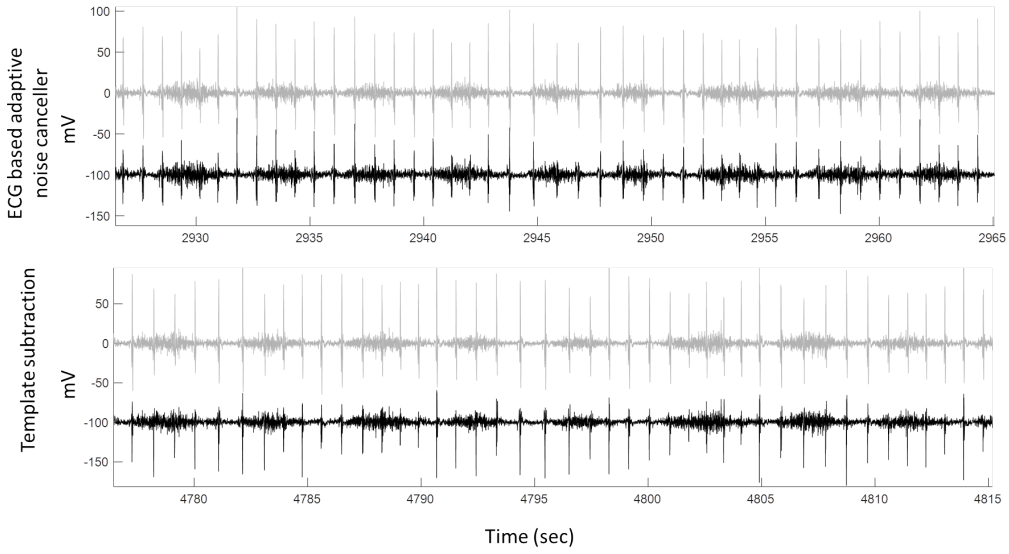

Figure 3.7: Results from a) ANC filter with ECG reference input signal and b) template subtraction using ensemble averaged artefact. Filter output (black) is offset from original signal (grey) by 100mv. Neither method satisfactorily removes cardiogenic artefact.

To test the suitability of intra-oesophageal EMGdi signal filtering methods here, preliminary tests using both template subtraction and ANC filters were performed on existing data and showed sub-optimal filtering (Figure 3.7). Recordings from intra-oesophageal data show strongly dominant ECG artefact, which may help explain poor results compared to those reported for surface EMGdi. Figure 3.7 shows example outputs using an ANC filter with an ECG noise reference signal and template subtraction attempts. Neither method is particularly successful in removing ECG artefact. The power of the cardiogenic waveform is so large that even a reasonable waveform template leaves quite substantial residual power which still dominates the signal.

Recently, new methods to filter EMGdi have been proposed that use wavelet transforms and independent component analysis (ICA) to help isolate and remove cardiogenic noise. ICA is a special case of blind signal separation and decomposes multivariate signals into separate components, with no prior knowledge of sources other than an assumption that each source is independent. This has been used to identify ECG components and remove

them from EMGdi, but its effectiveness is determined by the independence of the signals (Cao et al., 2002). Traditional wavelet transform filter methods decompose the signal into a wavelet basis, which is then used to define thresholds to remove finite bandwidths. However, significant overlap in frequency spectra between EMGdi and ECG make this approach inappropriate. Several papers have looked to combine these two methods and overcome the problems associated with each individually (Azzerboni et al., n.d.; Wu et al., 2016). Similar methods have been used successfully in electroencephalogram (EEG) signal analysis (Akhtar et al., 2012).

An ICA-based wavelet filter was created based on the work of Wu et al (Wu et al., 2016). ICA decomposition was performed using the Fast-ICA package in MATLAB , which is free software to perform fixed-point ICA, and widely used for estimating the de-mixing matrix to separate multiple channels into the same number of independent components (Hyvarinen and Oja, 1997). Once separated, any independent components containing solely noise were removed entirely, while any pure EMGdi signals were preserved fully. The remaining components underwent wavelet decomposition using the daubechies db1 wavelet, which is a highly localised wavelet, meaning it could reflect frequency characteristics of the cardiogenic signal. Decomposition was performed over 5 layers. Frequency bounds for the wavelet decomposition layers are determined by the sample frequency of EMGdi data, which, at 1kHz, gives upper frequency bounds for each layer with maximum frequency $f_{max} = 1000/2n$ where $n = 1, 2...5$. Given most of the ECG is centred in the 0-50Hz range, the low frequency wavelet decomposition levels have greatest noise components, primarily the 0-31.25Hz and 31.25-62.5Hz layers. Wavelet domain thresholds were adjusted based on both the average amplitude of raw signals and a factor corresponding to decomposition level, accounting for the fact that most noise will be distributed in the lower frequency band. Purified independent components were then reconstructed by a reverse of the ICA matrix into the original signal space.

3.2.3 Results

Figure 3.8 shows an example of these filtering techniques applied to intra-oesophageal EMGdi data. Visual inspection shows that clear preservation of respiratory EMGdi power is achieved, along with substantial reduction in the cardiogenic artefact. The power spectrum shows clear reduction in the 0-50Hz region, where ECG power is centred. It was found that this filter performs well for removing ECG from EMGdi, and was considered adequate for cleaning EMGdi for further analysis as a measure of inspiratory muscle activity in remaining thesis work. The tools are likely to provide particular benefit for analysis of within- and between-breath muscle responses which previously would have been sub-

(a)

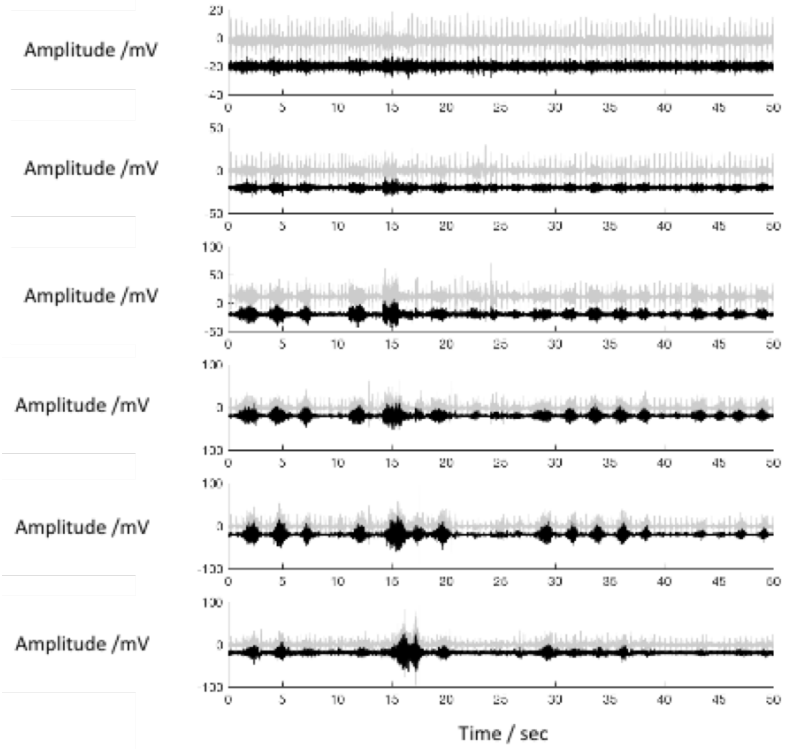

(b)

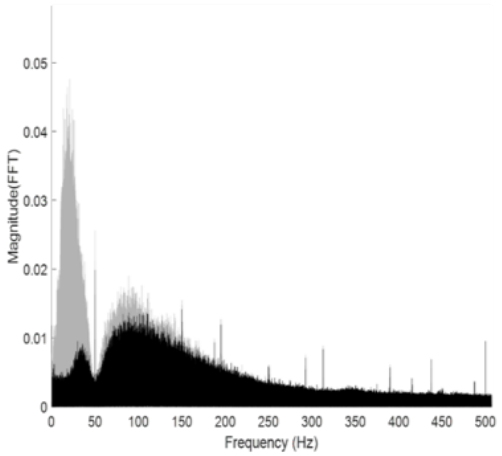

Figure 3.8: Filtered EMGdi using ICA decomposition and wavelet transform. a) Cardiogenic artefact in filter output (black) is significantly reduced compared to original signal (grey) in all six EMGdi channels. Output is offset by 20 mV for clarity. b) power spectra for original EMGdi (grey) and filtered output. Note significant reduction particularly in the 0-50Hz region, where ECG power is concentrated

stantially obliterated by traditional band-pass and/or ECG blanking methods.

3.3 Conclusions

Current methods for filtering oesophageal pressure and diaphragm EMG have been reviewed and strategies to optimise the respiratory components of these physiological signals whilst minimising cardiac noise have been proposed and tested. Good results were achieved using template subtraction methods for oesophageal pressure. EMGdi signals were successfully cleaned with a combined ICA-wavelet filter. Both methods have scope for future improvement, but performed sufficiently well in testing to provide valuable filtering methods for application in the ongoing analysis necessary for the remaining work described in this thesis.

Chapter 4

The effect of occlusion on pressure measurements

The previous chapter addressed one of the limitations of oesophageal pressure as a marker of effort: cardiogenic artefact that can distort respiratory signal information. The second limitation identified with oesophageal pressure was the possibility that airway occlusion directly alters measured pressure values through system mechanics. In the study presented in this chapter, an external occlusion was applied to OSA patients during sleep, and pressures at the mask, epiglottis and oesophagus were measured. The immediate effects of the applied occlusion on recorded pressure swings were quantified.

This aligns with Aim 2 of the thesis: to determine relative effects to an applied external occlusion on the current gold standard measures of respiratory effort in sleep (oesophageal and epiglottic pressure).

4.1 Background

Augmented inspiratory effort during airway obstruction is a defining characteristic of sleep disordered breathing (Guilleminault et al., 1976). Oesophageal pressure (Poes) is generally regarded as the gold standard measure of ventilatory drive or effort in sleep and pulmonary medicine, as it closely approximates pleural pressure changes (Cherniack et al., 1955; Dornhorst and Leathart, 1952). Upper airway collapse usually occurs in the oropharynx above the epiglottis. Consequently, epiglottic pressure changes recorded via an epiglottic catheter provide similar but more convenient pressure deflection measurements compared to measuring oesophageal pressure during occlusion. Thus epiglottic pressure recordings are more commonly used for the assessment of ventilatory drive and for defining the respiratory-related arousal threshold during sleep in patients with obstructive sleep apnoea (OSA) where frequent obstructions cause repeated arousals that can profoundly disrupt sleep.

Arousal from sleep is strongly associated with increased inspiratory effort around the termination of obstructive events in OSA (Berry and Gleeson, 1997; Vincken et al., 1987) and in upper airway resistance syndrome (UARS) (Guilleminault et al., 1976). OSA is now established to be a highly heterogeneous condition with both anatomical and non-anatomical contributions to its pathogenesis (Eckert et al., 2013). The arousal threshold, often quantified as the peak nadir oesophageal or epiglottic pressure on the breath prior to arousal, has been identified as a key phenotypic trait in OSA (Eckert and Younes, 2014). Therefore pressure deflection measurements for defining ventilatory drive associated with arousal have become increasingly common.

Additionally, given that airflow recovery has been shown to occur largely independently of

arousal (Younes, 2004), other compensatory mechanisms must clearly be more important than arousal for overcoming obstruction in OSA. The only two established mechanisms for non-arousal recruitment of upper airway dilator muscles during sleep are via negative pharyngeal pressure mechano-reflexes or increasing central ventilatory drive (Younes, 2003). Negative pressure changes at the pharynx are dependent on inspiratory pump muscle activity, which is primarily controlled by central chemo-reflex drive. Thus a better understanding of the complex relationship between negative pressure changes in the airway and ventilatory drive in the presence of airway occlusion is fundamental to understanding these mechanisms.

Abrupt airway collapse in OSA will to some extent alter the mechanical behaviour of the respiratory system itself, and this will affect the dynamics of airway and oesophageal pressure changes resulting from ongoing diaphragm and chest wall movements. Furthermore, relationships between neural drive to upper airway and inspiratory pump muscles, and the resulting negative pressure collapsing forces generated within the upper airway may well be non-linear, and could importantly influence airway collapse and subsequent airway reopening in OSA. Studies to date have given very little consideration to the effect of increased airway resistance or occlusion on the magnitude of oesophageal and airway pressure deflections, and the resulting measurements of ventilatory effort and the respiratory arousal threshold, independent of changes in inspiratory drive. A useful analogy is to consider a reciprocating piston pump, where abrupt occlusion of the pump opening will produce larger volume (Boyle's law) dependent pressure deflections within the pump itself with ongoing piston movements. Similar effects should be expected to operate in the human respiratory system, and therefore to influence airway and oesophageal pressure changes independent of mechano- and chemo-reflexes. These effects have important implications for the interpretation of oesophageal or epiglottic pressure changes as both markers of the underlying neural drive to breathe and estimates of the respiratory arousal threshold.

Consideration of simple theoretical pump models may be useful for helping to understand these effects, but may not adequately account for the more complex diaphragm and chest wall configurational and volume changes, muscle tension and loading, and respiratory reflex responses. Therefore the purpose of this study was to examine both theoretical and measured effects of abrupt airway occlusion on oesophageal and epiglottic pressure deflections throughout an acutely occluded breath, before more substantial inspiratory augmentation through neural drive pathways would be expected to develop. As supported by the literature above, we hypothesised that inspiratory epiglottic and oesophageal pressure changes would abruptly become more negative immediately following occlusion, due to volume dependent airway pressure and chest wall effects. We aimed to examine the mag-

nitude of these effects may be relatively modest and potentially amenable to correction towards more accurate estimates of inspiratory neural drive related changes in epiglottic and oesophageal pressure in the presence of abrupt airway occlusion.

4.2 Theoretical considerations

The total neural drive to inspiratory muscles can be thought of as muscle pressure, Pmus. In order to generate airflow, Pmus must increase chest wall volume and overcome lung elastic recoil and airflow resistance effects (Akoumianaki et al., 2014). Using the respiratory system equation of motion, total muscle pressure can be separated into two components, one to overcome the recoil pressure of the chest wall and the other to induce changes in pleural pressure which drive airflow:

$$\Delta P_{mus} = \Delta P_{cw} + \Delta P_{pl} \tag{4.1}$$

$$\Delta P_{mus} = E_{cw}.\Delta V + E_{rs}.\Delta V + R_{rs}.\Delta \dot{V} \tag{4.2}$$

where P_{cw} is chest wall pressure, P_{pl} is pleural pressure, E_{cw} is the chest wall elastance, E_{rs} is the elastance of the respiratory system and R_{rs} is the resistance of the respiratory system, ignoring any inertance effects, considered to be negligible (Mead and Agostoni, 1964). ΔV is the change in volume and $\Delta \dot{V}$ change in flow at any given point in time.

The difference between oesophageal (Poes) and epiglottic pressure (Pepi) depends on the lung elastance (E_L) and resistance (R_L).

$$P_{oes} - P_{epi} = E_L.\Delta V_L + R_L.\Delta \dot{V}_L \tag{4.3}$$

Similarly, the reduction in negative pressure from the epiglottis to the airway opening, which is typically enclosed within a mask necessary for reliable flow and pressure measurements, corresponds to pressure overcoming upper airway elastance (E_{UA}) and resistance (R_{UA}) to drive airflow.

$$P_{epi} - P_{mask} = E_{UA}.\Delta V_{UA} + R_{UA}.\Delta \dot{V}_{UA} \tag{4.4}$$

Using these equations, Pmus can be related to both oesophageal and epiglottic pressure

$$\Delta P_{mus} = E_{cw}.\Delta V_L + \Delta P_{oes} \tag{4.5}$$

$$\Delta P_{mus} = (E_{cw} + E_L).\Delta V_L + R_L.\Delta \dot{V}_L + \Delta P_{epi} \tag{4.6}$$

On occlusion, the elastic and resistive terms dependent on flow and volume change at both the upper airway and lung go to zero and there would be no expected inspiratory pressure change difference between the lung and the pharynx. Therefore, measured pressure deflections would be expected to be similar at both the epiglottis and oesophagus.

$$\Delta P_{mus} \approx \Delta P_{oes} \approx \Delta P_{epi} \tag{4.7}$$

Neural drive over the course of the first breath following airway occlusion would be expected to remain relatively constant as the circulatory delay time from central or peripheral chemo-receptor inputs that dominate ventilatory drive changes will substantially exceed breath time. However, there are likely to be additional mechano-receptor mediated reflex effects of load compensation which will be discussed later. Theoretically, then, equating Pmus on each breath, and considering $\Delta V = \Delta \dot{V} = 0$ on occlusion, for both Poes and Pepi

$$E_{cw}.V_{open} + (\Delta P_{oes})_{open} = (\Delta P_{oes})_{occ.} \tag{4.8}$$

$$(E_{cw} + E_L).V_{open} + R_L.V_{open} + (\Delta P_{epi})_{open} = (\Delta P_{epi})_{occ.} \tag{4.9}$$

Thus, on the basis of respiratory mechanics alone, the difference in oesophageal pressure from an open to an occluded breath would be expected to be dependent on the difference in volume from the non-occluded breath. Similarly, the difference in epiglottic pressure should be dependent on both the difference in volume and flow from the open to occluded breath. Therefore, a volume or flow dependent correction to epiglottic and oesophageal pressures could help correct for mechanical effects of abrupt airway occlusion, and produce a measure of the total underlying neural drive, or Pmus, which would be expected to remain consistent in the period immediately following occlusion.

In order to test these theoretical effects, we undertook a systematic analysis of measurements previously obtained from a study of obese OSA patients who underwent abrupt airway occlusion during sleep to investigate abdominal compression effects on upper airway closing pressure (Stadler et al., 2009).

Our hypotheses were that epiglottic and oesophageal pressure swings would be immediately more negative on occlusion due to effects of respiratory mechanics, and that these effects would be predictably flow and volume dependent. Additional augmentation by load

compensation or mechano-reflex modulation of drive could potentially also occur following occlusion onset. Mechano-reflex responses to abrupt pressure changes can be rapid and are known on a within breath basis (Jeffery et al., 2006*b*), however would not be expected to exhibit the same flow or volume dependence predicted above for mechanics related effects. Therefore, we will test how well any observed negative pressure differences fit the theoretical model developed above.

4.3 Methods

4.3.1 Study sample

This study made use of data obtained prior to this PhD and more detailed methods have been reported previously (Stadler et al., 2009). Briefly, complete data were obtained from 13 obese male patients (body mass index [BMI] 30-40 kg/m2) with moderate-to-severe OSA (apnoea-hypopnoea index [AHI] >30 events/h) who previously underwent detailed physiological recordings during sleep. The study was approved by the Daw Park Repatriation General Hospital and Adelaide University Human Research and Ethics Committees. All patients gave informed written consent to participate.

4.3.2 Study setup and protocol

Patients were set up for overnight sleep study recordings on a breathing circuit to provide nasal CPAP and rapid external occlusion via a computer-controlled balloon occlusion valve close to the inspiratory port of a nasal mask. Inspiratory flow and volume were recorded via a pneumotachograph (PT16, Jaeger, Germany) connected to the nasal mask, using mouth tape to ensure nasal breathing and prevent mouth leaks. End tidal CO_2 was measured at the mask (Capstar-100, CWE Inc, PA). Epiglottic pressure (Pepi) was measured via an air-perfused catheter passed through a sealed port on the mask. Oesophageal (Poes) and gastric (Pgas) pressures were measured via two separate 5-cm latex balloon catheters (Viasys Healthcare, Hoechberg, Germany) also passed through the mask, with both catheters connected to separate differential pressure transducers (Validyne Engineering, Northridge, CA) referenced to atmospheric pressure. Mask pressure (Pmask) was measured via a separate pressure transducer. All respiratory signals were acquired using a computerised data acquisition system (Model DI-720, DataQ Instruments, Ohio, USA), with each channel sampled at 200 Hz.

The original study examined the effects of abdominal compression on airway collapsibility,

so patients also wore an abdominal cuff that was inflated and deflated over the course of the night. Throughout the night, repeated external occlusions were commenced near end-expiration by rapidly inflating a balloon occlusion valve encased within the inspiratory limb of the breathing circuit (Stadler et al., 2009). Unidirectional breathing valves, constant positive airway pressure and careful attention to avoid mask leaks ensured that rapid airway occlusion commenced only during expiration and with no change in CPAP level. Occlusion continued for several breaths until the first sign of either EEG arousal or clearly discernible upper airway collapse as evidenced by a stable plateau in inspiratory mask pressure over several consecutive breaths. For this analysis, only events that lasted at least one full respiratory effort prior to airway collapse (i.e. closing pressure as defined by flattening of mask pressure despite ongoing inspiratory effort) or arousal, were included to avoid potential confounding from either airway collapse downstream from the external occlusion or arousal effects. An example occlusion event is shown in Figure 4.1.

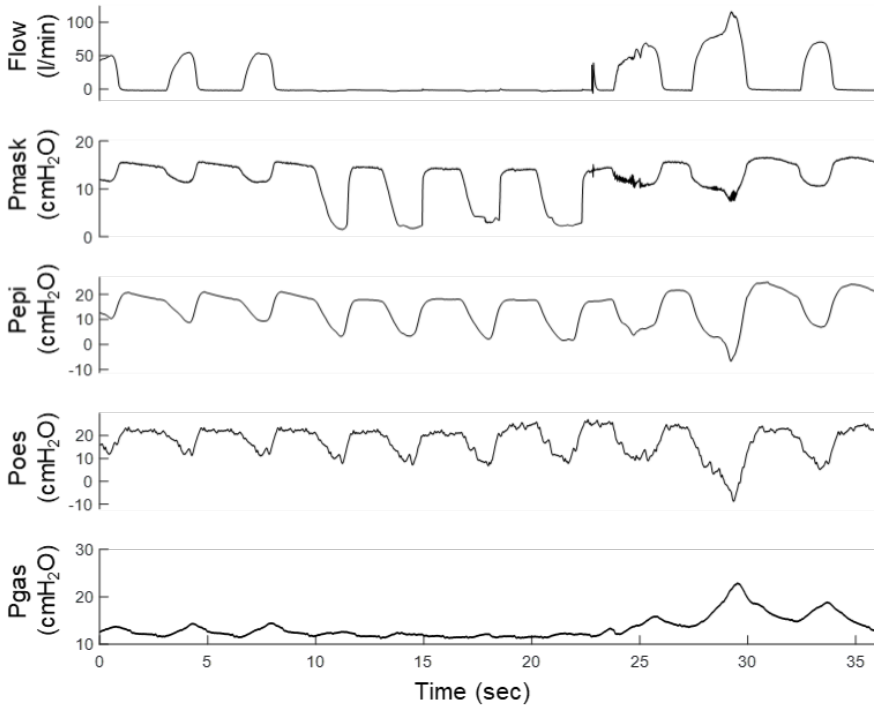

Figure 4.1: An example trace showing events during a brief mask occlusion. To compare the immediate effects of external occlusion on pressure at the epiglottis and oesophagus, pressure traces for the first occluded effort were compared to those from the effort immediately prior to occlusion.

4.3.3 Data analysis

Oesophageal pressure deflections on the initial occlusion breath were compared with the breath immediately prior to occlusion. For each occlusion the starts of the inspiratory effort immediately prior to and following occlusion onset were identified using custom software in MATLAB (The MathWorks, Natick, 2017), described in more detail in Appendix A. Fixed 10-second windows of patient flow, Pmask, Pepi, Poes and Pgas centred on effort onset for the breath directly prior to and following occlusion onset were then ensemble averaged in each cuff condition separately and in combination, within each patient before group ensemble averaging. Breath parameters including inspiratory, expiratory and total breath time (Ti, Te, Ttot), breathing frequency (FB), peak inspiratory flow (PIF), inspiratory tidal volume (Vti), minute ventilation (VI) and end tidal CO_2 (ETCO2) were calculated for the breath prior to occlusion. Baseline, minimum (maximum Pgas) and change in Pmask, Pepi, Poes and Pgas were measured for each occluded and non-occluded breath then averaged within each participant for each breath and cuff condition.

4.3.4 Respiratory mechanics based analysis

Any observed changes in pressure with occlusion could be due to changes in the mechanics of the system, reflex inspiratory muscle compensation, flow effects or augmented neural drive. If the contribution is dominated by system mechanics, then pressure differences between the non-occluded and occluded breath should be proportional to the difference in flow and volume changes between conditions, and correspond to the difference between measured pressure and muscle pressure, according to respiratory mechanics based predictions described earlier.

$$\Delta P_{mus} = E.\Delta V_{open} + R.\Delta \dot{V}_{open} + \Delta P_{open} = \Delta P_{occ.} \tag{4.10}$$

where ΔPmus is the total pressure generated by the respiratory muscles, and corresponds to the pressure measured on occlusion, $\Delta P_{occ.}$ as there is no generated flow or volume change. ΔP_{open} is the pressure measured with an unoccluded airway, and the difference between this and muscle pressure consists of additional flow and volume terms dependent on the elastance and resistance of the respiratory system portion between the respiratory muscles and point of pressure measurement.

Pre-occlusion breath data were fit to this equation, optimising values of constants E and R in the model to minimise the sum-of-squares error to the occlusion breath using a gener-

alised reduced gradient non-linear minimisation algorithm. The Pearson product-moment correlation coefficient was calculated between the two signals to determine how closely the corrected pre-occlusion breath correlated to the occlusion breath. This is used to examine how well mechanical effects alone, as modelled by the respiratory equation of motion, could explain observed pressure differences between occluded and non-occluded breaths. By experimental set up with a unidirectional breathing valve, only inspiratory flow was recorded. Given variable inspiratory times, ensemble averaged flow became artifactually distorted after the end of inspiration. Therefore, this analysis period was confined to the minimum inspiratory time, which occurred at 1.45 seconds.

4.3.5 Statistical analysis

Linear mixed model analyses were used to assess the effects of occlusion and cuff condition on each breath parameter. Each model used an auto-regressive co-variance structure and included a separate intercept for each subject to account for between-subjects effects. Mixed model analyses were also used to compare changes in pressures over time between occluded and the previous non-occluded breaths using pressures down-sampled to 20 Hz. Statistically significant differences were inferred when $p < 0.05$. Statistical analyses were performed using IBM SPSS Statistics version 22. All data are reported as mean ± SEM unless otherwise specified.

4.4 Results

4.4.1 Participants

Of 25 participants consented into the original study (Stadler et al., 2009), 5 had insufficient sleep, another 5 showed residual mask or mouth leaks and 2 were unable to tolerate the oesophageal catheter and were therefore excluded. Thus, data from 13 patients remained for analysis. 2 patients did not have usable epiglottic pressure signals so these were excluded from analysis. The characteristics of these participants are shown in Table 4.1. Subjects underwent an average of 44 ± 6 occlusion tests [range 17 – 84] over the course of the night.

Table 4.1: Patient characteristics (N=13)

	Mean±SEM
Age (years)	50 ± 3
BMI (kg/m^2)	34 ± 1
AHI (events/h)	58 ± 7
Waist Circumference (cm)	119 ± 3
Hip Circumference (cm)	119 ± 3
CPAP level (cmH_2O)	14.1 ± 0.8

4.4.2 Effect of abdominal cuff

Breath measurements from occluded and non-occluded breaths with each cuff condition are presented in Table 4.2. The abdominal cuff did not change tidal volume, peak inspiratory flow or ETCO2 prior to occlusion onset, but did increase Ti and reduce Te without changing Ttot or breathing frequency. Pmask and Pepi were not altered with cuff inflation. However, cuff inflation did significantly increase baseline Poes and Pgas, reduce minimum Poes and increase maximum Pgas, increasing the overall pressure swing in both channels. The time to peak Pgas was also increased in the cuff inflated condition. Pressure traces in the two conditions are illustrated in Figure 4.2.

4.4.3 Effect of occlusion

Pressure changes over the pre-occlusion and occluded breath under the cuff deflated condition are shown in Figure 4.2. Pressure swings at the mask, epiglottis and oesophagus were all more negative with occlusion, while gastric pressure increases during inspiration were markedly reduced. These effects were greatest in mask pressure, more modest in epiglottic pressure and smallest in oesophageal pressure. Corresponding breath parameters are presented in Table 4.2.

Simple linear flow and volume dependent corrections to open airway pressures to derive the total muscle pressure, Pmus, produced excellent fits to pressure measured with occlusion (Figure 4.3). This suggests that most of the epiglottic and oesophageal pressure differences between open versus occluded airway conditions can be explained via traditional respiratory mechanics models including flow and volume dependent terms. For the unoccluded breath, the Pmus signal can essentially fully account for the difference between the pressure generated by the respiratory muscles to the pressure mea-

Table 4.2: Ventilatory parameters for occlusion and pre-occlusion breath. Values are mean ± SEM, N=13. * indicates a main effect of cuff, † a main effect of occlusion, ‡ a cuff x occlusion effect.

	No Cuff		Cuff		
	Unoccluded	Occluded	Unoccluded	Occluded	
PIF (l/min)	25.9 ± 1.3		25.6 ± 1.3		
Vti (l)	0.54 ± 0.02		0.55 ± 0.03		
Ti (s)	1.7 ± 0.0		1.8 ± 0.1		*
Te (s)	2.5 ± 0.2		2.3 ± 0.2		*
Ttot (s)	4.2 ± 0.2		4.1 ± 0.2		
FB (breaths/min)	14.7 ± 0.6		15.1 ± 0.6		*
VI (l/min)	7.9 ± 0.4		8.1 ± 0.4		
CO2 (mmHg)	41.8 ± 0.6		40.9 ± 0.8		
Baseline Pmask (cmH_2O)	14.0 ± 1.2	14.0 ± 1.2	14.1 ± 1.2	14.1 ± 1.2	
Baseline Pepi (cmH_2O)	15.6 ± 2.2	15.7 ± 2.2	16.3 ± 2.4	16.3 ± 2.4	
Baseline Poes (cmH_2O)	18.1 ± 1.2	18.1 ± 1.2	18.9 ± 1.6	18.8 ± 1.5	*
Baseline Pgas (cmH_2O)	11.5 ± 0.9	11.5 ± 0.9	17.0 ± 0.8	17.1 ± 0.7	*
Min Pmask (cmH_2O)	11.4 ± 1.2	1.3 ± 1.0	11.7 ± 1.2	1.5 ± 1.0	†
Min Pepi (cmH_2O)	9.5 ± 1.6	3.1 ± 1.7	10.2 ± 1.7	3.2 ± 1.9	†
Min Poes (cmH_2O)	5.5 ± 1.1	0.5 ± 1.3	4.4 ± 1.5	-0.7 ± 1.6	*†
Max Pgas (cmH_2O)	13.5 ± 0.8	12.1 ± 0.8	21.3 ± 0.8	18.1 ± 0.7	*†‡
Time to min Pmask (s)	0.90 ± 0.06	1.3 ± 0.1	1.0 ± 0.1	1.2 ± 0.1	†‡
Time to min Pepi (s)	1.23 ± 0.10	1.4 ± 0.1	1.2 ± 0.1	1.4 ± 0.1	
Time to min Poes (s)	1.24 ± 0.05	1.5 ± 0.1	1.3 ± 0.1	1.5 ± 0.1	†
Time to max Pgas (s)	1.50 ± 0.07	1.5 ± 0.1	1.6 ± 0.1	1.5 ± 0.1	*
Pmask Swing (cmH_2O)	2.6 ± 0.1	12.7 ± 0.5	2.4 ± 0.1	12.6 ± 0.5	†
Pepi Swing (cmH_2O)	6.1 ± 0.9	12.6 ± 1.7	6.1 ± 1.1	13.1 ± 1.8	†
Poes Swing (cmH_2O)	12.6 ± 0.9	17.6 ± 1.2	14.4 ± 1.2	19.5 ± 1.3	*†
Pgas Swing (cmH_2O)	-2.0 ± 0.3	-0.6 ± 0.2	-4.2 ± 0.5	-1.0 ± 0.3	*†‡

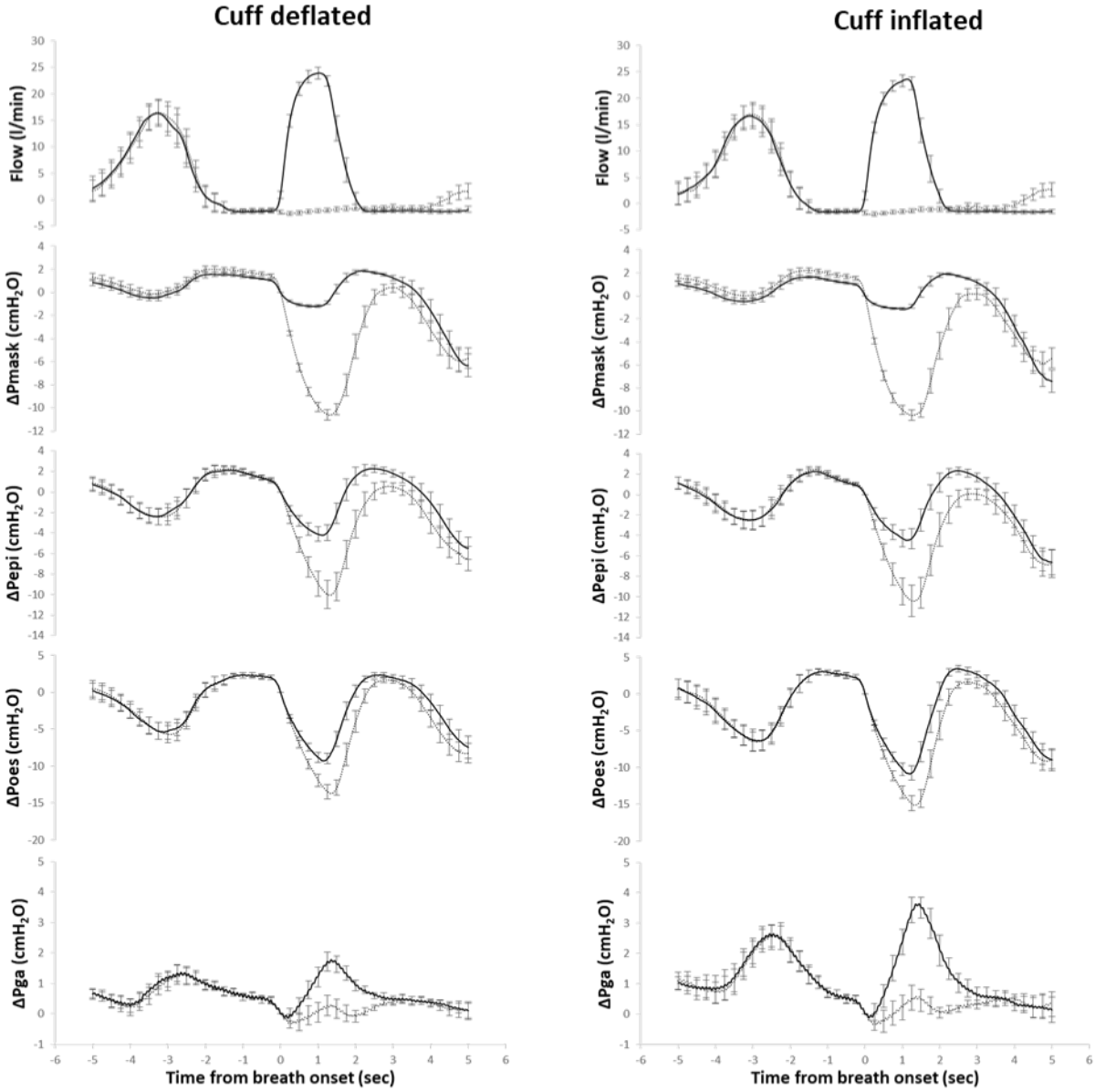

Figure 4.2: Group ensemble average flow and pressure profiles centred on the onset of the pre-occlusion breath (black line) and occluded breath (grey line) for cuff deflated and inflated conditions (N=13). All pressures are calculated as relative change from time zero. Note that although the second breath (black line pre-occluded breath) appears to be larger and sharper than the previous pre-occluded breath, this reflects temporal smoothing effects of ensemble averaging as there were no differences between the penultimate and anti-penultimate breaths before occlusion (corresponding to the grey vs black lines on the first plotted breath). Values are mean±SEM with error bars plotted every 5th data point for clarity.

sured at either the oesophagus or the epiglottis, taking into account additional chest wall elastance and lung elastance and resistance terms in the presence of flow (Mean±SEM Pepi; E=14.7±1.7 cmH2O/l, R=1.7±0.5 cmH2O.s/l, r^2=0.995±0.003; Poes E=9.8±1.2 cmH2O/l, R=0.2±0.1 cmH2O.s/l, r^2=0.991±0.003). Individual subject values are given in Table 4.3.

Table 4.3: Individual subject model fits for epiglottic and pressure difference between occlusion and pre-occlusion breaths

	Pepi			Poes		
Subject	E	R	r^2	E	R	r^2
1	14.37	0.00	0.998	4.47	0.00	0.993
2	14.34	3.38	0.994	14.66	0.88	0.998
3	10.50	0.14	0.999	8.72	0.00	0.996
4	25.14	0.00	0.995	15.74	0.00	0.986
5	13.49	1.49	1.000	9.34	1.64	0.995
6				13.92	0.00	0.962
7	13.50	3.79	1.000	8.57	0.56	0.998
8	5.39	1.48	0.984	10.47	0.00	0.996
9	12.47	5.24	0.997	10.70	0.00	0.998
10	13.35	0.10	0.992	0.55	0.00	0.982
11				9.14	0.00	0.999
12	14.76	2.14	0.998	14.92	0.00	0.999
13	24.92	0.71	0.992	6.70	0.00	0.975
Group	14.75	1.68	0.995	9.84	0.24	0.991

Occlusion effects on oesophageal pressure appeared to be almost entirely volume dependent with no resistive component, whereas effects on epiglottic pressure showed contributions from both flow and volume, as predicted from theoretical models of mechanics. However, even after correction for these mechanical effects quite substantial differences remained between peak Pmus estimated from Pepi (around -9 cmH2O, Figure 4.3) compared to estimates from Poes (around -13 cmH2O).

4.5 Discussion

This study specifically examined the effect of abrupt experimental airway occlusion on epiglottic and oesophageal pressure swings typically used for assessing inspiratory effort.

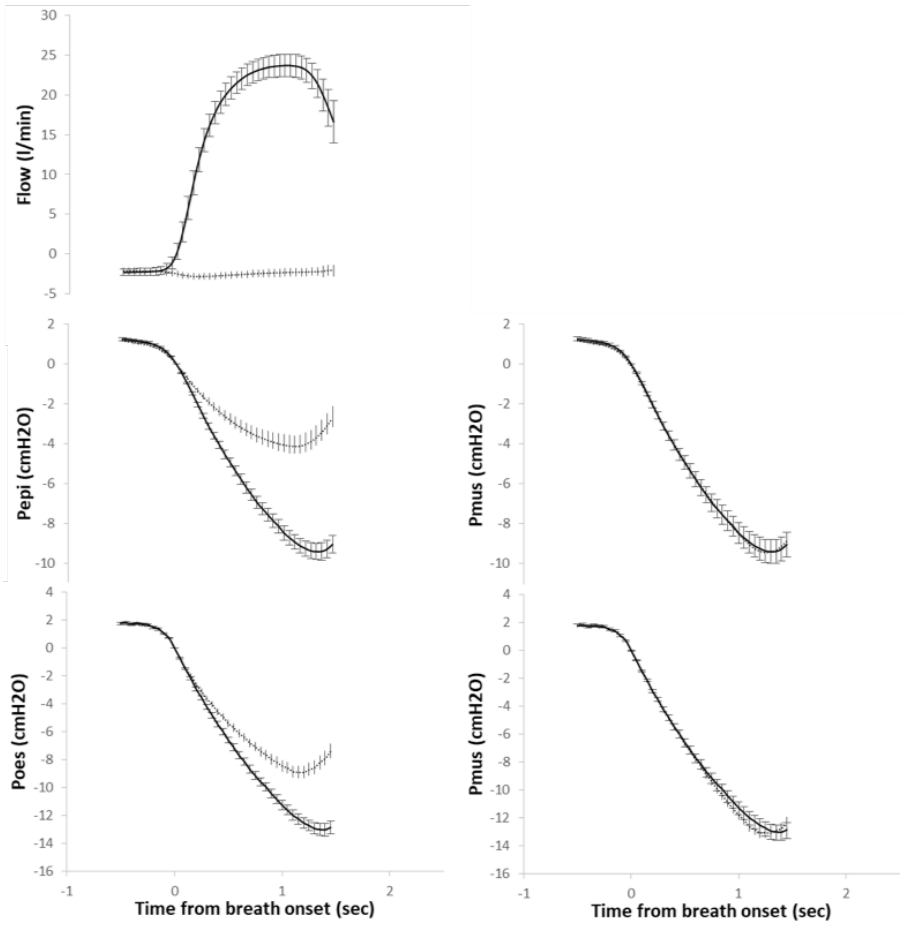

Figure 4.3: Oesophageal and epiglottic traces on the pre-occluded (black line) and occluded breath (dotted line) under the cuff-deflated condition. Plots on the right include a correction applied to the pre-occlusion breath by optimising constants E and R to fit the occluded breath to derive total muscle pressure, Pmus. Excellent fits of a mechanics-based correction from the traditional respiratory system equation of motion suggest most of the observed difference between the two conditions is due to these effects.

As hypothesised, both Poes and Pepi deflections became more negative on the breath immediately following abrupt external occlusion, when mechano- and chemo-reflex changes in underlying ventilatory effort would be expected to be relatively minimal or absent, particularly during early inspiration. These changes were especially pronounced in epiglottic pressure, where occlusion itself led to just over a 100% increase in the magnitude of the epiglottic pressure swing. In contrast Poes showed of the order of a 20% increase in the magnitude of the inspiratory pressure swing during occlusion. However, it is also worth considering that the degree of over-estimation of ventilatory drive changes from obstruction effects on Poes or Pepi deflections would be expected to diminish as ventilatory drive augments over subsequent breaths.

The substantial difference in pressure swings between occluded and non-occluded breaths could be accounted for via flow and volume dependent correction terms to the non-occluded breaths, with excellent corrected fits to observed measurements. These findings strongly support the hypothesis that pressure differences associated with occlusion reflect mechanical effects arising from abrupt changes in flow and volume with occlusion, and that ongoing muscle pressure related changes from neural drive remained largely unchanged. However, differences remaining between the magnitude of epiglottic and oesophageal pressure swings and corresponding estimates of Pmus on occlusion are consistent with expected residual pressure differences across the lung with occlusion not present in airway pressure.

These findings have important implications for the use of Poes and Pepi deflections for estimating changes in inspiratory effort, for example in arousal threshold determination. For the same central respiratory drive, the measured pressure changes during an apnoea would likely be substantially more negative than those measured during a hypopnoea, where there are still some inspiratory flow and volume changes. In light of the results of this study, care is warranted in the interpretation of studies noting associations between arousal and more negative pressure deflections, particularly when based on epiglottic pressure to assess arousal threshold. Events with cortical arousals have been associated with more negative epiglottic pressure deflections compared to events terminated without arousal. However, events with arousal have also been shown to be more severe, with greater oxygen desaturation and a higher proportion arising from apnoea vs hypopnoea (Li et al., 2019). Given that the results from this study indicate measured pressure deflections are substantially more negative in the presence of total occlusion, before chemo-reflex mediated increases in ventilatory drive would be expected, future studies clearly warrant more careful analysis to help separate direct effects of occlusion from underlying changes in respiratory drive and arousal threshold.

The findings from this study are also relevant to understanding the mechanics of airway

collapse and obstruction recovery in OSA. For example, substantially greater negative pressure swings at the epiglottis due to the mechanical effects of occlusion are likely to exacerbate airway collapse. The additional collapsing force will inevitably oppose upper airway dilator recruitment central to re-establishing patency. This may help explain phenomena such as negative effort dependence (Genta et al., 2014), and why airway obstruction is so difficult to reverse once it is established. Strong evidence supports that upper airway dilator muscles are driven by both brainstem-mediated central neural ventilatory drive and reflex activation from changes in airway pressure (Akahoshi et al., 2001; Horner et al., 1991; Malhotra et al., 2002; Wheatley et al., 1993) , whilst pump muscles are primarily activated by central drive itself, but with reflex modulated inhibition in the presence of airway obstruction (Jeffery et al., 2006*a*). This study showed that the immediate increase in negative pressure swings that occur on occlusion could be reasonably well captured with a linear model based on mechanics. If airway pressure swings become more negative as a result of occlusion itself, it means the relationship between central drive and the resulting negative airway pressure around the site of collapse becomes non-linear following commencement of airway obstruction. More negative pressure at the pharynx for a given level of central ventilatory drive would increase collapsing forces at and below the initial site of airway collapse. This might also favour upper airway dilator muscle recruitment via augmented negative pressure reflex activation, which could be important for airway recovery without arousal, although reduced negative pressure reflex activation above the site of collapse could also partly offset these effects.

4.5.1 Study limitations

There are several limitations to this study that warrant discussion. An external occlusion was used, applied upstream from a nasal CPAP mask. Consequently the effective dead-space volume below the site of external occlusion would be larger than with natural obstruction of the upper airway itself. We estimate the air volume from the site of external occlusion to the bottom of the pharyngeal space would likely be in the order of 160ml (approximately 20cm tubing at 2cm diameter 60ml, nasal mask approx. 80ml, average pharyngeal volume 20ml (Grauer et al., 2009). However, this is a relatively small volume compared to end-expiratory lung volume from which subsequent occlusion pressure change effects would then operate, so is unlikely to have substantially influenced our main findings. Subsequent airway collapse induced by negative airway pressure would also negate these effects, although we ensured mask pressure showed no sign of flattening to indicate airway collapse on the first breath. Use of an external occlusion as opposed to pharyngeal collapse occurring naturally during sleep could also have impacted on the

mechano-receptor response to negative pressure, as receptors above the site of naturally occurring collapse in OSA would still be subject to negative pressure. CPAP drops could be used to induce a more natural pharyngeal collapse, but this would occur on a background of substantially larger dynamic changes in airway pressure and lung volume over multiple breaths. We only examined acute effects of total external occlusion and did not consider partial collapse and Starling resistor-like behaviour more commonly exhibited in the human upper airway during hypopnoeas and snoring. Given that pressure swing changes were remarkably well explained on the basis of flow and volume changes, we would predict that the effects of partial airway obstruction should be more modest, and remain amenable to the same correction strategy.

Central and peripheral CO_2 chemo-reflex response times should substantially exceed the period examined in this study ($\pm$1 breath either side of occlusion), so chemo-reflex drive is highly unlikely to have influenced inspiratory drive over the same period. However, upper airway and inspiratory pump muscle mechano-reflex effects from more negative pressure or muscle loading, with much shorter latencies (<100ms (Eckert et al., 2007), are likely to have at least partly influenced responses over the course of the occluded breath. Strong relationships between pressure differences and models of respiratory mechanics on the breath before and after occlusion suggest that flow- and volume-dependent changes were much more dominant than reflex responses. Nonetheless, additional reflex-related augmentation of drive most likely did still contribute, and may explain a later peak in negative Poes and extended Ti with occlusion.

Given the additional effect of collapse on pressure signals, it is worth considering whether other measures of ventilatory neural drive may be superior. EMGdi signals are potentially more immune to flow and volume effects, and several studies have illustrated their utility as a measure of neural drive (Luo et al., 2009, 2008; Xiao et al., 2015). However, obstruction-induced configurational changes in the chest wall and diaphragm are also likely to alter muscle loading and length-tension relationships, thereby altering how neural drive is converted to muscle force and shortening velocity. EMGdi only reflects activity from an individual muscle, albeit the primary inspiratory pump muscle. Strong evidence supports that ventilatory neural drive is distributed to inspiratory motorneurones differentially according to muscle mechanical advantage (Butler and Gandevia, 2008). There is some indication that during apnoea, the relative recruitment of the diaphragm, intercostal and accessory muscles is altered such that in most patients the diaphragm remains the primary inspiratory muscle, but in a subset of patients this shifts to intercostal or accessory muscles (Wilcox et al., 1990). Pressure changes reflect the system as a whole, so should better encapsulate changing patterns of recruitment across different muscle groups, if mechanical effects can be largely accounted for. This study did not examine EMGdi over the

same period, but it would be of great interest to directly compare EMGdi and pressure measurements in future studies.

4.6 Conclusion

In summary, this study addressed concerns with the use of oesophageal and epiglottic pressure deflections as a measure of ventilatory drive in OSA, and for the first time clearly demonstrates quite substantial effects of occlusion itself on oesophageal and epiglottic pressure swings before chemo-reflex augmentation in underlying ventilatory drive. Given excellent fits based on theoretical considerations of respiratory system mechanics, relatively straight-forward corrections to consider Pmus instead of Poes or Pepi as a marker of underlying drive are possible. However, uncorrected Poes and Pepi swings remain relevant for understanding changing collapsing forces on the airway itself, and mechanoreceptor mediated stimuli to upper airway dilator and inspiratory pump muscles. However, the translation of neural ventilatory drive into pressure changes clearly involves complex interdependencies with respiratory mechanics such that using oesophageal or epiglottic pressure changes alone will systematically overestimate ventilatory drive changes in the presence of obstruction. The magnitude of obstruction effects were in the order of 20% for Poes, and around 100% for Pepi on the first occluded breath, although the relative contribution of these effects would be likely to diminish with subsequent ventilatory drive augmentation. Future studies relying on Poes or Pepi pressure swings for inferring changes in ventilatory drive or arousal threshold should consider these effects along with a flow and volume based correction.

Chapter 5

A novel method to quantify respiratory effort

The final limitation with oesophageal pressure identified at outset of this project was the inherent inter-subject variability in pressure measurements, reflective of physiological differences in the respiratory system. This chapter describes the theory and implementation of a novel method to derive an attempted ventilation signal from oesophageal pressure, using respiratory mechanics equations. This provides a more easily interpretable marker of respiratory effort that can be compared directly to measured ventilation in units of flow.

This aligns with aim 3 of the thesis: to implement and test a novel method to quantify respiratory effort and obstruction breath-by-breath in OSA using the classic respiratory equation of motion.

5.1 Background

Oesophageal and epiglottic pressure changes on inspiration provide the current "gold-standard" measures of breathing effort and the respiratory arousal threshold in sleep (Eckert and Younes, 2014; Gleeson et al., 1990). However, units of pressure change are inherently difficult to interpret and to compare between individuals. Absolute values of pressure are highly dependent on the mechanical properties of each individual's respiratory system, and on catheter placement and body position (Gulati et al., 2013; Guérin and Richard, 2012). Relative pressure swings, including in muscle pressure (Pmus) calculated using the Campbell diagram (Campbell, 1958), and diaphragm muscle electrical activity (EMG) changes are potentially more informative, but how these relate to the magnitude of the underlying neural respiratory drive to breathe and translate into achieved ventilation remains difficult to discern. Comparisons between individuals are especially problematic, particularly in obstructive sleep apnoea patients where complex and dynamic relationships between achieved ventilation, breathing effort and arousal from sleep likely reflect features of OSA combined with obesity effects on respiratory mechanics and the translation of neural activity into respiratory motion.

Obstructive sleep apnoea is characterised by periods of partial airway obstruction and flow limitation or total airflow cessation from complete obstruction, despite continued respiratory effort (see Figure 5.1). However, physiologically meaningful quantification of obstruction in OSA is inherently problematic. For clinical diagnosis, obstructive events are traditionally scored visually based on arbitrary and changing scoring criteria designed around manual scoring practicalities and reproducibility. Conventional definitions for adults require a substantial reduction in peak nasal cannula pressure and/or oro-nasal thermistor signal deflections of $\geq$90% for an apnoea and $\geq$30% for hypopnoea that last at least 10 seconds. Hypopnoea events also require an oxygen desaturation and/or an

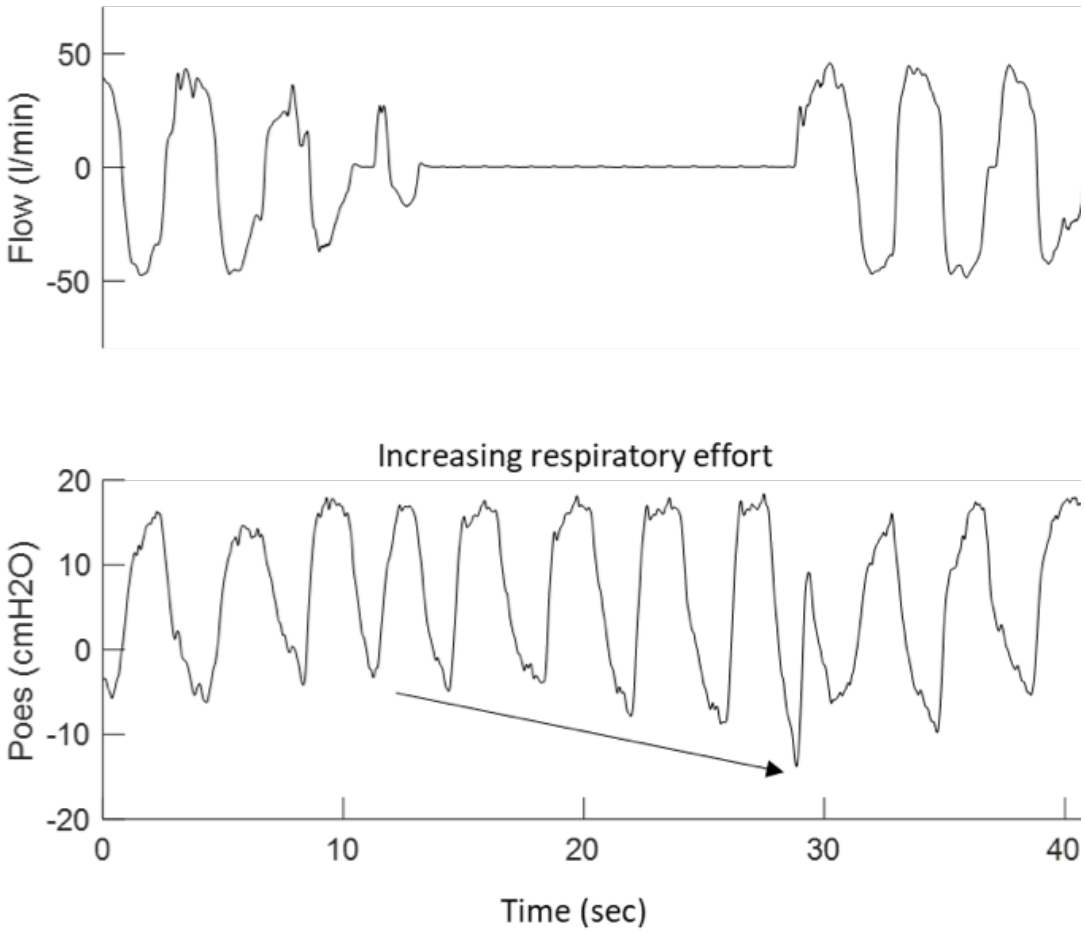

Figure 5.1: Oesophageal pressure changes during an apnoea event. Pressure swings become increasingly more negative as respiratory drive increases. However, relative pressure changes are inherently difficult to relate to airflow and to compare between individuals with potentially quite different respiratory mechanics.

arousal according to more variable American Academy of Sleep Medicine (AASM) scoring criteria (Iber et al., 2007). OSA is then defined on the basis of the average event count per hour of sleep, termed the apnoea-hypopnoea index (AHI), exceeding a pre-defined cut-off most appropriate for the specific scoring criteria used. This approach recognises the need for practical diagnostic signal acquisition and analysis methods, and greatly simplifies quantification of highly dynamic processes in sleep, but has several problems. Firstly, conventional event scoring takes no account of obstruction duration or the degree of reduction in ventilation beyond passing pre-specified arbitrary minimum duration and amplitude reduction threshold criteria. Secondly, nasal cannula pressure and oro-nasal thermistor signals are highly non-linear, which limits their utility for reliable quantitative ventilatory measurements. Square-root transformation can help to linearise nasal cannula pressure. Similar linearisation of thermistor signals is also possible, but ultimately, snug-fitting masks fitted with calibrated flow sensors are necessary for reliable quantitative measurements of airflow and ventilation. However, these measurements reflect only the achieved level of ventilation rather than the level of ventilatory drive of effort required to achieve them, which is also strongly influenced by upper airway patency in OSA. Thus, measures of inspiratory effort are also often of interest for understanding pathophysiological processes in respiratory problems such as OSA and central sleep apnoea (CSA), and potentially other respiratory conditions such as chronic obstructive pulmonary disease (COPD) and asthma.

During sleep, peak nasal cannula pressure or thermistor based deflections relative to chest and abdominal movements are further used to help classify central and mixed events characterised by pauses in the central neural drive to breathe. Whilst this remains a practical and accepted diagnostic approach, considerable uncertainty remains regarding the clinical significance of these events and the importance of absent or reduced ventilatory effort for precipitating cyclical airway obstruction in OSA.

Thus new tools are required to better quantify ventilatory effort and the severity of airway obstruction within and between breaths, as well as the relationships with other variables such as sleep stage, arousal and upper airway and ventilatory pump muscle activity. This is fundamentally needed to help better understand pathophysiological mechanisms in OSA, and to advance improvements in diagnostic methods and treatments.

An understanding of breathing effort is also vital to understanding the mechanisms of collapse and airway recovery in OSA. There is evidence to support that augmenting respiratory effort is the main compensatory mechanism ultimately responsible for the recovery of sufficient airflow to support stable breathing, and for restoring airway patency following partial or complete upper airway obstruction. Firstly, deep sleep is associated with fewer

respiratory events and increased oesophageal pressure swings (Ratnavadivel et al., 2009). Mild flow limitation can be counteracted by either increased pump muscle recruitment or duty cycle changes (Jordan et al., 2007). Finally, increasing respiratory effort appears to play the major role in promoting both arousal and stimulating upper airway dilator muscle activity through a combination of augmented inspiratory effort and negative pressure mechano-receptor mediated activity (Younes, 2003). Clearly, better tools are still needed to measure these changes over periods of interest across the course of the night.

To more comprehensively examine these concepts, we have developed a new analytic method to circumvent the main issues with current inspiratory effort measurements. This classic respiratory system equation of motion model-based method provides continuous estimates of airflow and volume expected to result for any given change in transpulmonary pressure, assuming the resistive and elastance properties of the respiratory system remain constant. This method provides a clear, visual and quantifiable measure of obstruction on a breath-by-breath basis, and has significant potential to help validate future tools that could potentially provide less invasive measures of obstruction and respiratory effort without the need for intrathoracic pressure measurements. This chapter first outlines the underlying theory, using basic respiratory mechanics, to derive a set of equations to model the respiratory system. This model was then tested on data collected from a small group of patients with severe OSA to demonstrate the significant utility of this new method for quantifying inspiratory effort in units of attempted airflow, volume and minute ventilation. These derived measurements were then directly compared to achieved levels to provide quantitative information about the complex inter-relationships between inspiratory effort, airway patency, achieved ventilation and arousal underpinning OSA.

5.2 Theory

During active breathing, the respiratory system is driven by transpulmonary pressure changes created by recruitment of inspiratory muscles to expand the thorax. The total driving pressure must overcome the elastic and resistive properties of the respiratory system in order to achieve airflow and lung volume changes. This relationship is well described by the classic respiratory system equation of motion (Campbell, 1958; Mead and Agostoni, 1964);

$$\Delta P(t) = R.\Delta \dot{V}(t) + E.\Delta V(t) \tag{5.1}$$

where $P(t)$, $V(t)$ and $\dot{V}(t)$ are pressure across the respiratory system, volume and flow (1st derivative of volume) at any time t, R and E are total respiratory system resistance

and elastance respectively. Inertance effects are ignored as negligible (Mead and Agostoni, 1964).

Assuming linearity, R and E are taken to be constants of the system. Mechanically, this corresponds to a two-compartment model where the respiratory system is modelled as a resistive tube (airway) in series with an elastic balloon (lung) with a pressure difference applied across it. This simplified linear system relating pressure and volume is commonly used in respiratory medicine to derive parameters of respiratory mechanics, and has been shown to be highly effective in modelling mechanics in the normal ranges of lung volume changes (Campbell, 1958). The system becomes non-linear at more extreme lung volumes, though this is unlikely to be a significant factor in most OSA patients where end-expiratory lung volume changes are likely to be relatively modest and ventilatory changes rarely depart too far from the tidal volume range. Nevertheless, for large changes in lung volume and in patients with lung disease where the compliance curve can shift considerably and breathing efforts may traverse less linear parts of the respiratory system compliance curve, the assumption of linearity would become progressively more problematic.

The total pressure generated by the patient's inspiratory muscles, Pmus, must overcome both the static recoil pressure of the chest wall, Pcw, and generate negative pleural pressure, Ppl, that drives inspiratory flow. In much of sleep medicine, oesophageal pressure deflections have been used as a direct measure of respiratory effort, with no consideration of chest wall effects. As shown in the previous chapter, this is likely to be more of a problem during airway obstruction, where impeded lung volume changes will reduce chest expansion and hence the contribution from the Pcw term. Assuming respiratory drive remains constant, a greater proportion of Pmus would be expected to be transformed into negative Ppl during obstruction, such that recorded Poes values become more negative, despite the same underlying ventilatory drive.

To account for this when using Poes as a measure of drive, we propose a volume-dependent chest wall component ($E_{cw}.\Delta V$ where E_{cw} is the elastance of the chest wall) to Poes prior to analysis to provide a better estimate of Pmus.

$$P_{mus} = P_{pl} + P_{cw} \approx P_{oes} + E_{cw}.\Delta V \tag{5.2}$$

where pressure P_{mus} is now the total muscle pressure generated. In the previous chapter, we showed that this approach could well account for a quite substantially more negative Poes deflection, in the order of 20-25%, on the breath immediately following externally applied airway occlusion in a group of OSA patients. The estimated average chest wall elastance value to account for occlusion was found to be approximately 9.8 cmH_2O.

Inserting this into equation 5.1, we find

$$\Delta P_{oes} + E_{cw}.\Delta V(t) = R.\Delta \dot{V}(t) + E.\Delta V(t) \tag{5.3}$$

The chest wall behaviour is now accounted for on both sides of the equation, with a correction to Poes on the left and in adjusted constants of elastance E and resistance R to account for total impedance across the respiratory system, including both flow related and chest wall related effects. In a patent airway, the chest wall term could be cancelled from both sides by using an adjusted effective elastance, $E' = E - E_{cw}$. However, for the sake of modelling attempted ventilation from in the presence of obstruction, actual volume change and attempted volume change will not always correspond and so we include the mechanical chest wall effects separately on the left hand side of Equation 5.3.

Equation 5.2 can be solved via an integration factor to obtain a function for V(t) which is then differentiated to give $\dot{V}$(t);

$$V(t) = \frac{1}{R} e^{\frac{-E}{Rt}} \int_0^T P_{mus}(t) e^{\frac{E}{Rt}} dt \tag{5.4}$$

$$\dot{V}(t) = \frac{-E}{R^2} e^{\frac{-E}{Rt}} \int_0^T P_{mus}(t) e^{\frac{E}{Rt}} dt + \frac{1}{R} e^{\frac{-E}{Rt}} P_{mus}(t) e^{\frac{E}{Rt}} \tag{5.5}$$

R, E and Pmus(0) can be estimated from airflow and oesophageal pressure during unobstructed breathing via Equation 5.1 and multiple linear regression. Equations 5.4 and 5.5 can then predict continuous volume and flow from Pmus and best fit E and R values, assuming that these remain constant. Whilst this assumption is clearly untrue when the airway partially or completely collapses, this approach is simply a re-arrangement of classic respiratory mechanics which elegantly avoids problems with resistance changes through to infinite (closure) in sleep and greatly simplifies visualisation, quantification and interpretation of obstruction. Continuous flow and volume can readily be derived analytically with simple code from Equation5.3. The script to perform this can be found in Appendix B.

5.3 Methods

The model was tested on previously recorded airflow (mask and pneumotachograph) and Poes (latex balloon catheter) from 8 males with severe OSA (mean±SD age 44±9 yr, BMI 35±5 kg/m^2, AHI 77±29 /hr). These data were available from a previous study (Stadler et al., 2010) approved by the Southern Adelaide Clinical Human Research Ethics

Committee and for which participants provided informed written consent. Signals were recorded using a DataQ acquisition system (Model DI-720, DataQ Instruments, Ohio, USA) and imported into MATLAB (The MathWorks, Natick, 2017) for analysis. Standard polysomnogram signals were also collected using a separate acquisition system and respiratory events and sleep staging were scored by a trained sleep technician. Events were time matched between the two acquisition systems using linear interpolation between event markers placed in both systems.

Oesophageal pressure signals were first filtered using a custom template-based method described in Chapter 3 to remove cardiogenic artefact. Volume was integrated from flow, after first accounting for any mask leak or baseline drift. Pmus was then derived by subtracting a volume dependent chest wall component from Poes, using the average value E_{cw} = 9.8 cmH_2O determined in Chapter 4. Individual patient values of chest wall elastance, E_{cw}, are likely to vary due to physiological differences in each respiratory system, as shown by the inter-subject variability observed in the results of Chapter 4. However, the standard error ($\pm$1.2cmH_2O) was relatively small so it seems this is a reasonable approximation. To determine a more accurate value of chest wall elastance for each subject, an abrupt total occlusion is required so that changes in pressure swings can be quantified, as per the methodology in Chapter 4. In naturally occurring obstruction events, airway collapse is much more dynamic, and often gradual, such that chest wall effects in pressure cannot be separated from other drive-related augmentation to pressure swings.

For a five minute period of stable breathing awake, pneumotachograph flow and both Poes and Pmus were separately fitted to the model to estimate values of respiratory system resistance and elastance for each subject using multiple regression. Attempted airflow and minute ventilation ("effort") expected from Pmus during the remainder of the night were subsequently derived on the basis that the airway had remained open with the same values of elastance and resistance. In this way, two attempted ventilation signals were derived, one from Poes and one from Pmus, to compare the effect of the chest wall correction on signals. Attempted flow signals were then compared to achieved airflow as measured via the pneumotachograph. Attempted volume was calculated by integrating the attempted flow signal. Achieved and attempted inspiratory minute ventilation values were then determined for each breath using the inspiratory tidal volumes and the derived attempted ventilation signal to determine breathing frequency from effort. In this way, an effort-by-effort value of the achieved ventilation could be compared to that which was expected had the airway remained patent, even if the airway is in fact completely collapsed. The breath-by-breath ratio of achieved to attempted ventilation was used to define an obstruction ratio, in which a value of 0 is fully obstructed and 1 fully patent. This provides a marker of changes in airway patency over the course of the night.

Table 5.1: Individual patient fits for E, R and r^2

Subject	E (cmH2O/l/s)	R (cmH2O/l/s2)	r^2
1	8.1	15.4	0.92
2	15.2	10.3	0.99
3	5.5	27.1	0.93
4	4.2	19.8	0.91
5	13.5	16.0	0.98
6	6.5	8.9	0.92
7	4.5	6.5	0.95
8	6.5	21.6	0.96

5.4 Results

The model produced excellent fits to the respiratory equation of motion, with (mean ± SD) r^2 values of 0.94±0.06 during periods of stable breathing in OSA patients. Individual patient fits for E, R and r^2 are given in 5.1. An example of the model fit from both Poes and Pmus during a 60 second stable breathing is shown in Figure 5.2. Pmus pressure swings are greater than those in Poes, exhibiting more negative nadir values, as a result of the additional chest wall term. However, the attempted ventilation traces derived from Pmus and Poes are very similar during the period of stable breathing, and both closely match the measured pneumotachograph flow signal. There is some residual cardiogenic artefact, but oscillations are reduced relative to the unfiltered pressure trace. Inspiratory and expiratory volume changes calculated by integrating flow are similar from both attempted and measured ventilation.

The derived values of constants E and R were then used in the model to calculate ventilation from Pmus and Poes. When applied to sleep data across the remainder of the night, the model clearly demonstrates marked changes in breathing effort during obstruction and airflow recovery. Figure 5.3 shows examples of the model applied to determine attempted flow and volume during periods of flow limitation and apnoea (total airway collapse). Over obstructed breaths, there is a clear difference between the attempted ventilation signals derived from Pmus (black line) and Poes (dotted line). The Poes-derived signal exhibits greater peak values of attempted flow during apnoea, and reduced attempted flow on the first recovery breath. The Pmus pressure deflection is more negative on the first recovery breath than in Poes, and the Pmus-derived ventilation signal more closely corresponds to the achieved flow signal on this breath. Minute ventilation was also calculated from achieved and attempted flow over the inspiratory effort, using the attempted flow baseline

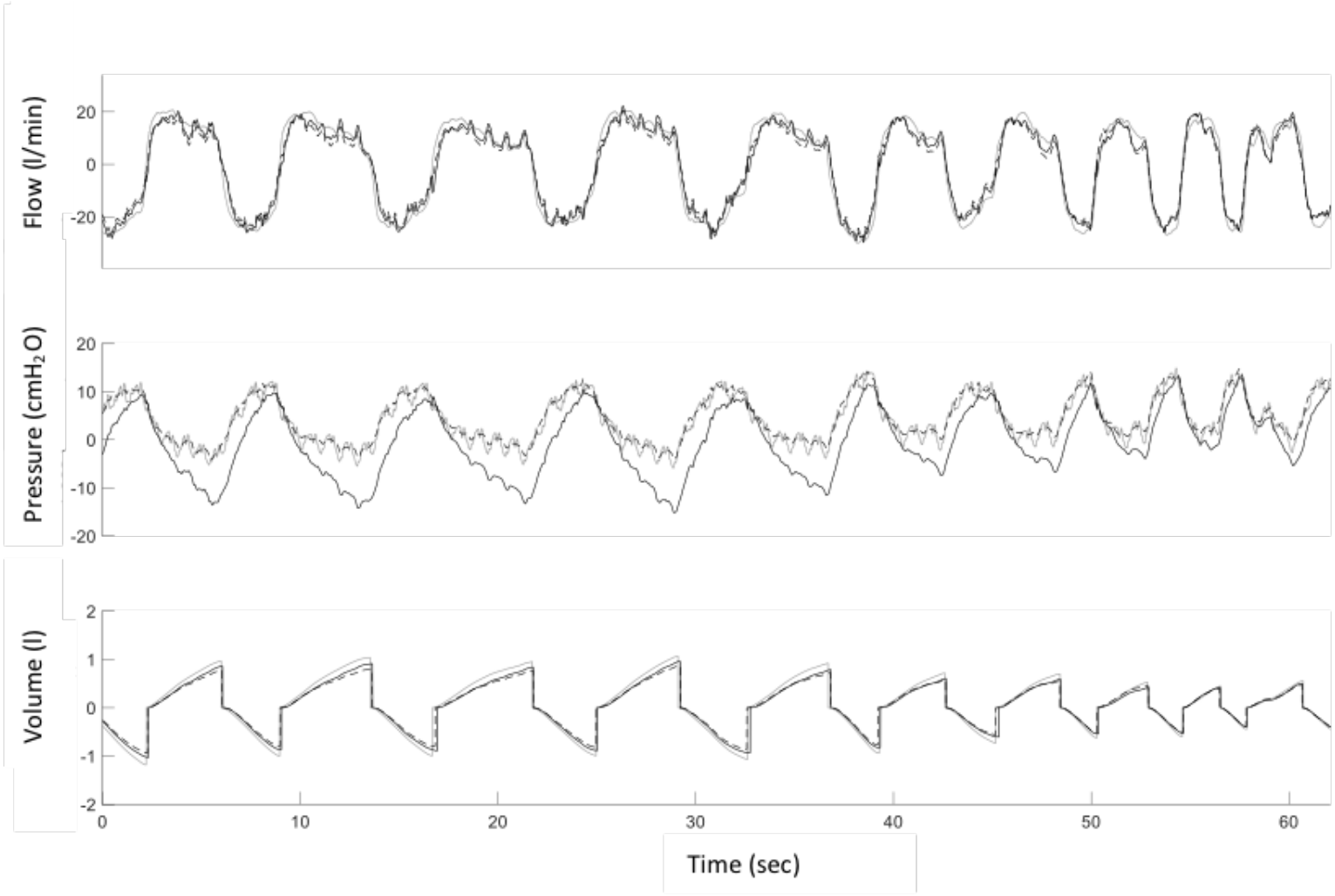

Figure 5.2: Attempted flow and volume derived from fits of filtered Poes (dotted lines) and Pmus (black lines) compared to measured flow and volume (grey line) at the mask during stable breathing. Pressures displayed are Pmus (black line), filtered Poes (dotted line) and unfiltered Poes (grey line).

crossing to define inspiratory effort duration. When the airway is patent, inspiratory effort duration closely corresponds to inspiratory breath duration, however during obstruction, the two do not always correspond. Therefore effort duration is used to calculate ventilation parameters and the obstruction ratio, as shown in Figure 5.4. A further example of ventilation parameters and the obstruction ratio from Pmus over a period of less severely obstructed breaths is given in 5.5.

5.5 Discussion

This novel method provides continuous estimates of attempted airflow and volume that should have resulted from dynamic driving pressure changes had the airway remained patent and the respiratory system continued to behave with the same mechanical properties as during stable breathing. Attempted airflow, volume and ventilation can then be compared directly with achieved flow, volume and ventilation traces, simplifying the interpretation of Poes and avoiding problems with modelling flow-pressure relations with continually changing resistance values through to infinite (at closure) during sleep. Unlike any previous Pmus, Poes or EMG derived measure, this estimates an individual's moment-to-moment attempted airflow (an index of inspiratory effort) in units of ventilation directly comparable to measured flow and ventilation. This provides information about when obstruction commences within and between breaths, and a comprehensive method for quantifying airway patency changes over time and over the course of obstructive events and their recovery. When combined with simultaneous EMG measures, greater insight into EMG translation to ventilation output and between group comparisons also become possible.

Furthermore, the zero-crossings in the attempted flow signal provide clear start and end points of inspiratory effort. These are much more easily and more reliably determined algorithmically than turning points in pressure, which requires rate-of-change thresholds that vary between individuals and can be distorted by artefact. Effort start and end points can be used as the timing basis of breath-by-breath measures from achieved flow over the course of obstruction, as is shown for ventilation and the obstruction ratio during apnoea in Figure 5.4. This circumvents issues in analysis when individual breaths cannot be clearly defined from flow during apnoea.

Pmus swings, with the additional chest wall correction, continue to increase on the first two breaths after airway reopening, unlike Poes swings which reduce immediately on the first breath of airflow recovery. Central ventilatory drive would be expected to be consistent over this period, as both the central and peripheral chemo-reflex systems have delays

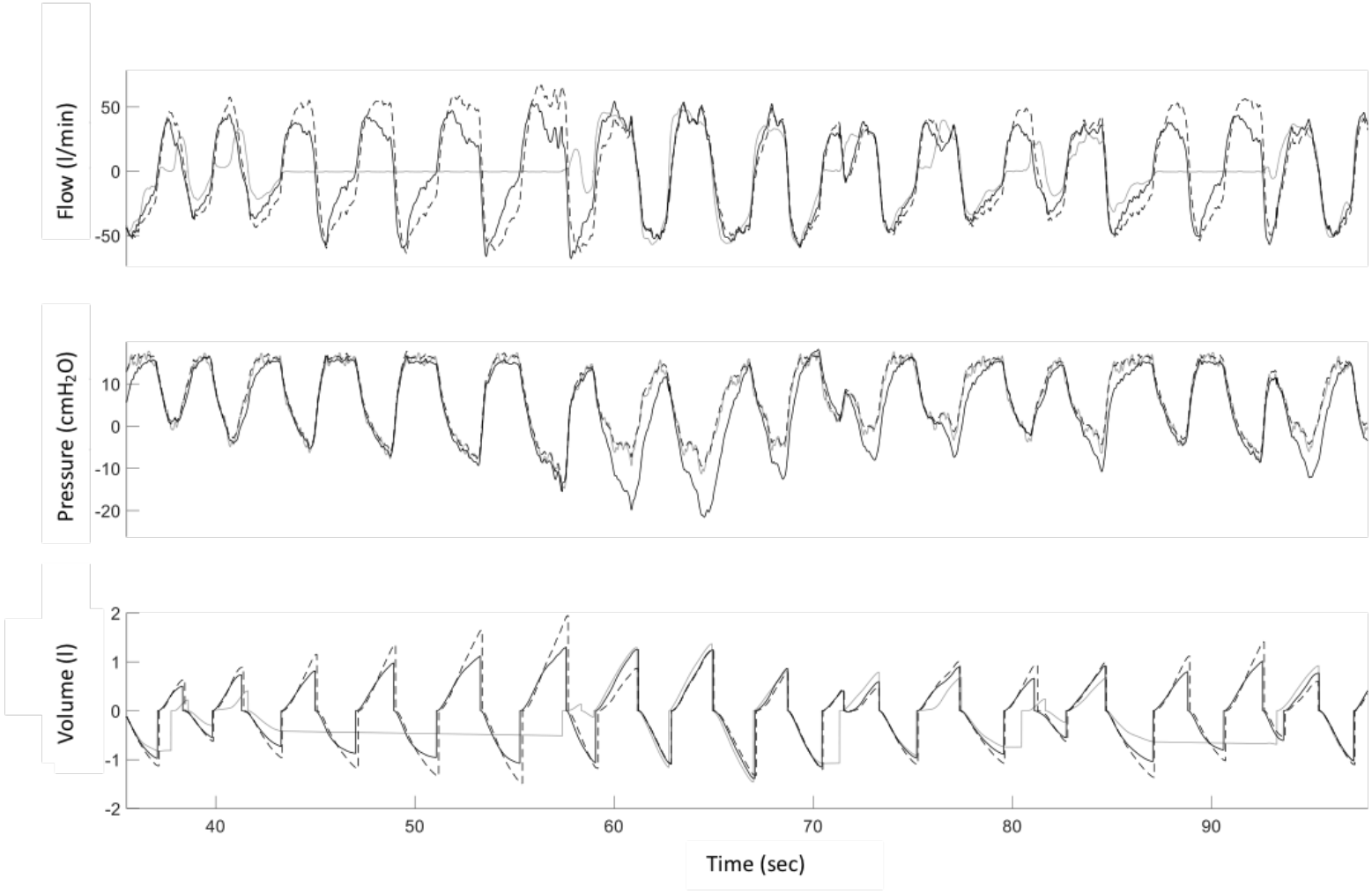

Figure 5.3: Attempted flow and volume derived from fits of Pmus (black lines) and Poes (dotted lines) compared to measured flow and volume (grey line) at the mask during a four breath total obstructive apnoea event, a subsequent 2 breath apnoea and intervening partially obstructed breaths. Pmus, with a volume dependent chest wall correction, provides a better fit to flow at the resumption of airflow.

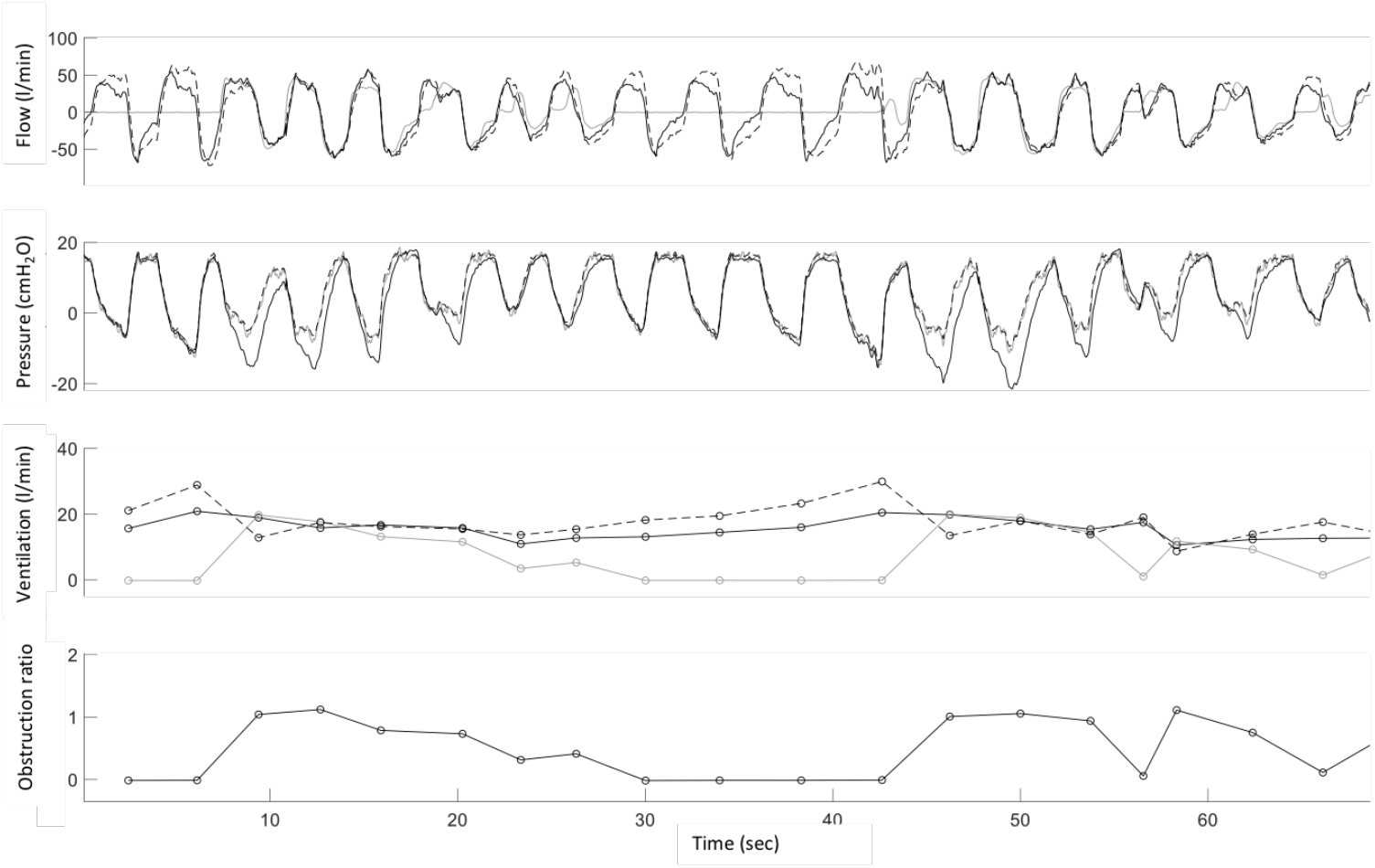

Figure 5.4: Attempted flow and ventilation derived from fits of Pmus (black line) and Poes (dotted line) compared to measured flow (grey line) at the mask during an obstructive event. Minute ventilation is calculated from attempted ventilation start and end points for both achieved and attempted ventilation, and the ratio of achieved to attempted ventilation provides an effort-by-effort obstruction ratio useful to quantify airway patency.

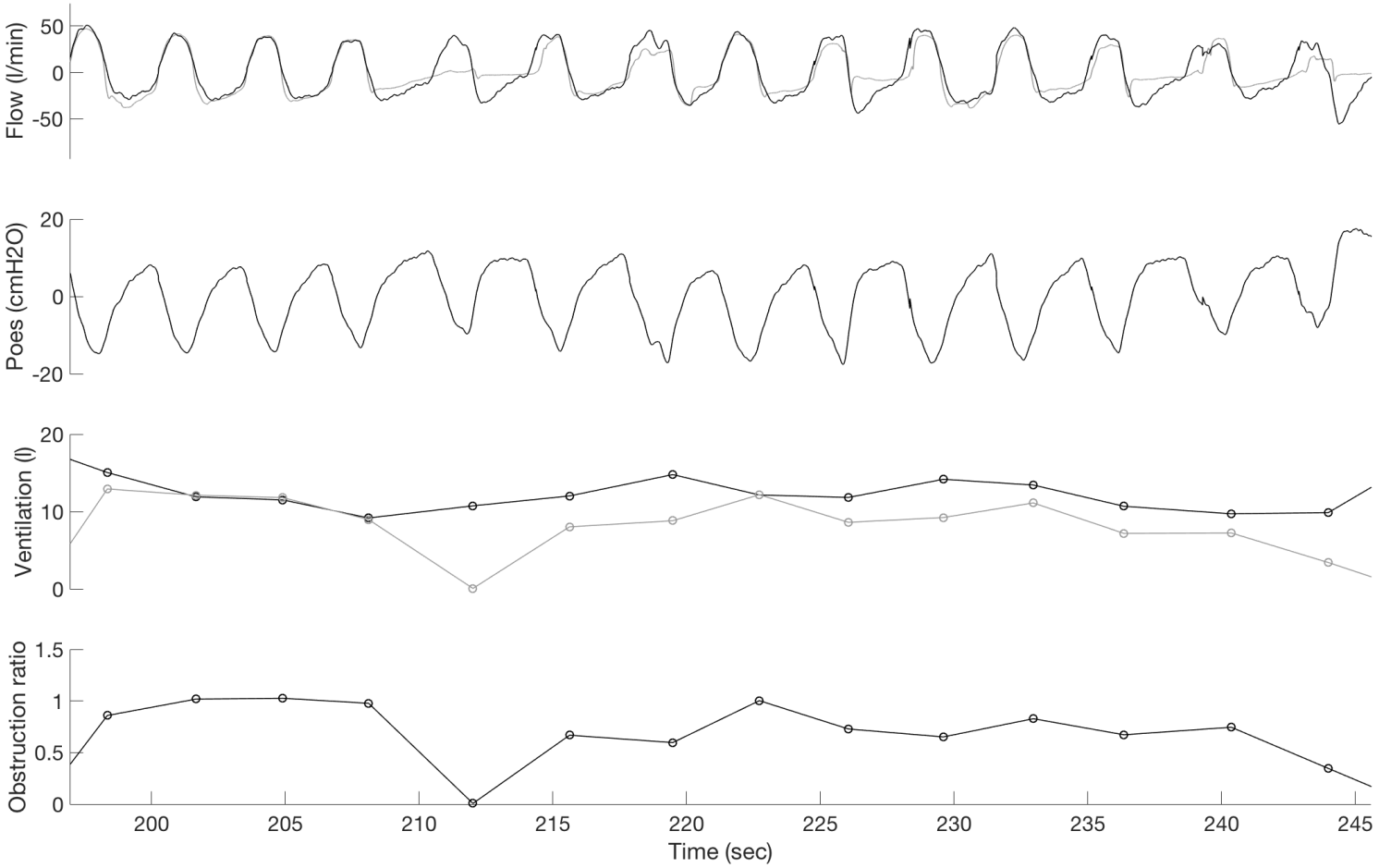

Figure 5.5: Attempted flow and ventilation derived from fits of Pmus (black line) compared to measured flow (grey line) at the mask during a less severe obstructive. Minute ventilation is calculated from attempted ventilation start and end points for both achieved and attempted ventilation, and the ratio of achieved to attempted ventilation provides an effort-by-effort obstruction ratio useful to quantify airway patency.

exceeding this time frame. Therefore, as an effort signal, it appears Pmus more closely corresponds to central drive than Poes. This further supports the use of a chest wall correction when using Poes as a marker of effort.

The use of the equation of motion is well established in respiratory medicine, but has never been used to derive a ventilatory signal from oesophageal pressure. The interpretation of breath-by-breath measurements is greatly simplified when using a flow signal as opposed to a pressure or EMG signal where units are not directly comparable to ventilation. Attempted inspiratory start and end times and volumes are much more easily quantified from baseline crossings in the modelled flow signal as opposed to turning points in raw oesophageal pressure, particularly for defining where end inspiration occurs during the passive recoil of the breathing cycle.

A key difference with this tool and other models is its simplicity. In the 1980s Younes and Riddle used a series of assumptions regarding how neural drive converts into pressure changes to advance a theoretical model for relating ventilatory effort to output (Riddle and Younes, 1981; Younes and Riddle, 1981; Younes et al., 1981). As Younes and Riddle pointed out, the relationship between dynamic inspiratory driving pressure and flow is modelled simply by the classical respiratory equation of motion. However the relationship between inspiratory muscle activity and pressure output is much more complex. We acknowledge that modelling the respiratory system response to airway collapse, including the flow and volume effects and configurational change, is highly complex, and indeed not possible with the basic respiratory system equation of motion, as laid out by Younes and Riddle. However, our method makes no attempt to do so, but instead simply models the flow expected from measured driving pressure had airway patency been maintained. This approach has fewer assumptions, fewer model terms and is more easily fitted and applied to experimental data. This method enables direct comparison of modelled flow to achieved flow to provide an obstruction metric that can assess airway patency on a breath by breath basis.

Obstruction is known to elicit load compensation responses throughout the respiratory system, which alter how neural drive is converted into muscle pressure. This is a highly complex process, with three main components: reflex responses mediated by muscle sensory afferents or pulmonary stretch receptors; intrinsic muscular compensation due to altered force/length or force/velocity responses or reduced radius of curvature of the diaphragm; and finally ventilatory drive augmentation modulated by chemo-reflex responses. By measuring oesophageal pressure effectively downstream from these neuromuscular factors, these effects are encapsulated within the model, thereby incorporating both neural and mechanical components. The effect of occlusion on pressure values themselves, how-

ever, could additionally alter transpulmonary pressure. The previous work described in Chapter 4 suggested a volume dependent chest-wall term could account for the majority of the variance between an acutely occluded compared to the pre-occluded breath, assuming ventilatory drive remained constant. Building this correction into the model through a volume-dependent chest wall term, should substantially help to account for such effects.

In summary, this new method for estimating ventilatory effort provides measurements with the same units of ventilation directly comparable to measured ventilation. This simplifies inter-subject comparisons and allows for a continuous breath-by-breath measure of airway obstruction. This new method holds significant promise for providing unprecedented new insights into moment-to-moment changes in inspiratory effort versus output across a broad range of respiratory problems such as OSA.

Chapter 6

Physiological measures around occlusion

In the previous chapter, a novel method of quantifying respiratory effort as a continuous measure of ventilation was developed and implemented in software with the aim of providing an enhanced understanding of ventilatory drive augmentation during sleep in OSA. This chapter describes the use of this new tool to explore relationships between respiratory effort augmentation, muscle recruitment and CO_2 chemo-reflex drive around both airway collapse and airway reopening.

This aligns with Aim 4 of the thesis: to use the new tools developed to investigate the underlying role of inspiratory drive and negative pressure during obstruction and in compensation mechanisms for dilator muscle recruitment and flow recovery, with and without arousal.

6.1 Background

Airflow recovery at obstructive event termination is thought to result once sufficient muscle recruitment is achieved to overcome collapsing forces and reopen the airway, often, but not always, in association with arousal (Younes, 2008). Those events in which arousal does occur have been found to be more severely obstructed and exhibit higher ventilatory overshoot when patency is re-established, and more often are associated with secondary obstruction events (Jordan et al., 2011; Younes, 2004). However, these changes were no longer significantly different between arousal conditions when matched for obstruction severity (Jordan et al., 2011). In theory, ventilatory overshoot is likely to promote hypocapnia and lower the chemo-reflex modulated neural drive to respiratory pump and upper airway dilator muscles, potentially leaving the airway more vulnerable to secondary collapse. Arousal has been shown to induce hypocapnia in the post-arousal period, however there was no sign of reduced genioglossus activity as a result (Cori et al., 2017). The authors propose this may reflect a form of respiratory after-discharge in upper airway muscles, in which muscle recruitment is elevated for an extended period after arousal to compensate for decreased ventilatory drive with hypocapnia. However, this analysis was limited to a relatively short period of five breaths following the return to sleep, which may be too short to fully encompass central chemo-reflex system delays. Falls in genioglossus activity below baseline levels may only be evident over time-periods beyond 10-20 seconds following hyperventilation. Invariably, however, over a longer observation period it is very difficult to control for other mechanisms like arousal or collapse further augmenting muscle behaviour. During sleep, where mild hypoventilation and hypercapnia normally develop relative to wake, it is also difficult to establish the most appropriate baseline levels of CO_2 and genioglossus muscle activity for comparison of subsequent changes, particularly in

those OSA patients who fail to achieve extended periods of stable breathing in sleep. Cori et al used the pre arousal breath as their baseline for subsequent comparisons of post-arousal changes in genioglossus activity (Cori et al., 2017). However other non-arousal mechanisms can recruit upper airway dilator muscles prior to arousal which may then systematically confound results expressed as changes from an immediate pre-arousal level. The relationship between hypocapnia, ventilatory drive and muscle recruitment is clearly complex, and currently inadequately understood in respect to its role in cyclic collapse of the upper airway.

A loss of wakefulness drive at sleep onset may be a factor in failure to maintain sufficient airway patency to support stable breathing, especially in OSA patients with an airway vulnerable to collapse in sleep. OSA severity as measured by AHI shows marked improvement during deep sleep, when ventilatory drive is elevated (Ratnavadivel et al., 2009). Genioglossus recruitment has also been shown to be elevated during periods of stable breathing in sleep, with activity levels closely related to drive levels (Jordan et al., 2009). Furthermore, the arousal threshold has a strong dependence on ventilatory drive. However, the relative role of ventilatory drive in augmenting upper airway muscle activity versus promoting arousal/hyperventilation responses around the time of airway reopening in OSA is still unclear. Most of the previous studies into breath parameters at event termination were performed with standardised CPAP manipulations to induce flow limitation and arousal. However, it remains unclear how well CPAP study results reflect mechanisms operating during naturally occurring respiratory events in OSA, where interdependencies between ventilatory drive and output in sequential neighbouring events may be particularly important. No studies have previously been able to systematically examine relationships between achieved ventilation and ventilatory drive over the course of naturally occurring apnoea events in OSA. To help better inform potential mechanisms of airway obstruction and recovery in OSA, the aim of this study was to use the new tools developed in this thesis to undertake a more detailed examination of ventilatory and muscle activity changes over the course of naturally occurring obstruction events in OSA than has previously been possible. Systematic examination of relationships between markers of upper airway versus diaphragm muscle activity, along with changes in ventilatory drive and end tidal CO_2 (ETCO2) over the full course of obstruction onset and airflow recovery, was thought likely to help better understand the mechanisms underpinning cyclical upper airway collapse in OSA.

6.2 Methods

6.2.1 Data analysis

Existing patient data from 6 males with severe OSA, recorded during a detailed physiological observational sleep study, underwent custom analysis (Stadler et al., 2010). This study was designed to investigate changes in lung volume and EMGdi activity at sleep onset. In addition to standard polysomnography signals, an oesophageal catheter was used to record pressure and intra-oesophageal diaphragm EMG (EMGdi). Per-oral intramuscular electrodes were used to measure genioglossus EMG (EMGgg). Data were recorded at 200Hz for respiratory signals and 1kHz for EMG signals. The tools developed earlier in this thesis were implemented in this study. Poes and EMGdi were first filtered to remove cardiogenic artefact, as discussed in Chapter 3. EMGgg and filtered EMGdi were rectified and smoothed with a 100ms window moving time average. A volume based correction was applied to Poes to derive Pmus, accounting for chest wall mechanics in order to better reflect drive during occlusion, where measured values would be more negative, as presented in Chapter 4. An attempted ventilation signal was derived from the equation of respiratory mechanics and Poes to provide a marker of respiratory drive, as described in Chapter 5. Obstruction severity was then defined on a breath-by-breath basis from the ratio of achieved to attempted ventilation. A novel parameter easily assessed from the modelled attempted ventilation signal is the effort duty cycle, representing the relative time in the expiratory phase relative to active inspiratory phase of attempted ventilation, as derived from oesophageal pressure. This provides a new method for tracking the modulation of inspiratory pattern generation over the course of apnoea events. Arousal and obstruction were scored from usual PSG signals by a highly experienced sleep technologist according to AASM 2007 criteria (Iber et al., 2007), as appropriate at the time of the original study. Extra care was taken to carefully identify the start and end timepoints of each arousal event to ensure these were as marked as accurately as possible.

Events for analysis were confined to apnoeas only, which required a flow reduction >90% baseline. The reasoning for this was four-fold. Firstly, apnoeas can be relatively unambiguously defined, unlike hypopnoeas which have much more variable obstruction severity. The point of airflow restoration is also much more sharply defined, aiding breath-by-breath averaging relative to clearly defined obstruction onset and offset. Additionally, the corrections derived for occlusion effects in pressure have so far only been tested on abrupt total airway collapse. Finally, arousal is known to be associated with more severe respiratory events. Consequently, limiting our analysis to apnoeas was considered to be important to avoid potential skewing towards hypopnoeas with non-arousal events, where airflow

recovery mechanisms may be somewhat different.

Analysis was performed in MATLAB (The MathWorks, Natick, 2017). Start and end points of obstruction were identified algorithmically with a flow threshold and then manually reviewed to ensure accuracy. A custom user interface was built to facilitate this analysis (discussed in more detail in Appendix A). The analysis period for each event was defined from 15 seconds prior to obstruction onset through to 30 seconds after airflow recovery from apnoea events with and without an arousal immediately before or within 5 seconds of airflow recovery. An example period is shown in Figure 6.1. All data is included for analysis during this window, even if further secondary collapse occurs. This is important in investigating how quickly the airway becomes unstable following an apnoea event.

For the period leading into and out of airway obstruction, signals underwent custom breath-by-breath analysis to determine inspiratory and expiratory time (Ti, Te), tidal volume (Vti, Vte), minute ventilation (VI, VE) and breathing frequency (FB) for both attempted and achieved ventilation signals. Ventilation signals were scaled relative to values recorded during a 3-minute stable breathing period of wake, taking average peak ventilation over this period. Averaged rectified inspiratory and expiratory genioglossus and diaphragmatic EMG were calculated for each breath over the inspiratory and expiratory time period respectively. EMG values were scaled relative to the pre-event baseline value on breath -3 from obstruction onset. This strategy was used instead of a wake baseline because several files required multiple gain changes in EMGgg signals over the course of the night, as well as electrode displacement altering signal quality, rendering wake comparisons problematic. This breath was selected as the baseline as was found to be consistently most stable, and unlikely to be an arousal breath from previous events or significantly obstructed. A comparison of EMGdi signals relative to both a wake and pre-event average tonic activity baseline is presented in Appendix C. Figure D.5 shows this choice does not significantly effect the results presented, which would be expected to hold true for EMGgg signals also. ETCO2 was recorded as the final plateau value during each expiratory period, assessed from all breaths showing a clear end-expiratory plateau, accounting for circuit delay.

6.2.2 Statistical analysis

Group data are presented as mean±SD or SEM of within-subject averages to account for different numbers of repeated events per subject. Linear mixed model analyses were used to investigate fixed main effects between arousal conditions and time across breaths for

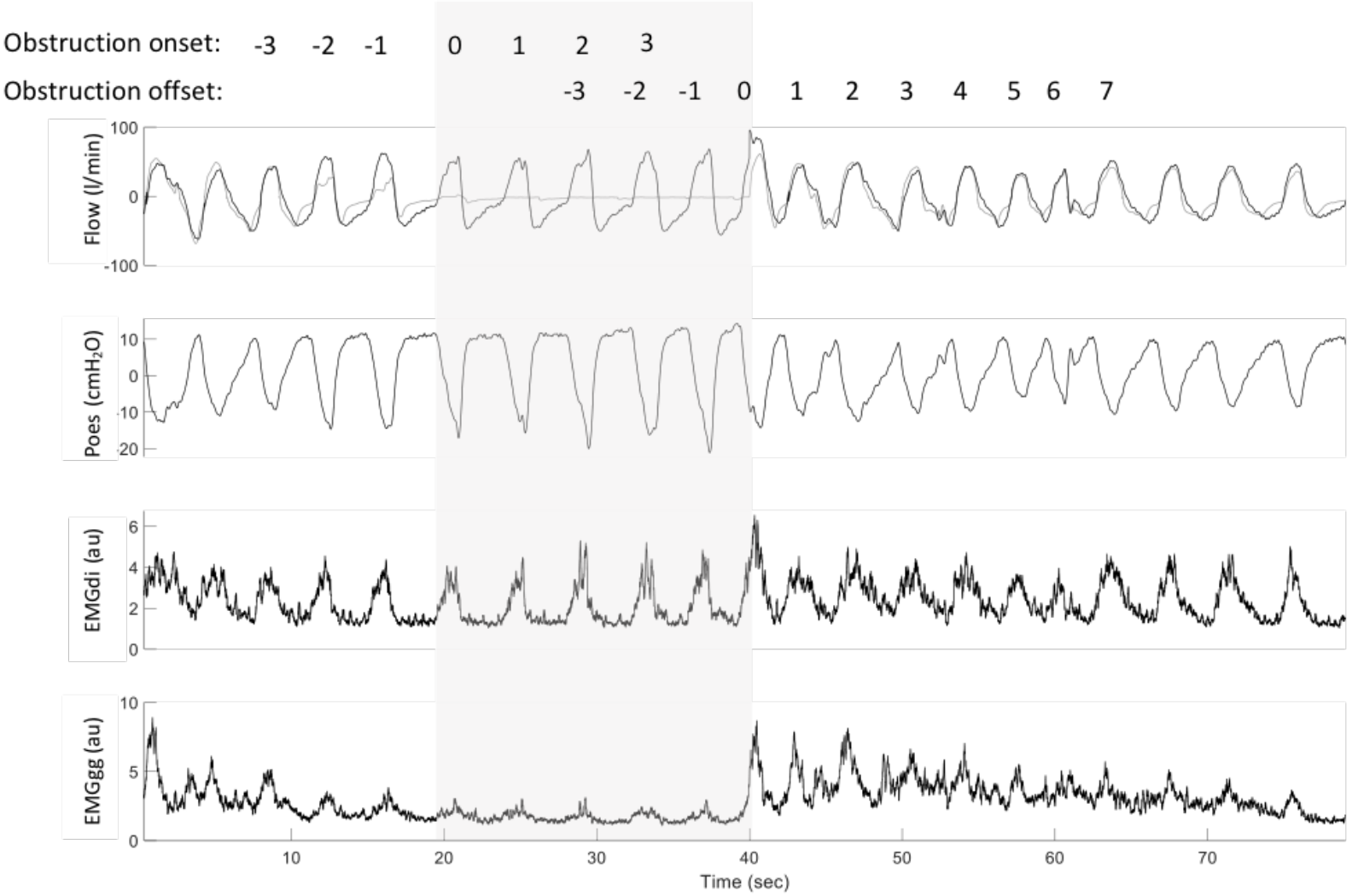

Figure 6.1: Example of an event for detailed analysis. Measured flow (grey) and attempted flow (black), derived from oesophageal pressure and respiratory mechanics had the airway remained patent, oesophageal pressure and EMGdi and EMGgg plotted over the course of an obstructive apnoea event. The obstruction region is shaded grey, and breaths are labelled relative to obstruction onset and offset. Achieved and attempted ventilation, inspiratory timings and average inspiratory and expiratory EMGgg and EMGdi were subsequently calculated for each breath for further quantitative analysis.

each respiratory parameter and their interaction, using breathing onset time as a covariate to account for the relative time of breaths from the airway obstruction or recovery. A random effect of subject ID was used to account for expected variance between-subjects. Where interactions were significant, breath-by-breath pair-wise comparisons were used to conduct pair-wise contrasts between arousal versus no-arousal conditions adjusted for multiple comparisons using Bonferroni corrections. Kaplan-Meier survival curves and Cox regression were performed to examine the likelihood of the airway remaining free of secondary obstruction following recovery, or re-obstruction free survival. The hazard of secondary airway re-obstruction in recovery cases with versus without an associated arousal event was determined, censored at 35-sec post airflow recovery. All statistical tests were run in SPSS (Version 22, IBM SPSS Statistics). $p<0.05$ was considered significant.

6.3 Results

Patients were all males with (mean±SD) BMI 36±5 kg/m^2, AHI 86±20 /hr, age 45±10 years and 129±88 obstruction events over the night. Across all subjects, 775 events were analysed. One subject lost EMGgg wires during the latter part of the night so these events were excluded from analysis.

6.3.1 Arousal distribution

The temporal distribution of scored cortical arousal relative to airway reopening is shown in Figure 6.3. The majority of airflow restoration events were associated with an arousal, with a sharp peak in the frequency distribution occurring a few seconds after airway patency had been re-established. Given the temporal distribution of arousals, obstruction events were divided into those in which arousal occurred within five seconds of airflow recovery, versus those with no arousal over the same interval for the remaining analyses. Apnoea events associated with arousal were of a greater obstruction duration (mean±SD 13.5±3.2 seconds vs 10.3±1.4 seconds, $p<0.02$). Figure 6.3 shows the arousal distribution within each individual.

Figure 6.2b shows Kaplan-Meier survival curves based on the time to the onset of the next scored obstructive event following airflow recovery (either apnoea or hypopnoea) from obstructive apnoeas with and without arousal events, demonstrating that obstruction recurred rapidly following airflow recovery in the majority of events. The presence versus absence of arousal did not alter the hazard of airway re-obstruction in the post airflow recovery period (Hazard Ratio±SE 1.01±0.11, $p=0.914$).

(a)

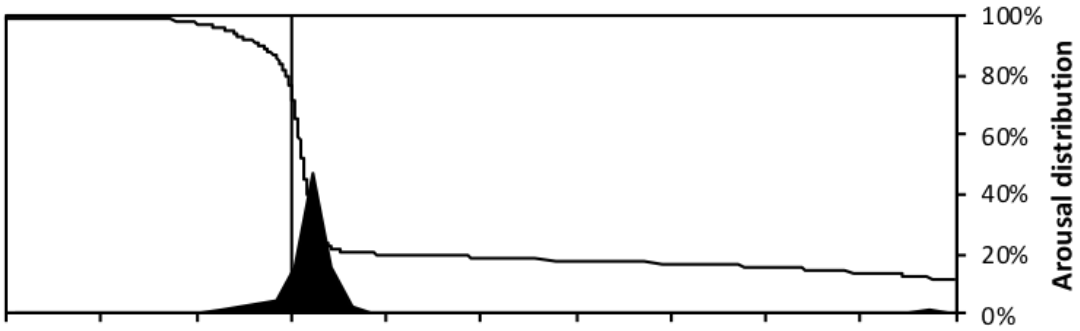

(b)

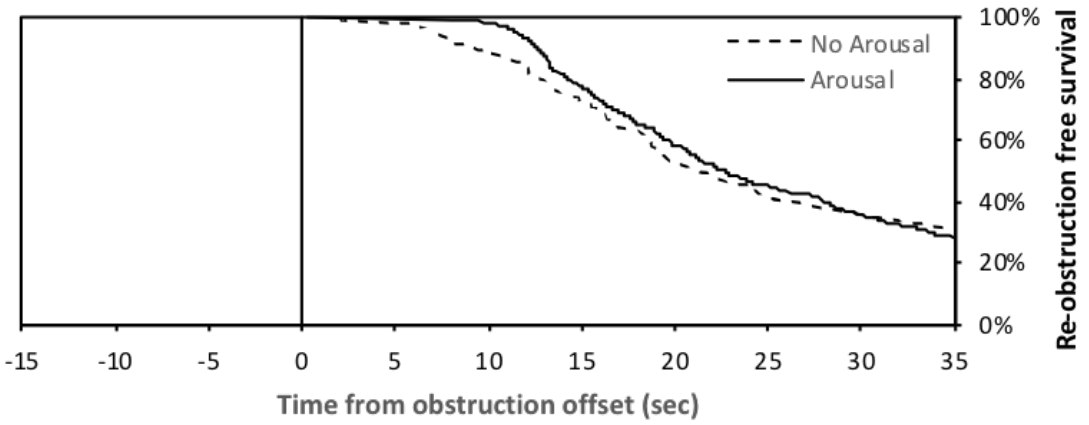

Figure 6.2: Distribution of arousal and re-obstruction relative to airflow recovery. a) Time relative to airflow restoration versus arousal frequency distribution for all obstructive apnoea events (n=775). Black shading indicates arousal frequency in 1-sec wide time bins and the solid line indicates the cumulative distribution and thus arousal free 'survival' up to 35 sec post airflow recovery. b) Re-obstruction survival curves for arousal events (solid line) and no arousal (dotted line) for the post recovery period relative to the time the airway reopened. Airway re-obstruction was classified on the basis of the onset of any scored hypopnoea or apnoea event.

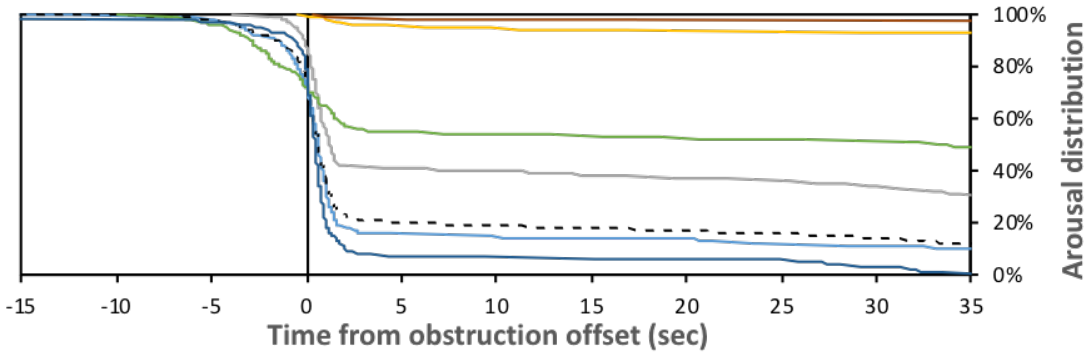

Figure 6.3: Time relative to airflow restoration versus arousal frequency distribution for individual subjects. The black dotted line shows the average of all the events as displayed in figure . The coloured solid lines each correspond to the arousal distribution of each individual subject.

6.3.2 Breath-by-breath analysis

Group average breath-by-breath values for key physiological parameters are shown in Figure 6.4 for the three breaths either side of obstruction onset and the three breaths prior to and eight breaths following obstruction offset, plotted at mean end inspiration time, relative to occlusion onset and offset respectively. Events are separated into those with and without arousal within 5 seconds of airway reopening. There was no statistically significant interaction effects between arousal conditions and the breaths around obstruction onset for any of the parameters calculated. Significant arousal versus breath number interaction effects were evident in attempted ventilation ($p=0.02$), obstruction ratio ($p=0.01$) and ETCO2 ($p<0.001$) over the end obstruction period. Individual patient data can be found in Appendix C.

6.3.3 Respiratory effort and ventilation

Respiratory effort as measured by attempted ventilation decreased on the three breaths preceding obstruction onset, then steadily increased, although the time effect was not statistically significant ($p=0.07$, Figure 6.4). There was no difference between arousal and non-arousal events over the same period. Attempted ventilation increased prior to airway reopening, and was significantly higher on the breath prior to airway recovery in events associated with arousal ($p=0.001$).

Over the following four breaths, attempted ventilation dropped to below the initial pre-event value at breath -3 from obstruction onset, but remained elevated relative to wake,

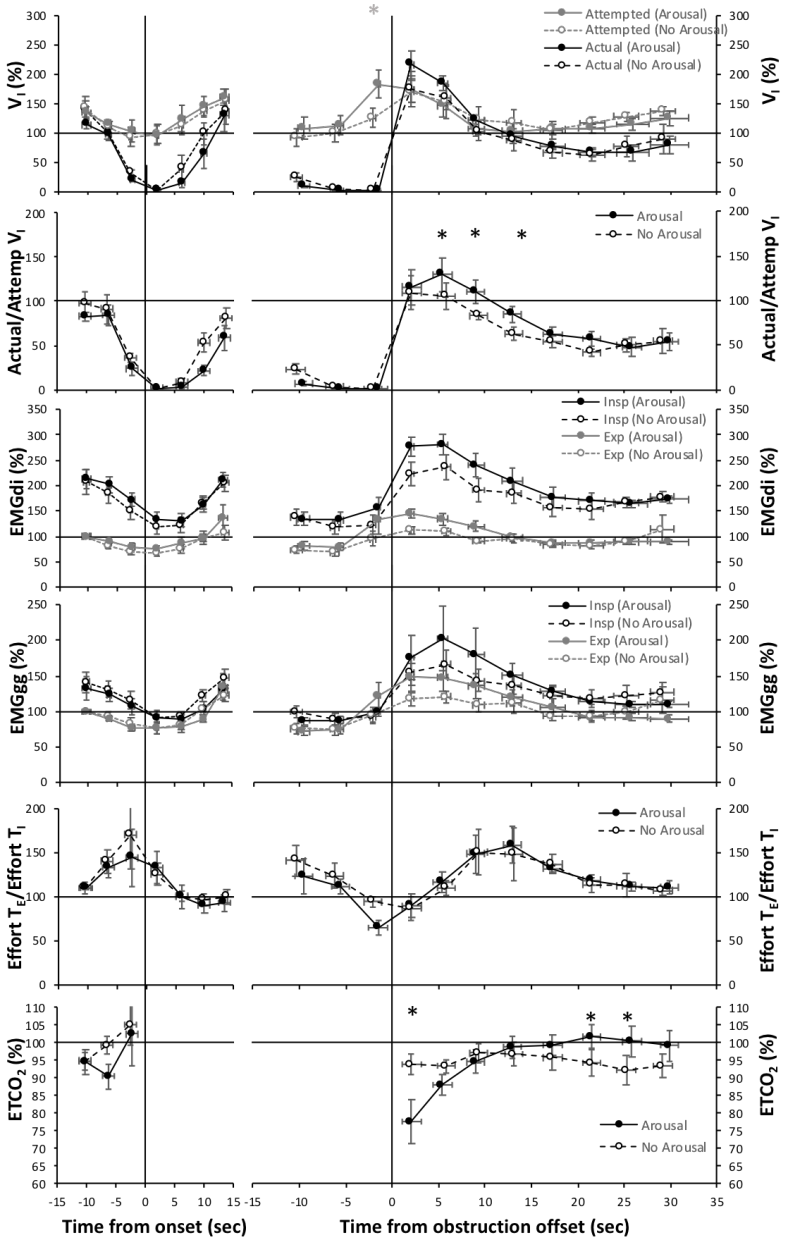

Figure 6.4: Breath-by-breath physiological measures with arousal (black) or no arousal (grey). Measured minute ventilation, attempted minute ventilation as derived from oesophageal pressure, inspiratory and expiratory EMGdi and EMGgg, effort duty cycle and ETCO2 plotted for the three breaths prior to and three breaths following obstruction onset, and three breaths prior to and eight breaths following airway re-opening. Data are means ± SEM, n=6, plotted at time relative to obstruction onset and offset respectively, and expressed as percentage of stable wake values for all variables except EMGgg and EMGdi which are expressed as a percentage of expiratory EMG activity on the third breath prior to total airway occlusion. *indicates significant post-hoc pair-wise differences between arousal versus no-arousal conditions in the presence of a significant condition by time interaction effect.

suggesting overall respiratory drive remained high. However, despite relatively high breathing effort, this was clearly not sufficient to maintain airway patency, given that the ratio of attempted to achieved ventilation fell below 100% by the 3rd breath post airway reopening in both arousal versus no-arousal conditions, and then continued to deteriorate. Measured ventilation was elevated above wake levels on the 3rd breath prior to total obstruction, and markedly elevated compared to both wake and pre-obstruction levels for the first two breaths after airway re-opening, but quickly dropped thereafter, consistent with the onset of conventionally scored secondary events as seen in the re-obstruction survival plot (Figure 6.2b).

6.3.4 Duty cycle

There were clear changes in the effort duty ratio during obstruction where expiratory time progressively reduced relative to the inspiratory phase of the effort cycle (Figure 6.4, time effect p=0.021). Following the initial breath of airflow recovery, the Te/Ti effort ratio increased over the subsequent three breaths. It was also observed that often airflow recovery occurred out of phase with the effort cycle, often late in the inspiratory phase and sometimes even into the passive or potentially active recoil phase of respiration. Around this point, another active inspiratory effort often commenced with a markedly reduced effort Te/Ti ratio. An example of this behaviour is shown in Figure 6.5. This occurred quite frequently in some patients, and may have contributed to the observed abrupt reduction in expiratory time on the breath prior to airflow recovery.

6.3.5 Muscle activity and ETCO2

Inspiratory diaphragm muscle activity showed few signs of increasing activity until the last breath during obstruction immediately prior to the point of airway re-opening (Figure 6.4). Post-recovery, EMGdi activity was elevated in both arousal and non-arousal conditions to above pre-event levels for the three breaths following airway reopening, but then fell below pre-obstruction levels. There was no statistically significant difference between the arousal conditions across the period. Genioglossus recruitment was substantially elevated on the breath during which the airway re-opened, and remained elevated for the following five breaths. There was some sign of augmented expiratory genioglossus muscle activity on the breath immediately prior to airflow recovery, although this did not reach statistical significance compared to the previous breath. ETCO2 was reduced on the first breath following airflow recovery, particularly in the event of an arousal (Figure 6.4).

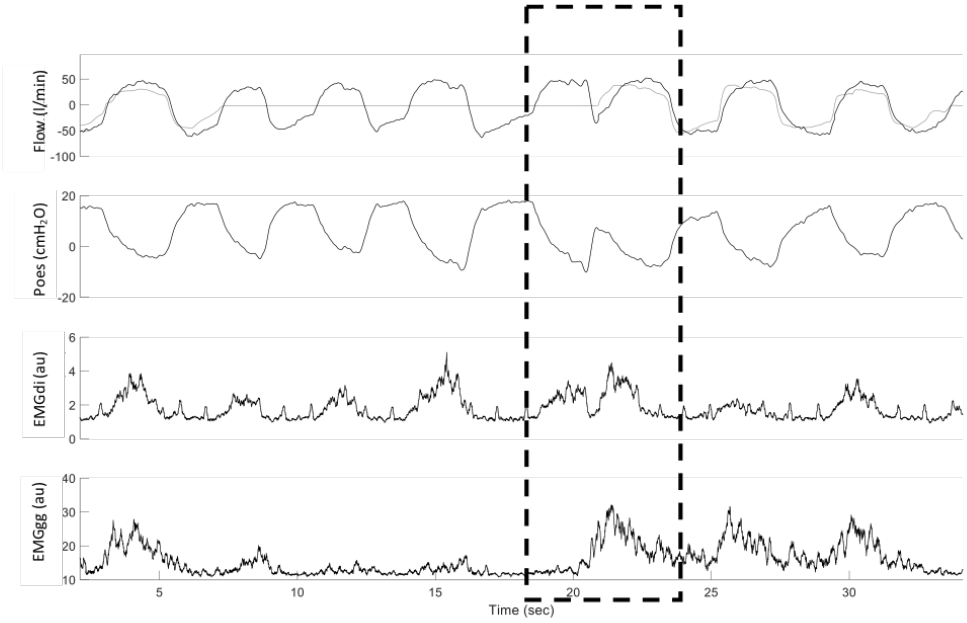

Figure 6.5: Example of augmented effort duty cycle. Attempted (black) and measured (grey) flow, pressure, EMGdi and EMGgg at airflow recovery. The airway did not always re-open in phase with the effort cycle at the start of a negative pressure deflection. Instead, secondary efforts were triggered later in the cycle, which may explain some of the observed breath by breath changes in relative expiratory time on the breath prior to airflow recovery.

6.4 Discussion

This is the first study to have systematically examined comprehensive estimates of respiratory effort derived from oesophageal pressure in OSA patients. This detailed exploration of relationships between inspiratory effort, upper airway and diaphragm muscle activity, ventilation and arousal over the course of obstructive apnoea events and their recovery highlights several important observations for understanding cyclical airway obstruction in OSA. A comparison of the attempted and achieved ventilation over the period of obstruction onset and offset provides evidence of decreasing breathing effort and upper airway muscle activity in precipitating airway obstruction, and signs of progressively augmenting effort and muscle activity in recovering airway patency largely irrespective of the presence or absence of arousal. It appears that in this group of patients, with very severe OSA and complete obstructive apnoeas, a consistent reduction in respiratory effort preceded obstruction onset developed after a prior period of mild hyperventilation and hypocapnia relative to wake. Furthermore, and consistent with this obstruction, deteriorating airflow rapidly recurred following the first few breaths of airflow recovery. Whilst this occurred largely irrespective of the presence or absence of arousal, transient hypocapnia and subse-

quent hypercapnia were more exaggerated following arousal, consistent with more severe ventilatory disturbances in the presence of arousal. These findings support that ventilatory disturbances and associated transient airflow recovery responses, both with and without arousal, reflect complex and dynamic inter-relationships between breathing effort, upper airway muscle activity and airway collapsibility that promote ongoing cyclical airway collapse over relatively short time periods.

In general, the presence of arousal made little difference to the physiological measures over the period of obstruction onset and airflow recovery. This supports the concept arousal is a distinct phenomena that often occurs around the time of flow recovery, likely driven by similar stimulus (Eckert and Younes, 2014). There was some evidence of increased ventilatory drive prior to the end of the obstructive event in events accompanied by arousal, but this was only statistically significant in the derived measure of attempted ventilation and not in EMG muscle activity measures. The ratio of achieved to attempted ventilation was significantly lower in the absence of arousal for the first three breaths following airflow recovery. However, values were not different from breath 4 onwards, suggesting obstruction recurred quickly regardless of the presence or absence of arousal. Previous studies have shown inconsistent results regarding associations between ventilatory overshoot responses and arousal. Although initial evidence suggested an elevated ventilatory response with arousal intensity (Younes, 2004), when matched for obstruction event severity and duration, Jordan et al. found that changes in peak flow, ventilation, epiglottic pressure swings and peak and tonic EMGgg were no longer significantly different between arousal and no arousal events (Jordan et al., 2011). The current study systematically examined all complete obstructive apnoea events. Consequently, event severity was not specifically matched between events with versus without arousal on the basis of obstruction duration, which was greater in events with versus without arousal. However, apart from evidence to support greater accumulated ventilatory drive arising from more prolonged severe events, the very close similarity between arousal versus non-arousal airflow recovery responses supports that cortical arousal itself does not greatly influence ventilatory recovery from obstruction.

This work supports the current understanding of arousal as a largely independent process from airway reopening. 14% of events occurred entirely without an associated arousal during the 30 seconds following the obstructive apnoea events examined in detail in this analysis. This is consistent with a previous study investigating arousal frequency in response to CPAP dial downs showing around 17% of obstructive events recover without arousal, and that airflow recovery without an associated arousal is less likely with more severe events (Younes, 2004). In Younes's work, the majority of arousals occurred prior to airway re-opening. However, in this study of obstructive apnoeas alone, the arousal dis-

tribution was centred a few seconds after flow resumed with only a fifth of events showing arousal preceding airflow restoration. Nevertheless, the results from this study are largely consistent with previous findings that the concept of competing arousal and upper airway re-opening recruitment thresholds is likely to be highly patient dependent (Jordan et al., 2007; Younes, 2003, 2004). Given the small sample of severe OSA patients in this study, event distributions are likely to differ somewhat compared to other studies. Methodologic differences between induced events on CPAP and naturally occurring apnoeas could also affect arousal responses and the baseline level of inspiratory and upper airway muscle activity from which obstruction develops. Arousal events exhibited higher drive on the breath prior to airflow recovery, consistent with the concept of an inspiratory effort-related arousal threshold.

A key observation in this study was the difference in responses between our derived metric of ventilatory drive based on oesophageal pressure and our measure of EMGdi, particularly during occlusion. On the breath prior to airflow recovery, attempted ventilation substantially increased. However, there was no clear corresponding recruitment of either diaphragm or genioglossus inspiratory muscle activity over the same period. This may be evidence of inspiratory diaphragm muscle suppression in response to muscle loading by airway obstruction, or differential distribution of drive to inspiratory muscles favouring other accessory muscles. It is also possible that our method overestimates ventilatory drive from oesophageal pressure. We have used a basic model for the respiratory system that relies on a linear volume correction during occlusion. This may not adequately account for respiratory system responses to obstruction. On the other hand, substantial inaccuracies of this nature may be unlikely given there was a relative increase in drive from breath -2 to breath -1, both of which clearly remained occluded.

Expiratory diaphragm and genioglossus activity were elevated on the breath prior to airway recovery, despite no sign of inspiratory muscle activity increases. This may reflect an important mechanism for restoring airway patency. Duty cycle changes over the course of airflow restoration may be a reflection of increasing drive, or load compensation mechanisms responding to lung volume and flow changes over this period. The abrupt reduction in expiratory time relative to inspiratory time on the breath prior to airflow recovery is strongly suggestive of reflex-modulation of the breathing effort duty cycle potentially involved in re-establishing airway patency. This has not previously been reported in the literature and clearly warrants further investigation. These results together point to potential rapid physiological changes around airflow restoration. However, it is not yet clear whether this response reflects non-linear upper airway versus inspiratory pump muscle recruitment, in which upper airway muscle activity rapidly becomes sufficient to restore patency. Alternatively, this may reflect some other reflex mediated response that rapidly

augments upper airway muscle activity to restore flow, or potentially a reflex response to abrupt spontaneous airflow restoration itself.

6.4.1 Methodological considerations

A clear limitation of this study is its observational nature and relatively small sample size. Recruitment for such instrumentally intensive studies and detailed breath-by-breath analysis of this nature are very challenging. However, detailed and systematic quantitative analyses of many replicate events gained through this approach provide important new insights into the physiological mechanisms underpinning airway obstruction and airflow recovery with versus without arousal. The understanding gained from this analysis helps to inform future studies and analysis using these powerful new techniques. Clearly further physiological data collection in larger groups with more diverse patient and respiratory event selection is needed. Further analyses segmented into different sleep stages would also be useful to help determine the contribution of augmented ventilatory drive and potential interactions with altered arousability and thus arousal thresholds for explaining more stable breathing and upper airway function in deep sleep. Unfortunately, this heavily instrumented group of patients with very severe OSA had almost no deep sleep available for such comparisons.

Given abrupt withdrawal of wakefulness influences on respiratory and upper airway muscle control, and marked cyclical changes associated with unstable breathing and frequent arousal, there are also fundamental challenges in defining what should constitute baselines and 'low drive' in the context of obstructive events. Wake-sleep changes are well documented in muscle activity and ventilatory drive, such that the level of activity required to maintain airway patency in wake versus sleep, or stage 1 versus stage 3, could potentially be quite different. Comparisons made to a pre-event value may artificially elevate or potentially reduce the apparent baseline, as OSA patients may already be at an increased or reduced drive state from previous compensation responses to airway obstruction. This study used a period of stable breathing in wake to define baselines where possible. However, for EMG channels, gain adjustments during the night made this overly complicated so a pre-event baseline of the 3rd breath prior to event commencement was used as a relative baseline. Expressing EMG activity as a percentage of maximum activity is common, but within-subject baseline comparisons were considered to be more informative for this analysis. Future studies should consider comparable measurements during periods of stable breathing during wake and ideally also during periods of stable breathing in deep sleep for comparisons.

In summary, the powerful new tools applied in this work provide important new methods to explore the pathophysiological mechanisms responsible for cyclical airway obstruction and airflow recovery in OSA. The results of this study strongly support the importance of dynamic changes in ventilatory effort for precipitating upper airway obstruction and for airflow recovery both with and without an accompanying arousal.

Chapter 7

Airway recovery mechanisms

The previous chapter investigated breath-by-breath changes in ventilatory drive, ETCO2 and respiratory muscle recruitment over the course of obstructive apnoea events and recovery in OSA. Results highlighted that arousal had relatively little effect on breath-by-breath parameters over the post-obstruction recovery period, including on the ventilatory overshoot and likelihood of re-obstruction, though there was some evidence of elevated ventilatory drive immediately prior to airflow recovery in arousal events.

Given that it has already been established that arousal is not the primary mechanism for airway recovery itself, pharyngeal dilator muscles must be recruited by some other compensatory mechanism around the point of airflow recovery. The results of Chapter 6 suggest that genioglossus and diaphragm muscle activity does not gradually increase over the course of severe obstructive events, but instead increases more abruptly just prior to and over the course of the first breath of flow recovery with levels then remaining elevated for several breaths. Simultaneously, abrupt changes in inspiratory cycle timing often occur, strongly suggestive of reflex modulation of the ventilatory duty cycle to either promote airflow recovery or in response to airflow recovery itself. The aim of this chapter is to further explore short-term changes in muscle recruitment and ventilatory pressures at the time the airway re-opens with the aim of better understanding physiological mechanisms around the point of airflow recovery.

This further builds on Aim 4 of the thesis: to use the new tools developed to investigate the underlying role of inspiratory drive and negative pressure during obstruction and in compensation mechanisms for dilator muscle recruitment and flow recovery, with and without arousal.

7.1 Background

Arousal is widely accepted to be non-essential to airway recovery in OSA. Therefore, patency must be restored primarily by other compensatory mechanisms. Effort or duty cycle augmentation can increase inspiratory time to promote greater tidal volume in the presence of ongoing flow limitation, but additional upper airway dilator muscle recruitment is needed to more successfully augment airflow and inspiratory volume in the presence of partial or complete airway obstruction.

Upper airway dilator muscles are primarily stimulated by wakefulness related drive inputs to the hypoglossal motor neuron pool, central drive and negative airway pressure, which itself only increases with increased inspiratory pump recruitment according to ventilatory drive (Younes, 2008). Therefore, ventilatory drive is a primary source of upper airway

dilator recruitment. Indeed, upper airway dilator muscle activity does not increase immediately in response to obstruction (Pierce et al., 2007; Schwartz et al., 1998), and this delay is likely due to two main factors. Firstly, given quite prolonged central chemo-reflex delays, periods of diminishing ventilatory drive would be expected to take some time to reach a nadir. Secondly, different muscle groups should be expected to have different recruitment thresholds and sensitivities to both common drive inputs, and local sensory inputs specific to each muscle such as airway mucosal pressure and intramuscular load/tension receptors. Thus the effective recruitment threshold, TER , reflecting the level of drive required for a dilator muscle response to obstruction, likely differs between muscle groups and between patients, due to differences in anatomy, viscous properties of the pharynx, the site of collapse and the relative recruitment rates of pharyngeal and pump muscles affecting the balance of forces in the upper airway (Younes et al., 2007).

In the previous chapter, it was observed that the timing of airflow recovery was quite variable across the respiratory effort cycle. A better understanding of the distribution of airflow recovery within the breathing cycle could help to inform the underlying mechanisms of airflow recovery. In the presence of airway collapse it is important to consider that both the patterns of upper airway versus inspiratory pump muscle recruitment and dynamic changes in airway pressure may simultaneously reinforce airway collapse.

Thus, a key purpose of this study was to undertake a detailed examination of EMG responses of both an upper airway dilator muscle (genioglossus, EMGgg) and the main centrally controlled respiratory pump muscle (diaphragm, EMGdi) to better understand the relative recruitment of both muscle groups around the point of airflow recovery. Upper airway phasic muscles, such as the genioglossus, have shown well documented reflex responses to abrupt negative pressure in human studies in both wake and sleep, though the response is reduced during sleep (Berry et al., 1995; Horner et al., 1991; Wheatley et al., 1993). Negative pressure stimuli produce a genioglossus reflex response consisting of a brief excitatory phase followed by a more prolonged period of suppression (Eckert et al., 2007). Tonic muscles like the tensor palatini also exhibit reflex responses to negative pressure, though these are markedly reduced during sleep (Wheatley et al., 1993). In these studies, ensemble averaging of raw rectified EMGgg responses to multiple trials revealed short-latency reflex responses temporally related to sharp changes in pressure drops. In this study, it was reasoned that similar signal averaging around the point of abrupt airflow recovery would help to reveal preceding patterns of EMG and/or pressure changes temporally related to the process of airflow recovery itself. The novel advanced filtering techniques developed in Chapter 3 were used to support this analysis. Previously, cardiogenic artefact strongly dominated signal power in EMGdi, and methods of gating signal analysis restricted to segments between QRS complexes resulted in significant signal

loss. The use of more sophisticated alternative methods allowed for short timeframe, raw, rectified EMG analysis to more reliably determine patterns of respiratory pump versus upper airway dilator muscle activation around the time of airflow recovery. These methods were used in combination with a detailed assessment of oesophageal pressure related changes in breathing effort to examine airflow recovery responses from apnoea both with and without accompanying arousal. A closer analysis of the timing of flow restoration relative to effort commencement on a within-breath basis was also used to provide further insight into duty cycle modulation towards an enhanced understanding of compensatory mechanisms by which airway patency is restored following total airway collapse. A more detailed knowledge of these processes could help to advance more effectively targeted treatments.

7.2 Methods

A secondary analysis was performed using the same obstructive event data from six OSA patients examined in Chapter 6. Periods of airway collapse were identified by a reduction in flow to less than 10% of the average stable peak flow and were reviewed manually, using a custom MATLAB (The MathWorks, Natick, 2017) user interface (Appendix A). The point of airway reopening was also manually reviewed to ensure reliable identification. Flow, oesophageal pressure, gastric pressure and filtered, rectified EMGdi and EMGgg were ensemble averaged over a window spanning the preceding five seconds and the initial two seconds of inspiration about this point, to examine activity over the breath prior to recovery and the following inspiratory period. Events were segmented into those that occurred with and without arousal, as in Chapter 6. Ensemble averages were performed on an individual subject basis to help examine inter-subject variability in responses. Averaged flow and pressure responses are still presented in Appendix D, Figure D.5.

To identify any fundamental physiological differences that may help to explain temporal events responsible for airway reopening, ensemble averaged muscle responses at the point of airflow onset at obstruction end were compared to those at several other time points in the apnoea event. The attempted flow signal developed in Chapter 5 was used to define start and end point of efforts during occlusion. Examples of these time-points are identified on an example occlusion in Figure 7.1. These included the point of initial oesophageal pressure deflection on the effort in which flow recovery occurred (point B), given this was not always synchronous with flow onset (point C), and the initial oesophageal pressure deflection on the effort prior to flow recovery, which remained occluded (point A). As a comparison, a fourth baseline condition was included by taking a period of stable breathing in wake

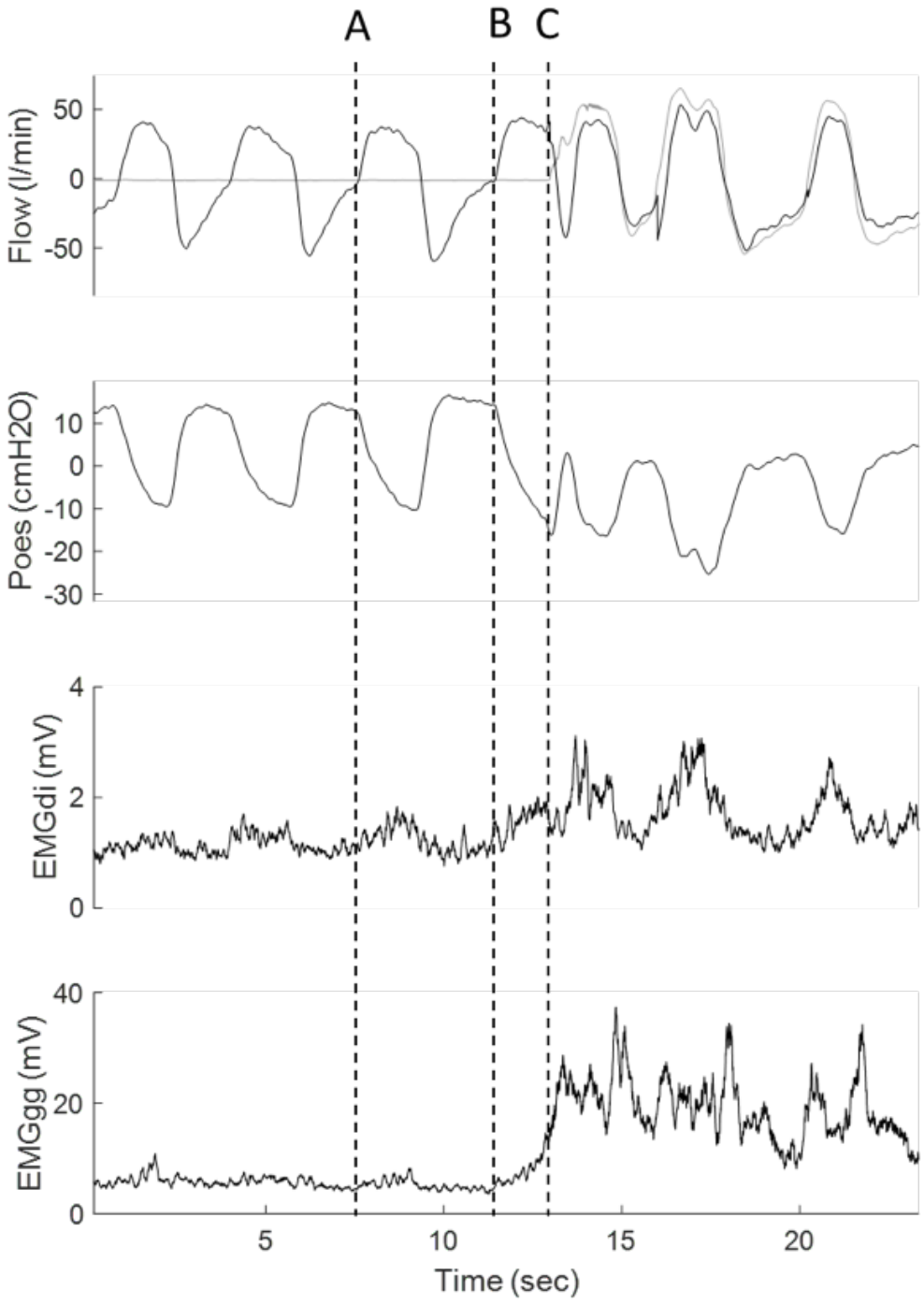

Figure 7.1: An example airflow recovery event, with attempted flow (black line) and measured flow (grey line), oesophageal pressure and rectified, MTA EMGdi and EMGgg (100ms window). The time anchors for ensemble averaged are displayed with A: start of previous occluded effort, B: start of successful effort and C: flow onset point. Windows of 5 seconds prior and 2 seconds post each anchor point were ensemble averaged for responses.

averaged over multiple breaths around the initial oesophageal pressure deflection to provide a baseline pattern of muscle activity, flow and pressure change at the commencement of flow during normal breathing activity. Each individual's within-subject flow and pressure traces are displayed in grey and the ensemble average overlayed in black. Given the level of electrical noise and variability in individual EMGdi and EMGgg traces only ensemble averages (black line) are plotted with 95% confidence intervals (grey line).

Due to temporal differences in the point of flow resumption during breathing efforts, I chose to take averages about three different time points (A,B,C in Figure 7.1). At point C, where recovery takes place, pressure signals are out of phase and so peak and minimum values from the ensemble average are poorly reflective of individual values. For this reason, ensemble averages are also taken at point B (the commencement of the effort) where pressure values are initially aligned and flow and EMGgg signals show more signs of temporal smear. In order to examine average levels of activity at key time points, values of oesophageal pressure, EMGdi and EMGgg at time zero for each breath were calculated for comparisons between breaths at the point of averaging. A 50ms window centred on time zero was used to reduce variability associated with residual noise in instantaneous values of rectified averaged EMG signals at time zero.

Group data are presented as mean±SEM of within subject averages. Linear mixed model analyses were used to investigate fixed main events of arousal (presence versus absence) and breath type (wakefulness breaths, effort associated with airflow recovery, effort prior to recovery and start of flow onset). Each model used an auto-regressive covariance structure and included subject ID as a random effect each with a different intercept to account for expected between subject variability. Where interaction or main effects were significant, relevant Bonferroni adjusted pair-wise comparisons were used to test for more specific pair-wise differences. All statistical tests were run in SPSS (Version 22, IBM SPSS Statistics).

To better investigate changes in duty cycle over the course of obstruction and recovery, attempted flow was used to derive ventilatory timing parameters from the effort signal, as discussed in Chapter 5. These were calculated for the three breaths prior to and three breaths following airflow recovery. The period of stable wake was used as baseline.

To quantify the level of asynchrony between effort onset and flow recovery, the time from commencement of effort to the start of inspiratory flow on the breath airflow resumed was calculated for each event. In order to establish the relative phase of inspiration independent of absolute inspiratory time to allow for comparisons between subjects, this time was divided by the total previous inspiratory effort duration, as derived from the attempted flow signal. Given frequent signs of additional and prolonged effort augmentation, this

duration was chosen as a baseline instead of the total effort time of the recovery breath. Inspiratory time is known to augment progressively during obstruction, so it was felt the obstructed breath immediately prior provided the best baseline inspiratory time for comparison.

7.3 Results

Six patients, with (mean±SEM) BMI 36±5 kg/m^2, AHI 86±20 /hr, age 45±10 years and an average of 129±88 obstruction events over the night, provided data for analysis. In one subject the genioglossus signal was lost during the night, and there were other problematic gain changes in EMGdi recordings so these signals were excluded from analysis.

An example of one participant's arousal and non-arousal responses at the point of airflow recovery are shown in Figure 7.2. Corresponding group values of mean oesophageal pressure, gastric pressure, EMGdi and EMGgg at time zero for each condition are presented in Table 7.1. There was no difference between arousal and non-arousal responses in the degree of muscle recruitment at airway re-opening (EMGgg 2.5±0.3 vs 2.3±0.2, EMGdi 2.4±0.3 vs 2.3±0.2). However oesophageal pressure at the point of airflow recovery was more negative in the arousal condition (-7.2±3.1 vs -1.5±2.3 cmH2O, p=0.03).

To compare physiological differences between obstructed breaths in which flow recovery did and did not occur, Figure 7.3 plots each of the breath conditions for comparison in one example subject. Similar figures for the remaining subjects can be found in Appendix D. There was minimal evidence of EMGgg recruitment during the occluded breaths prior to flow onset. However, EMGgg rapidly increased in the 200ms prior to airflow recovery, and was significantly higher compared to levels at the commencement of the previous two occluded inspiratory efforts ($p<0.001$) but not to levels at flow onset during wake. A similar pattern of behaviour was observed in all subjects. Unlike EMGgg, EMGdi continued to display phasic activity during obstruction, closely following the pattern of change in oesophageal pressure. In general, airflow recovery occurred during the inspiratory effort phase of the respiratory duty cycle, when inspiratory oesophageal pressures, EMGdi activity, and particularly EMGgg activity were augmented compared to the preceding effort. Oesophageal pressure at flow recovery was significantly more negative than at the start of any of the other comparator breaths ($p<0.001$), and was out of phase with a broad spread of airflow compared to downward deflection in oesophageal pressure and EMGdi activation across recovery events. There was no statistically significant difference in gastric pressure at the start of effort onset or at flow recovery between any condition.

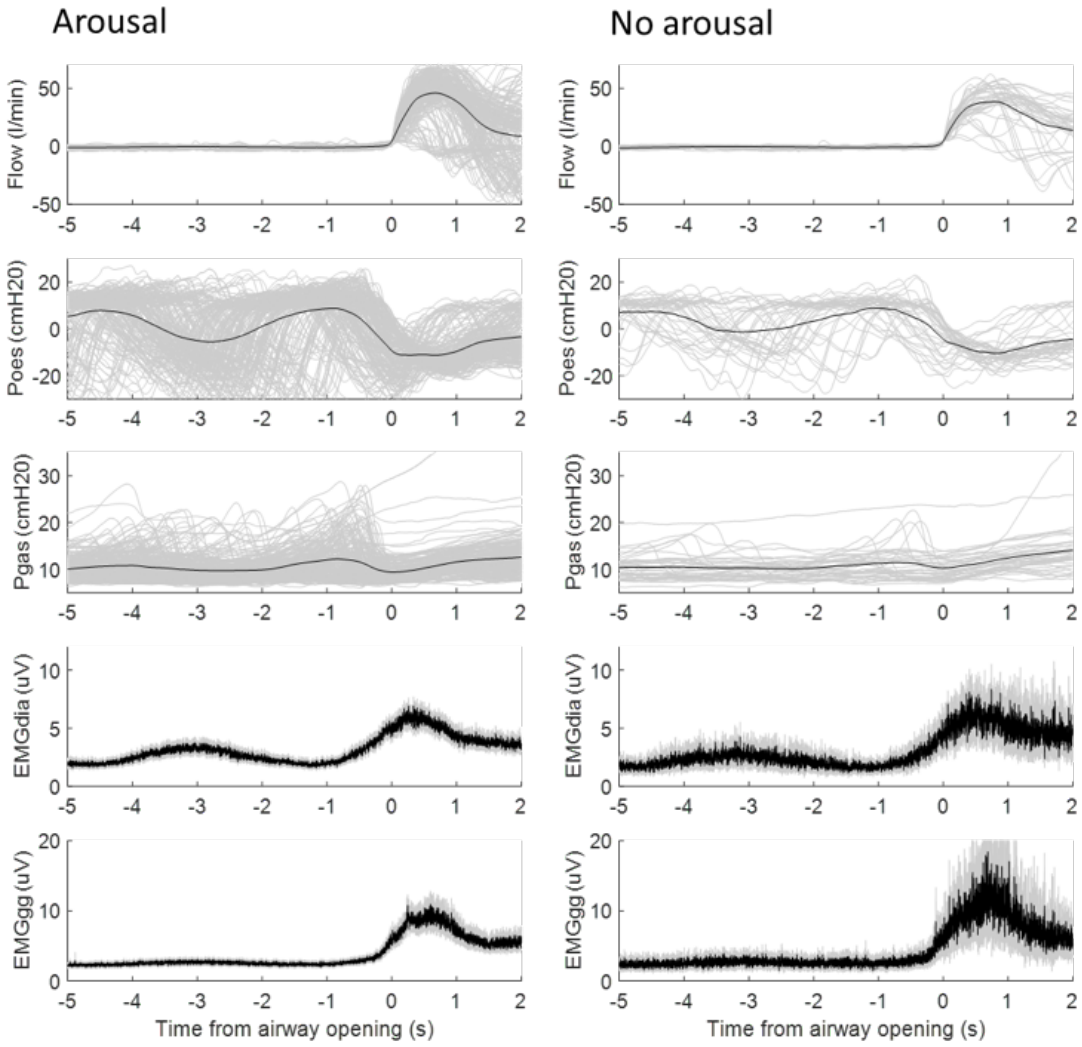

Figure 7.2: Example arousal and non-arousal flow recovery responses from one participant. Arousal N=213, Non-arousal N=39. For Flow, Poes and Pgas, individual events are plotted in grey and the ensemble average overlaid in black. For EMG responses, mean curve (black) and 95% confidence intervals (grey) are displayed.

Table 7.1: Pressure and muscle activity at time zero for each breath and arousal condition. Values are group mean±SEM, N=6. Effort -1 and 0 correspond to the inspiratory efforts immediately prior to and most closely associated with the point of airflow recovery. EMGgg and EMGdi activity are expressed as a percentage of the average minimum level of activity recorded during expiration in baseline wake period. Statistical tests compared levels at airflow recovery to other conditions, * indicates $p<0.05$ vs all other conditions, † indicates $p<0.05$ vs effort start but not different to wake

	Baseline	Effort -1 Start		Effort 0 Start		Flow recovery point		
	Wake	Arousal	No Arousal	Arousal	No Arousal	Arousal	No Arousal	
Poes (cmH_2O)	7.0±1.0	9.7±1.3	10.2±1.1	8.4±1.2	9.6±1.3	-7.2±3.1	-1.5±2.3	*
Pgas (cmH_2O)	12.1±1.0	11.7±1.3	11.1±0.9	11.6±1.1	11.4±0.9	10.8±1.0	10.8±0.9	
EMGgg (%min wake)	2.0±0.4	1.5±0.3	1.3±0.2	1.8±0.3	1.6±0.3	2.5±0.4	2.2±0.4	†
EMGdi (%min wake)	1.7±0.2	1.0±0.2	1.2±0.2	1.4±0.2	1.3±0.2	2.4±0.3	2.3±0.2	†

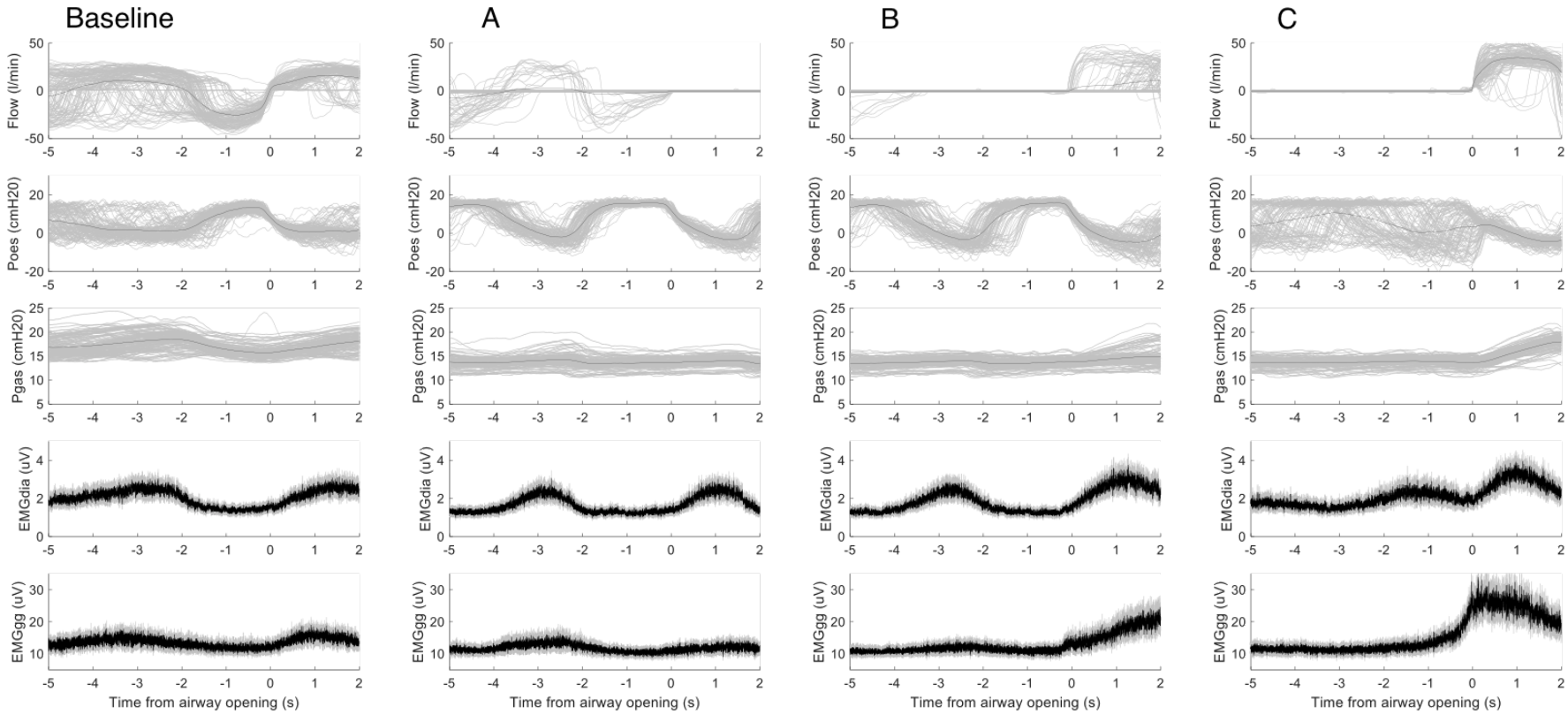

Figure 7.3: Example responses across all four averaging time-points from one participant (Baseline events N=100, A,B,C events N=174). Baseline shows responses averaged with time zero aligned with inspiratory flow onset during wake along with one preceding breath, A) with time zero aligned with inspiratory effort onset of the first occluded breath, B) with time zero aligned with inspiratory effort onset on the breath associated with airflow recovery and C) with time zero aligned with airflow recovery.

Table 7.2: Breath parameters from attempted ventilation derived from oesophageal pressure, giving a measure of effort timings during obstruction. Values are group mean±SEM, N=6, for 3 breaths prior to and post airway recovery. Average values from a baseline period of stable wake are provided for comparison.

	Baseline	Breath -3	Breath -2	Breath -1	Breath 0	Breath 1	Breath 2	Breath 3
Effort TI (sec)	1.8 ± 0.1	1.8 ± 0.1	1.8 ± 0.1	1.9 ± 0.1	2.2 ± 0.3	1.8 ± 0.1	1.6 ± 0.1	1.8 ± 0.2
Effort TE (sec)	1.9 ± 0.1	2.4 ± 0.2	2.2 ± 0.2	1.6 ± 0.1	1.9 ± 0.1	2.3 ± 0.3	2.4 ± 0.3	2.5 ± 0.3
Effort TTOT (sec)	3.7 ± 0.2	4.2 ± 0.3	4.0 ± 0.2	3.5 ± 0.2	4.1 ± 0.3	4.1 ± 0.3	4.0 ± 0.3	4.3 ± 0.4
Effort Ti/TTOT	0.48 ± 0.02	0.43 ± 0.02	0.45 ± 0.01	0.54 ± 0.02	0.54 ± 0.03	0.45 ± 0.03	0.40 ± 0.03	0.42 ± 0.02
Effort VTI (l/min)	0.6 ± 0.1	0.8 ± 0.1	0.9 ± 0.1	1.0 ± 0.1	1.2 ± 0.3	1.0 ± 0.2	0.7 ± 0.1	0.8 ± 0.1
Effort VTE (l/min)	0.6 ± 0.1	0.8 ± 0.1	0.8 ± 0.1	0.7 ± 0.1	1.0 ± 0.1	1.2 ± 0.2	1.0 ± 0.1	0.9 ± 0.1
Effort PIF (l/min)	32.4 ± 2.4	42.0 ± 4.8	44.0 ± 4.7	50.8 ± 3.5	53.3 ± 6.7	53.2 ± 10.2	44.7 ± 8.0	43.2 ± 6.8

Ventilatory duty cycle parameters derived from the attempted ventilation signal are shown in Table 7.2. The distribution of airflow recovery times in the effort duty cycle showed that flow typically resumed shortly after the start of the effort cycle, but with a broad tapering distribution of onset times extending throughout the inspiratory effort and well into the relaxation phase of the respiratory cycle (Figure 7.4). This wide-spread distribution was also evident in the ensemble averages of oesophageal pressure at flow onset (Figure 7.3).

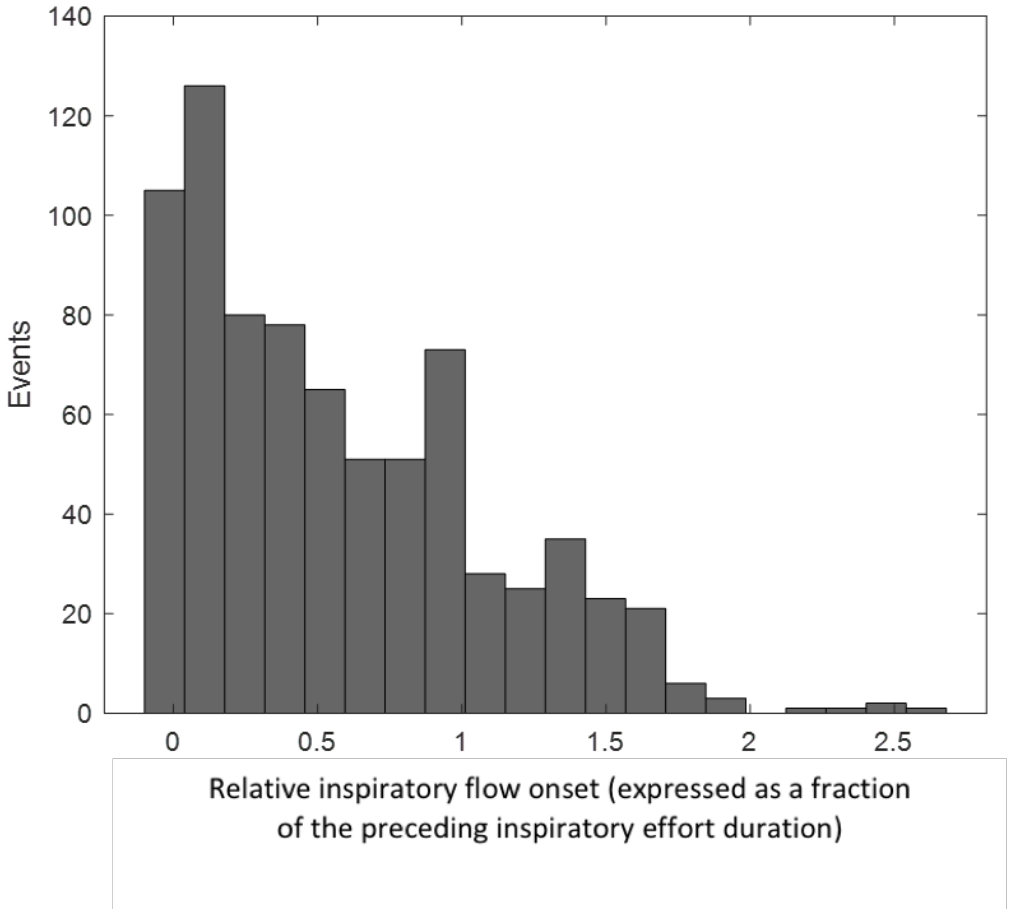

Figure 7.4: Group data distribution of flow onset relative to effort onset expressed as a fraction of inspiratory duration of the previous inspiratory effort.

7.4 Discussion

The aim of this study was to better understand the fundamental physiological compensatory mechanisms that enable airflow recovery following severe upper airway obstruction in OSA. Whilst it is now well accepted that airflow recovery from airway obstruction oc-

curs largely independent of arousal responses (Younes, 2003), and that both events are largely governed by augmenting inspiratory drive (Eckert and Younes, 2014), the more precise mechanisms and timing of EMG activation and airflow recovery responses remain poorly understood.

This study found consistent evidence of rapid pre-recruitment of genioglossus muscles in the 200ms leading up to flow onset. The ensemble averaged EMGgg response showed consistent and substantial augmentation of muscle activity well above preceding levels immediately prior to airflow recovery with sharper signal averaging when temporally aligned with flow onset compared to inspiratory effort onset. Abrupt further augmentation in EMGgg following airflow restoration was also evident with signal averaging aligned with flow or effort onset, likely indicating that abrupt re-opening of the airway provides an important stimulus for EMGgg activation via airway pressure receptor mediated effects. In contrast, the EMGdi activation produced a sharper response to effort onset. These observations support the hypothesis that upper airway dilator muscle recruitment is central to the process of airflow recovery following complete obstruction (Younes, 2008). EMGgg responses were not different with compared to without arousal, further supporting the concept that airflow recovery and arousal are independent events (Younes, 2003), but that both may be largely governed by the prevailing level of central ventilatory drive.

Whilst I acknowledge the limitations arising from substantial inter- and intra-breath and subject variability, which impacts all analytical strategies in this area, I believe that signal averaging techniques remain the best way to examine the key physiological phenomena of interest in this study (Figures 7.2, 7.3). This approach clearly shows interesting and previously unreported findings, highlighting the important different temporal correlations between signals. Peak values are not quantified from ensemble averages because invariably through averaging temporal smearing has occurred, and so they would not reflect actual peak effort values. Nevertheless, these figures provide important visual information about the different temporal relationships of the pressure and upper airway dilator responses around airflow recovery.

Arousal events showed significantly more negative oesophageal pressures at flow onset consistent with augmented inspiratory activation, with inspiratory flow and effort more out of phase in events that also triggered an arousal. As shown in Chapter 6, the majority of arousals in this study occurred very shortly after airflow recovery occurred. It is possible then that arousal occurs in response to sensorimotor efferent-afferent mismatch associated with chemo- and mechano-reflex augmentation in inspiratory effort in the presence of obstruction, but could also potentially reflect secondary responses to a sudden onset of flow later in the inspiratory cycle. Thus, in addition to the traditional concept of an

inspiratory effort arousal threshold (Gleeson et al., 1990), there may be another mechanistic pathway to help explain the close temporal association between arousal and airway recovery. Further studies are warranted to further investigate these mechanisms.

A secondary aim of this study was to further explore within-breath delays in flow onset relative to effort onset and the modulation of inspiratory timing. The distribution of flow onset relative to the duration of the preceding inspiratory effort was heavily skewed towards inspiratory effort onset, but then widely distributed over the remainder of the inspiratory phase extending well into the relaxation phase of the breathing cycle. Airflow restoration late in the inspiration effort cycle around the time of nadir oesophageal pressure and effort relaxation was also common.

The detailed analysis of effort augmentation at the point of airflow recovery frequently showed a secondary inspiratory effort following flow recovery relatively late and out of phase with the ventilatory drive cycle (e.g. Figure 7.4). This may be evidence of a sigh-like reflex, in which the inspiratory recruitment pattern is altered around the time flow recovery. Reflex behaviour to augment inspiratory activity and change the central timing pattern of breathing is not a new concept in respiratory mechanics. The Herring-Bruer reflex is a fundamental protective physiological response to excessive inflation of the lung, activated by pulmonary stretch receptors (Hering and Breuer, 1868). Inspiratory activity is inhibited by this sensory reflex through the augmentation of central nervous respiratory motor pattern in a protective response to muscle loading. Though clearly the observed results are a separate phenomenon, pulmonary or upper airway vagal afferent feedback could similarly modulate neural inspiratory pattern generation at the point of airflow recovery.

From this study, it is not yet clear if the observed reflex is itself mechanistically involved in generating flow, or whether it is a secondary response once flow has been restored. Brainstem or neural inspiratory pattern modulation to induce an additional effort late in inspiration, at a time when the upper airway muscles are at a greater level of phasic activation and the system is more mechanically favourable, could help shift the balance of forces towards flow generation. Alternatively, the observed reflex may be a response to the abrupt exposure of sensory receptors to changes in pressure or stretch, either in upper airway muscles or the lung, when patency is restored. It could also result from efferent-afferent mismatch between expected and achieved flow, volume and/or muscle length-tension when reflex activation occurs out of phase with a respiratory cycle. Upper airway reflex responses to negative pressure stimulus are well documented (Horner et al., 1991; Malhotra et al., 2002), but reflex modulation of central drive in an OSA context has not previously been documented.

Increasing inspiratory duty cycle (Ti/Ttot) is an established compensatory response to ongoing flow limitation, which helps to sustain tidal volume and ventilation despite obstruction through more sustained augmentation in inspiratory effort (Jordan et al., 2007; Onal and Lopata, 1986). Whilst this is a well-established mechanism to help counteract flow limitation effects, this is the first study that has been able to look more closely at inspiratory effort prolongation during complete airway obstruction, using the novel parameters of derived attempted ventilation. Inspiratory time does increase over the course of obstruction, but there are abrupt changes at breaths -1 and 0 which are likely related to the observed reflex behaviour. Duty cycle augmentation at end apnoea could serve to improve the balance of forces necessary to overcome obstruction to restore airflow. The observation that genioglossus recruitment appeared to substantially increase prior to signs of oesophageal pressure augmentation and flow restoration supports that duty cycle changes are more likely to reflect a secondary response to airway opening. Careful measurements in future studies to further examine the presence and temporal relationships of secondary turning points in oesophageal pressure with upper airway muscle recruitment and flow onset would be very useful.

Previous work in Chapter 4 showed that flow/pressure effects importantly influence respiratory mechanics between occluded and un-occluded breaths. Thus, it is worth considering if effects observed in this study could potentially reflect pressure related artefacts resulting from sudden airflow restoration and an inadequate model of the respiratory system. However, there are several reasons to support that this is unlikely to be the case. Firstly, whilst the respiratory mechanics model was used to help define inspiratory effort onset, assumptions affect model based amplitudes much more than timing, and the remaining analyses were minimally reliant on the model. Secondly, EMGdi showed similar phasic patterns entirely consistent with changes in oesophageal pressure (Figure 7.1) with both governed by central ventilatory drive. Thirdly, the total duration of the inspiratory phase of effort was clearly increased on sigh-like breaths, reflecting central pattern generation timing changes difficult to explain through potential artefacts or other mechanisms.

7.4.1 Potential Limitations

This study required highly instrumented physiological measurements including an oesophageal manometry catheter to record pressure and EMGdi, and intramuscular wire electrodes to record EMGgg. It is possible the presence of a catheter in the pharyngeal space may alter the behaviour of upper airway mechanoreceptors and alter physiological responses. However, to identify neural pattern augmentation during airway collapse, drive measures of either pressure or intraoesophageal EMG are required, so this is difficult

to avoid. Careful analysis of non-invasive drive measures (e.g. respiratory inductance plethysmography bands) may be useful to identify duty cycle changes, but these signals are invariably less reliable.

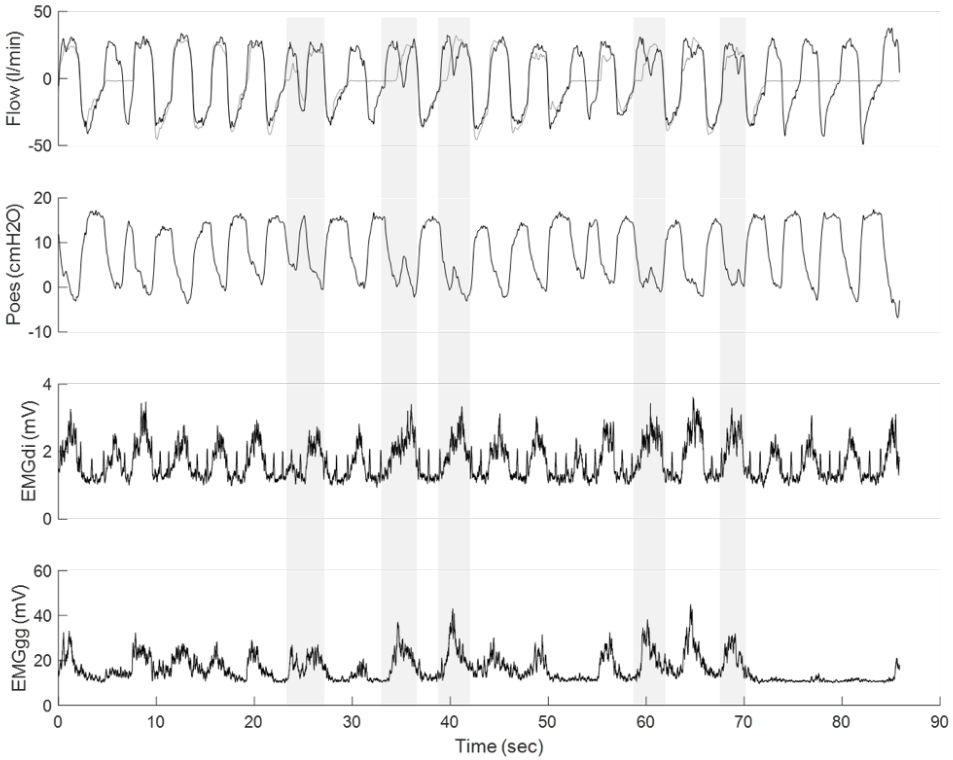

Figure 7.5: Examples of multiple augmented duty cycle responses within one subject, highlighted in grey, including responses to within-breath obstruction suggesting the phenomena is common in OSA

The current study only examined apnoea events, where abrupt flow onset occurs, facilitating use of ensemble average responses to a very well-defined event-offset time point. Future studies should explore whether similar patterns of responses and reflex behaviour also accompany less severe hypopnoea events. The subjects in the current study were selected to have very severe OSA and exhibited predominately apnoea events, so future studies should include OSA patients with more hypopnoeas for similar analysis. Preliminary observations of augmented effort in response to within-breath obstruction successfully achieving flow restoration (Figure 7.5) support that the phenomena observed in this study are likely to occur much more commonly than just at end-apnoea observed in this study. The method developed of deriving an attempted ventilation signal allows for clear identification of within breath obstruction and better characterisation of hypopnoea, so these tools should facilitate such an analysis in future. However, additional thought would be required of

how to identify and define flow restoration points within breath when obstruction start and end is less clearly defined than in an apnoea.

In summary, the findings of this study support the central importance of augmented inspiratory effort for overcoming the effects of markedly diminished upper airway dilator muscle activity in the presence of upper airway obstruction (Younes, 2008). Furthermore, non-linear patterns of upper airway muscle recruitment with augmenting inspiratory drive also appear to be important for restoring airflow. Findings were also consistent with previous studies indicating that arousal is a largely an epiphenomenon of augmented inspiratory effort and is not the main factor responsible for airflow restoration (Jordan et al., 2011; Younes, 2003, 2004). Furthermore, this study has identified a sigh-like reflex contributing to substantial changes in inspiratory timing not previously explored in sleep, and which appear to be remarkably common in response to severe airway obstruction. The presence of airflow recovery broadly distributed from early inspiratory effort right through to the early-mid relaxation phase of the respiratory effort cycle followed by more marked augmentation in upper airway muscle activity highlights the likely importance of the negative airway pressure stimulus for upper airway dilator muscle recruitment, and the impact of upper airway obstruction on this important airway dilator stimulus. Further exploration of these phenomena will be important for an improved understanding of the clearly very complex upper airway protective and compensatory mechanisms that largely fail to adequately protect airway function during sleep in OSA.

Chapter 8

Conclusion

8.1 Thesis Objectives

The overall objective of this thesis was to enhance current knowledge regarding the role of respiratory effort augmentation in obstructive sleep apnoea. In addition to poor anatomy, OSA is known to involve a series of non-anatomical impairments that alter the compensatory mechanisms that could otherwise help to counteract increased airway collapsibility (Eckert, 2018). These include decreased responses of upper airway dilator muscles, the over- or under-sensitivity of the central chemo-reflex control system and an overly sensitive arousal system. Increasing respiratory effort generates increasing negative pressure within the respiratory system, which has been shown to be a factor strongly associated with both the arousal response (Gleeson et al., 1990; Younes, 2004) and the dilator muscle recruitment reflex mechanism (Horner et al., 1991). Additionally, ventilatory effort or drive is intrinsically linked to central chemo-reflex control, as that is the primary pathway through which augmented respiratory pump muscle activity is recruited (Ramirez et al., 2013). Therefore oesophageal pressure swings are an important measure related to the two main stimuli for airflow compensation responses in OSA. However, few studies record this intrinsically invasive measure, and in those that do, analysis is generally limited to peak-to-nadir inspiratory pressure swing measures. A better understanding of this signal is important for understanding the role of negative pressure and effort augmentation in OSA pathophysiology. Doing this required the development of new tools and analysis methodologies, which were then implemented to explore mechanisms of airway collapse and airflow recovery in OSA.

The thesis focussed on four specific main aims:

Aim 1 To develop the new filtering techniques required to reduce cardiogenic artefact effect on oesophageal pressure and diaphragm EMG signals. This was addressed in Chapter 3.

Aim 2 To determine the relative effects of an applied external occlusion on oesophageal and epiglottic pressure. This was addressed in Chapter 4.

Aim 3 To implement and test a novel method to quantify respiratory effort and obstruction severity breath-by-breath in OSA patients using a method derived from the classic respiratory equation of motion. This was addressed in Chapter 5.

Aim 4 To use the tools developed to investigate inspiratory drive and negative pressure during obstruction and flow recovery, with and without arousal. This was addressed in Chapters 6 and 7.

8.2 Key Findings

1. Acute airway occlusion itself alters pressure values by an average factor of around 20% for oesophageal pressure and around 100% for epiglottic pressure measurements. This is the first time that acute occlusion effects have been systematically examined in detail. Pressure differences between occluded and non-occluded breaths were found to exhibit excellent fits to volume and flow differences, suggesting occlusion effects are predominantly governed by respiratory mechanics, likely involving abrupt changes in the chest-wall impedance term and resistance at the epiglottis in the presence of occlusion. Oesophageal and epiglottic pressure swings are commonly used as a measure of the arousal threshold and markers of inspiratory effort in physiology studies in OSA research. This finding has important implications for the interpretation of inspiratory pressure deflection values in both past and future studies.

2. The respiratory mechanics model derived measure of attempted ventilation provides a new and insightful measure of ventilatory effort and upper airway obstruction. Tools were created to do this on a breath-by-breath basis, providing new and detailed information regarding the development and restoration of upper airway obstruction in OSA.

3. Augmenting upper airway muscle recruitment appears to be the dominant mechanism for airway reopening. There is clear evidence of recruitment of genioglossus muscles directly preceding the point of airflow recovery. This suggests airway reopening occurs when dilator activity becomes sufficient to overcome collapsing forces.

4. Airflow recovery most often coincides with the commencement of a respiratory effort, but this can occur at any point during the inspiratory phase of the respiratory effort cycle, including into the relaxation phase as negative airway collapsing pressures appear to be abating. When flow recovery occurs late in inspiration, it was observed that a secondary active inspiratory effort re-commences. This observation appears to support reflex changes in inspiratory pattern generation. This is a new observation and may reflect an additional compensatory mechanism in OSA that has not yet been appreciated or studied in detail.

8.3 Research Implications

The findings in Chapter 4 that acute airway occlusion itself does affect both oesophageal and epiglottic pressure values is important to all studies that use these signals to determine

arousal threshold from peak negative pressure values immediately prior to arousal (Gleeson et al., 1990; Li et al., 2019; Xiao et al., 2015). None of these studies have considered the effects of severity of collapse and resultant changes in flow on the pressure values recorded during different events. Our results suggest that apnoea events, with a complete airway obstruction, will produce more negative pressure deflections that a hypopnoea, where some airway patency is retained, even if both had the same underlying neural drive. These effects are most dominant in epiglottic pressure measurements, though this technique is used regularly in studies to determine arousal threshold (Carter et al., 2016; Eckert et al., 2011; Li et al., 2019). It is therefore highly important to investigate these effects further, or at least to consider occlusion effects on pressure values in the interpretation of these studies.

The method developed in Chapter 5, and subsequently applied to physiological data in Chapters 6 and 7, seeks to define a new gold standard measure for neural drive derived from oesophageal pressure signals and address some of the limitations with interpreting drive from raw pressure signals themselves. Diaphragm EMG is an alternative drive measurement. In cases of obstruction,it has been shown oesophageal pressure and diaphragm EMG do not relate linearly (Luo et al., 2009, 2008). Therefore, there is some debate about which of these markers is a better reflection of 'true' underlying neural drive, particularly during events. The breath-by-breath analysis of Chapter 6 also shows differences between ventilatory drive derived from Pmus by the novel method of this thesis and the average inspiratory EMGdi values, in line with these previous studies. It is important this relationship is understood better, and further investigation is raised in the future recommendations below.

The in depth study of airway opening and arousal in Chapter 6 showed, very similarly to (Younes, 2003), that often airflow recovery occurs either prior to or entirely without arousal occurring. This adds to previous findings that arousal and airflow recovery are separate phenomena with likely shared stimulus (Amatoury et al., 2018; Jordan et al., 2007; Younes, 2004). In our study, the majority of arousals actually occur after patency is re-established, however Younes found arousal did predominantly precede airflow recovery. This could be due to the fact we analysed severe total collapse only, which were generally abrupt, short events or simply small sample patient differences. Scoring arousals accurately is also notoriously challenging, and there may be differences resulting from this.

It is also important to consider the clinical implications of the physiological findings of this thesis. Currently, there are a limited number of treatment options for OSA, with the most widely prescribed being CPAP therapy (Sullivan et al., 1981). Though this is highly efficacious when used correctly, tolerance is low, meaning the clinical benefits of CPAP

for an individual are variable (Weaver and Grunstein, 2008). Mandibular advancement devices are better tolerated than CPAP, but target anatomical traits alone, so are less widely applicable. Hypoglossal nerve stimulation directly targets the upper airway dilator muscles, and though results have been promising in a subset of patients, they are not yet widely applicable (Eastwood et al., 2011; Strollo Jr et al., 2014). Recently, a two drug combination of Atomoxetine and Oxybutynin designed to improve genioglossus muscle activity during sleep produced promising early results for reducing AHI across subjects (Taranto-Montemurro et al., 2019). The results from Chapter 7 that a sudden increase in upper airway muscle recruitment precedes airway reopening suggests that the response of these dilator muscles are of central importance to airflow recovery. This supports the value of treatments which target upper airway muscle responses, either through electrical stimulation or via pharmacological pathways. This thesis has also highlighted the role of neural drive augmentation across events, which is still not well understood. By creating a better framework of tools to systematically measure these changes in patients, it will be possible to determine in wider samples the role this plays in OSA.

8.4 Limitations

The studies presented in this thesis contain small numbers of patients with severe OSA, who may not be representative of physiological phenomena operating in mild-to-moderate OSA. Analysis was limited to apnoea events, which are less common than partial airway collapse and flow limitation, and solely confined to stages one and two of NREM sleep. Further work using similar techniques applied to milder obstruction events and in larger groups of OSA patients are clearly warranted.

The sleep studies presented in the final two chapters were observational. This provides the benefit of very detailed analyses of relevant physiological data obtained from naturally occurring apnoea events in OSA, of which there are very few documented studies. However, it also makes it impossible to draw firm conclusions about the causal role of different pathways and mechanisms in the observed results.

As with any studies with an intensive physiological focus, during data collection patients were highly instrumented, and it is unavoidable that instrumentation may have negatively impacted on sleep itself. Recording oesophageal pressure requires an intro-oesophageal catheter, which clearly limits widespread research use and clinical applicability of the presented methods of recording respiratory effort.

However, the tools developed in this thesis have the potential to enhance understanding

of the development, progression and resolution of upper airway obstruction in OSA. The studies in this thesis have helped to develop further testable hypotheses regarding the mechanisms underpinning OSA, for exploration in larger future studies.

8.5 Future Recommendations

Based on the work performed in this thesis, there are several recommendations for areas of future work:

- The method of deriving an attempted ventilation signal from oesophageal pressure showed major promise as a highly informative quantitative measure of inspiratory effort. It also provides the potential for continuous within-breath assessment of obstruction. The field of sleep is in need of new quantitative metrics to replace manual scoring and count-based threshold measures of disease severity like the AHI, which largely fails to quantify obstruction severity or inform pathogenic causal mechanisms. Due to the invasive nature of oesophageal pressure recording, the tools developed are unlikely to have direct wide-spread clinical applicability. However, tracking obstruction measures over the course of the whole night and comparing to AHI and oxygen desaturation would provide much needed detailed quantitative insight to help inform the design of more practical non-invasive metrics.
- In chapter 5, breath-by-breath measures of ventilatory drive from transpulmonary pressure and EMGdi diverged over the course of apnoea, even when accounting for chest wall effects through Pmus. Thus closer investigation of EMGdi and oesophageal pressure relationships would help to provide further insight into the contribution of mechanical versus neuromuscular influences on this phenomenon.
- Further analysis of reflex augmentation of inspiratory pattern generation is clearly warranted. A closer look at the temporal relation between airflow onset and secondary inspiratory pressure deflection and EMGdi recruitment would help to determine whether this reflex is a primary mechanism to generate flow or a secondary response to airflow recovery.

References

Akahoshi, T., White, D. P., Edwards, J. K., Beauregard, J. and Shea, S. A. (2001), 'Phasic mechanoreceptor stimuli can induce phasic activation of upper airway muscles in humans', *J Physiol* **531**(Pt 3), 677–91.

Akhtar, M. T., Mitsuhashi, W. and James, C. J. (2012), 'Employing spatially constrained ica and wavelet denoising, for automatic removal of artifacts from multichannel eeg data', *Signal processing* **92**(2), 401–416.

Akkiraju, P. and Reddy, D. (1992), 'Adaptive cancellation technique in processing myoelectric activity of respiratory muscles', *IEEE Transactions on Biomedical Engineering* **39**(6), 652–655.

Akoumianaki, E., Maggiore, S. M., Valenza, F., Bellani, G., Jubran, A., Loring, S. H., Pelosi, P., Talmor, D., Grasso, S. and Chiumello, D. (2014), 'The application of esophageal pressure measurement in patients with respiratory failure', *American journal of respiratory and critical care medicine* **189**(5), 520–531.

Amatoury, J., Jordan, A. S., Toson, B., Nguyen, C., Wellman, A. and Eckert, D. J. (2018), 'New insights into the timing and potential mechanisms of respiratory-induced cortical arousals in obstructive sleep apnea', *Sleep* **41**(11).

Aronson, R. M., Onal, E., Carley, D. W. and Lopata, M. (1989), 'Upper airway and respiratory muscle responses to continuous negative airway pressure', *Journal of Applied Physiology* **66**(3), 1373–1382.

Azarbarzin, A., Ostrowski, M., Hanly, P. and Younes, M. (2014), 'Relationship between arousal intensity and heart rate response to arousal', *Sleep* **37**(4), 645–53.

Azarbarzin, A., Sands, S. A., Taranto-Montemurro, L., Oliveira Marques, M. D., Genta, P. R., Edwards, B. A., Butler, J., White, D. P. and Wellman, A. (2017), 'Estimation of pharyngeal collapsibility during sleep by peak inspiratory airflow', *Sleep* **40**(1).

Azzerboni, B., Carpentieri, M., La Foresta, F. and Morabito, F. (n.d.), Neural-ica and wavelet transform for artifacts removal in surface emg, *in* '2004 IEEE International Joint

Conference on Neural Networks (IEEE Cat. No. 04CH37541)', Vol. 4, IEEE, pp. 3223–3228.

Baydur, A., Behrakis, P. K., Zin, W. A., Jaeger, M. and Milic-Emili, J. (1982), 'A simple method for assessing the validity of the esophageal balloon technique', *American Review of Respiratory Disease* **126**(5), 788–791.

Berry, R. B., Brooks, R., Gamaldo, C., Harding, S. M., Lloyd, R. M., Quan, S. F., Troester, M. T. and Vaughn, B. V. (2017), 'Aasm scoring manual updates for 2017 (version 2.4)', *Journal of Clinical Sleep Medicine* **13**(05), 665–666.

Berry, R. B., Budhiraja, R., Gottlieb, D. J., Gozal, D., Iber, C., Kapur, V. K., Marcus, C. L., Mehra, R., Parthasarathy, S. and Quan, S. F. (2012), 'Rules for scoring respiratory events in sleep: update of the 2007 aasm manual for the scoring of sleep and associated events', *Journal of clinical sleep medicine* **8**(05), 597–619.

Berry, R. B. and Gleeson, K. (1997), 'Respiratory arousal from sleep: Mechanisms and significance', *Sleep* **20**(8), 654–675.

Berry, R. B., Kouchi, K. G., Bower, J. L. and Light, R. W. (1995), 'Effect of upper airway anesthesia on obstructive sleep apnea', *American journal of respiratory and critical care medicine* **151**(6), 1857–1861.

Berry, R. B., McNellis, M. I., Kouchi, K. and Light, R. W. (1997), 'Upper airway anesthesia reduces phasic genioglossus activity during sleep apnea', *American journal of respiratory and critical care medicine* **156**(1), 127–132.

Bonnet, M. and Arand, D. (1997), 'Heart rate variability: sleep stage, time of night, and arousal influences', *Electroencephalography and clinical neurophysiology* **102**(5), 390–396.

Brouillette, R. T. and Thach, B. T. (1980), 'Control of genioglossus muscle inspiratory activity', *Journal of Applied Physiology* **49**(5), 801–808.

Butler, J. E. (2007), 'Drive to the human respiratory muscles', *Respiratory physiology & neurobiology* **159**(2), 115–126.

Butler, J. E. and Gandevia, S. C. (2008), 'The output from human inspiratory motoneurone pools', *The Journal of physiology* **586**(5), 1257–1264.

Campbell, E. J. M. (1958), *The respiratory muscles and the mechanics of breathing*, Lloyd-Luke.

Cao, J., Murata, N., Amari, S.-i., Cichocki, A. and Takeda, T. (2002), 'Independent component analysis for unaveraged single-trial meg data decomposition and single-dipole source localization', *Neurocomputing* **49**(1-4), 255–277.

Carter, S. G., Berger, M. S., Carberry, J. C., Bilston, L. E., Butler, J. E., Tong, B. K., Martins, R. T., Fisher, L. P., McKenzie, D. K., Grunstein, R. R. and Eckert, D. J. (2016), 'Zopiclone increases the arousal threshold without impairing genioglossus activity in obstructive sleep apnea', *Sleep* **39**(4), 757–66.

Carter, S. G., Carberry, J. C., Grunstein, R. R. and Eckert, D. J. (2018), 'Polysomnography with an epiglottic pressure catheter does not alter obstructive sleep apnea severity or sleep efficiency', *Journal of sleep research* p. e12773.

Cartwright, R. D. (1984), 'Effect of sleep position on sleep apnea severity', *Sleep* **7**(2), 110–114.

Chen, J., Lin, Z., Ramahi, M. and Mittal, R. (1994), 'Adaptive cancellation of ecg artifacts in the diaphragm electromyographic signals obtained through intraoesophageal electrodes during swallowing and inspiration', *Neurogastroenterology Motility* **6**(4), 279–288.

Cheng, Y.-P., Wu, H.-D., Jan, G.-J. and Wang, C.-Y. (2001), 'Removal of cardiac beat artifact in esophageal pressure measurement via a modified adaptive noise cancellation scheme', *Annals of biomedical engineering* **29**(3), 236–243.

Cheng, Y., Wu, H., Wang, C. and Jan, G. (1999), 'Removal of cardiac beat artifact in oesophageal pressure measurement by frequency analysis', *Medical biological engineering computing* **37**(6), 776–783.

Cherniack, R. M., Farhi, L. E., Armstrong, B. W. and Proctor, D. F. (1955), 'A comparison of esophageal and intrapleural pressure in man', *Journal of applied physiology* **8**(2), 203–211.

Chervin, R. D. and Aldrich, M. S. (1997), 'Effects of esophageal pressure monitoring on sleep architecture', *American journal of respiratory and critical care medicine* **156**(3), 881–885.

Conrad, W. A. (1969), 'Pressure-flow relationships in collapsible tubes', *IEEE Transactions on Biomedical Engineering* (4), 284–295.

Cori, J. M., Nicholas, C. L., Baptista, S., Huynh, I., Rochford, P. D., O'Donoghue, F. J., Trinder, J. A. and Jordan, A. S. (2012), 'Inspiratory-resistive loading increases the ventilatory response to arousal but does not reduce genioglossus muscle activity on the return to sleep', *Journal of Applied Physiology* **113**(6), 909–916.

Cori, J. M., O'Donoghue, F. J. and Jordan, A. S. (2018), 'Sleeping tongue: current perspectives of genioglossus control in healthy individuals and patients with obstructive sleep apnea', *Nat Sci Sleep* **10**, 169–179.

Cori, J. M., Thornton, T., O'Donoghue, F. J., Rochford, P. D., White, D. P., Trinder, J. and Jordan, A. S. (2017), 'Arousal-induced hypocapnia does not reduce genioglossus activity in obstructive sleep apnea', *Sleep* **40**(6).

De Troyer, A., Gorman, R. B. and Gandevia, S. C. (2003), 'Distribution of inspiratory drive to the external intercostal muscles in humans', *J Physiol* **546**(Pt 3), 943–54.

De Troyer, A., Leeper, J. B., McKenzie, D. K. and Gandevia, S. C. (1997), 'Neural drive to the diaphragm in patients with severe copd.', *American Journal of Respiratory and Critical Care Medicine* **155**(4), 1335–1340.

Dechman, G., Sato, J. and Bates, J. (1992), 'Factors affecting the accuracy of esophageal balloon measurement of pleural pressure in dogs', *Journal of Applied Physiology* **72**(1), 383–388.

Deng, Y., Wolf, W., Schnell, R. and Appel, U. (2000), 'New aspects to event-synchronous cancellation of ecg interference: an application of the method in diaphragmatic emg signals', *IEEE Transactions on Biomedical Engineering* **47**(9), 1177–1184.

Dornhorst, A. and Leathart, G. (1952), 'A method of assessing the mechanical properties of lungs and air-passages', *The Lancet* **260**(6725), 109–111.

Eastwood, P. R., Barnes, M., Walsh, J. H., Maddison, K. J., Hee, G., Schwartz, A. R., Smith, P. L., Malhotra, A., McEvoy, R. D. and Wheatley, J. R. (2011), 'Treating obstructive sleep apnea with hypoglossal nerve stimulation', *Sleep* **34**(11), 1479–1486.

Eckert, D. J. (2018), 'Phenotypic approaches to obstructive sleep apnoea - new pathways for targeted therapy', *Sleep Med Rev* **37**, 45–59.

Eckert, D. J., Malhotra, A., Wellman, A. and White, D. P. (2014), 'Trazodone increases the respiratory arousal threshold in patients with obstructive sleep apnea and a low arousal threshold', *Sleep* **37**(4), 811–819.

Eckert, D. J., McEvoy, R. D., George, K. E., Thomson, K. J. and Catcheside, P. G. (2007), 'Genioglossus reflex inhibition to upper airway negative pressure stimuli during wakefulness and sleep in healthy males', *The Journal of physiology* **581**(3), 1193–1205.

Eckert, D. J., Owens, R. L., Kehlmann, G. B., Wellman, A., Rahangdale, S., Yim-Yeh, S., White, D. P. and Malhotra, A. (2011), 'Eszopiclone increases the respiratory arousal

threshold and lowers the apnoea/hypopnoea index in obstructive sleep apnoea patients with a low arousal threshold', *Clinical science* **120**(12), 505–514.

Eckert, D. J., Saboisky, J. P., Jordan, A. S., White, D. P. and Malhotra, A. (2010), 'A secondary reflex suppression phase is present in genioglossus but not tensor palatini in response to negative upper airway pressure', *Journal of Applied Physiology* **108**(6), 1619–1624.

Eckert, D. J., White, D. P., Jordan, A. S., Malhotra, A. and Wellman, A. (2013), 'Defining phenotypic causes of obstructive sleep apnea. identification of novel therapeutic targets', *Am J Respir Crit Care Med* **188**(8), 996–1004.

Eckert, D. J. and Younes, M. K. (2014), 'Arousal from sleep: implications for obstructive sleep apnea pathogenesis and treatment', *J Appl Physiol (1985)* **116**(3), 302–13.

Edwards, B. A., Andara, C., Landry, S., Sands, S. A., Joosten, S. A., Owens, R. L., White, D. P., Hamilton, G. S. and Wellman, A. (2016), 'Upper-airway collapsibility and loop gain predict the response to oral appliance therapy in patients with obstructive sleep apnea', *Am J Respir Crit Care Med* **194**(11), 1413–1422.

Edwards, B. A., Sands, S. A., Eckert, D. J., White, D. P., Butler, J. P., Owens, R. L., Malhotra, A. and Wellman, A. (2012), 'Acetazolamide improves loop gain but not the other physiological traits causing obstructive sleep apnoea', *The Journal of physiology* **590**(5), 1199–1211.

Edwards, B. A., Sands, S. A., Owens, R. L., Eckert, D. J., Landry, S., White, D. P., Malhotra, A. and Wellman, A. (2016), 'The combination of supplemental oxygen and a hypnotic markedly improves obstructive sleep apnea in patients with a mild to moderate upper airway collapsibility', *Sleep* **39**(11), 1973–1983.

Feldman, J. L. and Del Negro, C. A. (2006), 'Looking for inspiration: new perspectives on respiratory rhythm', *Nature Reviews Neuroscience* **7**(3), 232.

Flemale, A., Gillard, C. and Dierckx, J. (1988), 'Comparison of central venous, oesophageal and mouth occlusion pressure with water-filled catheters for estimating pleural pressure changes in healthy adults', *European Respiratory Journal* **1**(1), 51–57.

Gandevia, S. C., Smith, J. L., Crawford, M., Proske, U. and Taylor, J. L. (2006), 'Motor commands contribute to human position sense', *The Journal of physiology* **571**(3), 703–710.

Genta, P. R., Owens, R. L., Edwards, B. A., Sands, S. A., Eckert, D. J., Butler, J. P., Loring, S. H., Malhotra, A., Jackson, A. C. and White, D. P. (2014), 'Influence of

pharyngeal muscle activity on inspiratory negative effort dependence in the human upper airway', *Respiratory physiology neurobiology* **201**, 55–59.

German, W. and Vaughn, B. V. (1996), 'Techniques for monitoring intrathoracic pressure during overnight polysomnography', *American Journal of Electroneurodiagnostic Technology* **36**(3), 197–208.

Gillespie, D. J., Lai, Y. and Hyatt, R. E. (1973), 'Comparison of esophageal and pleural pressures in the anesthetized dog', *Journal of applied physiology* **35**(5), 709–713.

Gleeson, K., Zwillich, C. W. and White, D. P. (1990), 'The influence of increasing ventilatory effort on arousal from sleep', *Am Rev Respir Dis* **142**(2), 295–300.

Gottfried, S., Rossi, A. and Milic-Emili, J. (1986), 'Dynamic hyperinflation, intrinsic peep, and the mechanically ventilated patient', *Crit Care Digest* **5**, 30–33.

Grauer, D., Cevidanes, L. S., Styner, M. A., Ackerman, J. L. and Proffit, W. R. (2009), 'Pharyngeal airway volume and shape from cone-beam computed tomography: relationship to facial morphology', *Am J Orthod Dentofacial Orthop* **136**(6), 805–14.

Graßhoff, J., Petersen, E., Eger, M., Bellani, G. and Rostalski, P. (n.d.), A template subtraction method for the removal of cardiogenic oscillations on esophageal pressure signals, *in* '2017 39th Annual International Conference of the IEEE Engineering in Medicine and Biology Society (EMBC)', IEEE, pp. 2235–2238.

Guerin, C., Coussa, M., Eissa, N., Corbeil, C., Chasse, M., Braidy, J., Matar, N. and Milic-Emili, J. (1993), 'Lung and chest wall mechanics in mechanically ventilated copd patients', *Journal of Applied Physiology* **74**(4), 1570–1580.

Guilleminault, C., Tilkian, A. and Dement, W. C. (1976), 'The sleep apnea syndromes', *Annual review of medicine* **27**(1), 465–484.

Gulati, G., Novero, A., Loring, S. H. and Talmor, D. (2013), 'Pleural pressure and optimal positive end-expiratory pressure based on esophageal pressure versus chest wall elastance: incompatible results', *Critical care medicine* **41**(8), 1951–1957.

Guérin, C. and Richard, J.-C. (2012), 'Comparison of 2 correction methods for absolute values of esophageal pressure in subjects with acute hypoxemic respiratory failure, mechanically ventilated in the icu', *Respiratory care* **57**(12), 2045–2051.

Haponik, E. F., Smith, P. L., Bohlman, M. E., Allen, R. P., Goldman, S. M. and Bleecker, E. R. (1983), 'Computerized tomography in obstructive sleep apnea: correlation of airway size with physiology during sleep and wakefulness', *American Review of Respiratory Disease* **127**(2), 221–226.

Henke, K. G., Badr, M. S., Skatrud, J. B. and Dempsey, J. A. (1992), 'Load compensation and respiratory muscle function during sleep', *J Appl Physiol (1985)* **72**(4), 1221–34.

Hering, E. and Breuer, J. (1868), Self-steering of respiration through the nervus vagus, *in* 'Ciba Foundation Symposium on Breathing: Hering-Breuer'.

Horner, R., Innes, J., Murphy, K. and Guz, A. (1991), 'Evidence for reflex upper airway dilator muscle activation by sudden negative airway pressure in man', *The Journal of Physiology* **436**(1), 15–29.

Horner, R., Mohiaddin, R., Lowell, D., Shea, S., Burman, E., Longmore, D. and Guz, A. (1989), 'Sites and sizes of fat deposits around the pharynx in obese patients with obstructive sleep apnoea and weight matched controls', *European Respiratory Journal* **2**(7), 613–622.

Hudgel, D. W., Chapman, K. R., Faulks, C. and Hendricks, C. (1987), 'Changes in inspiratory muscle electrical activity and upper airway resistance during periodic breathing induced by hypoxia during sleep', *Am Rev Respir Dis* **135**(4), 899–906.

Hudgel, D. W., Martin, R. J., Johnson, B. and Hill, P. (1984), 'Mechanics of the respiratory system and breathing pattern during sleep in normal humans', *J Appl Physiol Respir Environ Exerc Physiol* **56**(1), 133–7.

Hutter, D. A., Holland, B. K. and Ashtyani, H. (2004), 'Occult sleep apnea: the dilemma of negative polysomnography in symptomatic patients', *Sleep Med* **5**(5), 501–6.

Hyvarinen, A. and Oja, E. (1997), 'A fast fixed-point algorithm for independent component analysis', *Neural computation* **9**(7), 1483–1492.

Iber, C., Ancoli-Israel, S., Chesson, A. and Quan, S. F. (2007), *The AASM manual for the scoring of sleep and associated events: rules, terminology and technical specifications*, Vol. 1, American Academy of Sleep Medicine Westchester, IL.

Isono, S., Remmers, J. E., Tanaka, A., Sho, Y., Sato, J. and Nishino, T. (1997), 'Anatomy of pharynx in patients with obstructive sleep apnea and in normal subjects', *J Appl Physiol (1985)* **82**(4), 1319–26.

Jeffery, S., Butler, J. E., McKenzie, D. K., Wang, L. and Gandevia, S. C. (2006*a*), 'Brief airway occlusion produces prolonged reflex inhibition of inspiratory muscles in obstructive sleep apnea', *Sleep* **29**(3), 321–328.

Jeffery, S., Butler, J. E., McKenzie, D. K., Wang, L. and Gandevia, S. C. (2006*b*), 'Brief airway occlusion produces prolonged reflex inhibition of inspiratory muscles in obstructive sleep apnea', *Sleep* **29**(3), 321–328.

Jordan, A. S., Cori, J. M., Dawson, A., Nicholas, C. L., O'Donoghue, F. J., Catcheside, P. G., Eckert, D. J., McEvoy, R. D. and Trinder, J. (2015), 'Arousal from sleep does not lead to reduced dilator muscle activity or elevated upper airway resistance on return to sleep in healthy individuals', *Sleep* **38**(1), 53–9.

Jordan, A. S., Eckert, D. J., Wellman, A., Trinder, J. A., Malhotra, A. and White, D. P. (2011), 'Termination of respiratory events with and without cortical arousal in obstructive sleep apnea', *Am J Respir Crit Care Med* **184**(10), 1183–91.

Jordan, A. S., O'Donoghue, F. J., Cori, J. M. and Trinder, J. (2017), 'Physiology of arousal in obstructive sleep apnea and potential impacts for sedative treatment', *American journal of respiratory and critical care medicine* **196**(7), 814–821.

Jordan, A. S., Wellman, A., Heinzer, R. C., Lo, Y. L., Schory, K., Dover, L., Gautam, S., Malhotra, A. and White, D. P. (2007), 'Mechanisms used to restore ventilation after partial upper airway collapse during sleep in humans', *Thorax* **62**(10), 861–7.

Jordan, A. S., White, D. P., Lo, Y. L., Wellman, A., Eckert, D. J., Yim-Yeh, S., Eikermann, M., Smith, S. A., Stevenson, K. E. and Malhotra, A. (2009), 'Airway dilator muscle activity and lung volume during stable breathing in obstructive sleep apnea', *Sleep* **32**(3), 361–8.

Kezirian, E. J. and Goldberg, A. N. (2006), 'Hypopharyngeal surgery in obstructive sleep apnea: an evidence-based medicine review', *Archives of Otolaryngology Head and Neck Surgery* **132**(2), 206–213.

Kirkness, J. P., Madronio, M., Stavrinou, R., Wheatley, J. R. and Amis, T. C. (2003), 'Relationship between surface tension of upper airway lining liquid and upper airway collapsibility during sleep in obstructive sleep apnea hypopnea syndrome', *Journal of Applied Physiology* **95**(5), 1761–1766.

Kuna, S. T. (2000), 'Respiratory-related activation and mechanical effects of the pharyngeal constrictor muscles', *Respir Physiol* **119**(2-3), 155–61.

Kuna, S. T. and Smickley, J. S. (1997), 'Superior pharyngeal constrictor activation in obstructive sleep apnea', *Am J Respir Crit Care Med* **156**(3 Pt 1), 874–80.

Kuna, S. T., Smickley, J. S. and Vanoye, C. R. (1997), 'Respiratory-related pharyngeal constrictor muscle activity in normal human adults', *Am J Respir Crit Care Med* **155**(6), 1991–9.

Kushida, C. A., Giacomini, A., Lee, M. K., Guilleminault, C. and Dement, W. C. (2002), 'Technical protocol for the use of esophageal manometry in the diagnosis of sleep-related breathing disorders', *Sleep medicine* **3**(2), 163–173.

Legrand, A. and De Troyer, A. (1999), 'Spatial distribution of external and internal intercostal activity in dogs', *J Physiol* **518**(Pt 1), 291–300.

Levine, S., Gillen, J. S., Weiser, P. and Kwatny, E. (1986), 'Description and validation of an ecg removal procedure for emgdi power spectrum analysis', *Journal of Applied Physiology* **60**(3), 1073–1081.

Li, Y., Orr, J., Jen, R., Sands, S. A., DeYoung, P., Smales, E., Edwards, B., Owens, R. L. and Malhotra, A. (2019), 'Is there a threshold that triggers cortical arousals in obstructive sleep apnea', *Sleep* .

Loewen, A. H., Ostrowski, M., Laprairie, J., Maturino, F., Hanly, P. J. and Younes, M. (2011), 'Response of genioglossus muscle to increasing chemical drive in sleeping obstructive apnea patients', *Sleep* **34**(8), 1061–73.

Luo, Y. M., Tang, J., Jolley, C., Steier, J., Zhong, N. S., Moxham, J. and Polkey, M. I. (2009), 'Distinguishing obstructive from central sleep apnea events: diaphragm electromyogram and esophageal pressure compared', *Chest* **135**(5), 1133–1141.

Luo, Y. M., Wu, H. D., Tang, J., Jolley, C., Steier, J., Moxham, J., Zhong, N. S. and Polkey, M. I. (2008), 'Neural respiratory drive during apnoeic events in obstructive sleep apnoea', *Eur Respir J* **31**(3), 650–7.

Malhotra, A., Pillar, G., Fogel, R. B., Edwards, J. K., Ayas, N., Akahoshi, T., Hess, D. and White, D. P. (2002), 'Pharyngeal pressure and flow effects on genioglossus activation in normal subjects', *Am J Respir Crit Care Med* **165**(1), 71–7.

Marshall, N. S., Wong, K. K., Liu, P. Y., Cullen, S. R., Knuiman, M. W. and Grunstein, R. R. (2008), 'Sleep apnea as an independent risk factor for all-cause mortality: the busselton health study', *Sleep* **31**(8), 1079–1085.

McKenzie, D. K., Butler, J. E. and Gandevia, S. C. (2009), 'Respiratory muscle function and activation in chronic obstructive pulmonary disease', *Journal of applied physiology* **107**(2), 621–629.

Mead, J. and Agostoni, E. (1964), 'Dynamics of breathing', *Handbook of Physiology. Respiration* **1**, 411–427.

Mezzanotte, W. S., Tangel, D. J. and White, D. P. (1992), 'Waking genioglossal electromyogram in sleep apnea patients versus normal controls (a neuromuscular compensatory mechanism).', *The Journal of clinical investigation* **89**(5), 1571–1579.

Morrell, M. J., Harty, H. R., Adams, L. and Guz, A. (1995), 'Changes in total pulmonary resistance and pco2 between wakefulness and sleep in normal human subjects', *J Appl Physiol (1985)* **78**(4), 1339–49.

Newman, A. B., Foster, G., Givelber, R., Nieto, F. J., Redline, S. and Young, T. (2005), 'Progression and regression of sleep-disordered breathing with changes in weight: the sleep heart health study', *Archives of internal medicine* **165**(20), 2408–2413.

Nicholas, C. L., Jordan, A. S., Heckel, L., Worsnop, C., Bei, B., Saboisky, J. P., Eckert, D. J., White, D. P., Malhotra, A. and Trinder, J. (2012), 'Discharge patterns of human tensor palatini motor units during sleep onset', *Sleep* **35**(5), 699–707.

Nieto, F. J., Young, T. B., Lind, B. K., Shahar, E., Samet, J. M., Redline, S., D'Agostino, R. B., Newman, A. B., Lebowitz, M. D. and Pickering, T. G. (2000), 'Association of sleep-disordered breathing, sleep apnea, and hypertension in a large community-based study', *Jama* **283**(14), 1829–1836.

Onal, E. and Lopata, M. (1986), 'Respiratory timing during nrem sleep in patients with occlusive sleep apnea', *Journal of applied physiology (Bethesda, Md.: 1985)* **61**(4), 1444.

Onal, E., Lopata, M. and O'Connor, T. D. (1981), 'Diaphragmatic and genioglossal electromyogram responses to co2 rebreathing in humans', *Journal of Applied Physiology* **50**(5), 1052–1055.

Owens, R. L., Edwards, B. A., Sands, S. A., Butler, J. P., Eckert, D. J., White, D. P., Malhotra, A. and Wellman, A. (2014), 'The classical starling resistor model often does not predict inspiratory airflow patterns in the human upper airway', *J Appl Physiol (1985)* **116**(8), 1105–12.

Patrick, G. B., Strohl, K. P., Rubin, S. B. and Altose, M. D. (1982), 'Upper airway and diaphragm muscle responses to chemical stimulation and loading', *Journal of Applied Physiology* **53**(5), 1133–1137.

Peever, J. H., Shen, L. and Duffin, J. (2002), 'Respiratory pre-motor control of hypoglossal motoneurons in the rat', *Neuroscience* **110**(4), 711–722.

Penzel, T., Kantelhardt, J. W., Lo, C.-C., Voigt, K. and Vogelmeier, C. (2003), 'Dynamics of heart rate and sleep stages in normals and patients with sleep apnea', *Neuropsychopharmacology* **28**(S1), S48.

Pierce, R., White, D., Malhotra, A., Edwards, J. K., Kleverlaan, D., Palmer, L. and Trinder, J. (2007), 'Upper airway collapsibility, dilator muscle activation and resistance in sleep apnoea', *European Respiratory Journal* **30**(2), 345–353.

Pillar, G., Fogel, R. B., Malhotra, A., Beauregard, J., Edwards, J. K., Shea, S. A. and White, D. P. (2001), 'Genioglossal inspiratory activation: central respiratory vs mechanoreceptive influences', *Respir Physiol* **127**(1), 23–38.

Pinto, J. A., Godoy, L. B., Marquis, V. W., Sonego, T. B., Leal Cde, F. and Artico, M. S. (2011), 'Anthropometric data as predictors of obstructive sleep apnea severity', *Braz J Otorhinolaryngol* **77**(4), 516–21.

Punjabi, N. M. (2008), 'The epidemiology of adult obstructive sleep apnea', *Proceedings of the American Thoracic Society* **5**(2), 136–143.

Rama, A. N., Tekwani, S. H. and Kushida, C. A. (2002), 'Sites of obstruction in obstructive sleep apnea', *Chest* **122**(4), 1139–47.

Ramirez, J.-M., Garcia III, A. J., Anderson, T. M., Koschnitzky, J. E., Peng, Y.-J., Kumar, G. K. and Prabhakar, N. R. (2013), 'Central and peripheral factors contributing to obstructive sleep apneas', *Respiratory physiology & neurobiology* **189**(2), 344–353.

Ratnavadivel, R., Chau, N., Stadler, D., Yeo, A., McEvoy, R. D. and Catcheside, P. G. (2009), 'Marked reduction in obstructive sleep apnea severity in slow wave sleep', *J Clin Sleep Med* **5**(6), 519–24.

Remmers, J., DeGroot, W., Sauerland, E. and Anch, A. (1978), 'Pathogenesis of upper airway occlusion during sleep', *Journal of Applied Physiology* **44**(6), 931–938.

Riddle, W. and Younes, M. (1981), 'A model for the relation between respiratory neural and mechanical outputs. ii. methods', *Journal of Applied Physiology* **51**(4), 979–989.

Saboisky, J. P., Gorman, R. B., De Troyer, A., Gandevia, S. C. and Butler, J. E. (2007), 'Differential activation among five human inspiratory motoneuron pools during tidal breathing', *J Appl Physiol (1985)* **102**(2), 772–80.

Sands, S. A., Eckert, D. J., Jordan, A. S., Edwards, B. A., Owens, R. L., Butler, J. P., Schwab, R. J., Loring, S. H., Malhotra, A., White, D. P. and Wellman, A. (2014), 'Enhanced upper-airway muscle responsiveness is a distinct feature of overweight/obese individuals without sleep apnea', *Am J Respir Crit Care Med* **190**(8), 930–7.

Schuessler, T. F., Gottfried, S. B., Goldberg, P., Kearney, R. E. and Bates, J. H. (1998), 'An adaptive filter to reduce cardiogenic oscillations on esophageal pressure signals', *Annals of biomedical engineering* **26**(2), 260–267.

Schwab, R. J., Gupta, K. B., Gefter, W. B., Metzger, L. J., Hoffman, E. A. and Pack, A. I. (1995), 'Upper airway and soft tissue anatomy in normal subjects and patients

with sleep-disordered breathing. significance of the lateral pharyngeal walls', *American journal of respiratory and critical care medicine* **152**(5), 1673–1689.

Schwab, R. J., Pasirstein, M., Pierson, R., Mackley, A., Hachadoorian, R., Arens, R., Maislin, G. and Pack, A. I. (2003), 'Identification of upper airway anatomic risk factors for obstructive sleep apnea with volumetric magnetic resonance imaging', *American journal of respiratory and critical care medicine* **168**(5), 522–530.

Schwartz, A., O'Donnell, C., Baron, J., Schubert, N., Alam, D., Samadi, S. and Smith, P. (1998), 'The hypotonic upper airway in obstructive sleep apnea: role of structures and neuromuscular activity', *American journal of respiratory and critical care medicine* **157**(4 Pt 1), 1051.

Schweitzer, T. W., Fitzgerald, J. W., Bowden, J. A. and Lynne-Davies, P. (1979), 'Spectral analysis of human inspiratory diaphragmatic electromyograms', *J Appl Physiol Respir Environ Exerc Physiol* **46**(1), 152–65.

Seppä, V.-P., Hyttinen, J. and Viik, J. (2011), 'A method for suppressing cardiogenic oscillations in impedance pneumography', *Physiological measurement* **32**(3), 337.

Sforza, E., Bacon, W., Weiss, T., Thibault, A., Petiau, C. and Krieger, J. (2000), 'Upper airway collapsibility and cephalometric variables in patients with obstructive sleep apnea', *American journal of respiratory and critical care medicine* **161**(2), 347–352.

Skatvedt, O., Akre, H. and Godtlibsen, O. B. (1996), 'Nocturnal polysomnography with and without continuous pharyngeal and esophageal pressure measurements', *Sleep* **19**(6), 485–90.

Skiba, V., Goldstein, C. and Schotland, H. (2015), 'Night-to-night variability in sleep disordered breathing and the utility of esophageal pressure monitoring in suspected obstructive sleep apnea', *J Clin Sleep Med* **11**(6), 597–602.

Smales, E. T., Edwards, B. A., Deyoung, P. N., McSharry, D. G., Wellman, A., Velasquez, A., Owens, R., Orr, J. E. and Malhotra, A. (2015), 'Trazodone effects on obstructive sleep apnea and non-rem arousal threshold', *Annals of the American Thoracic Society* **12**(5), 758–764.

Stadler, D. L., McEvoy, R. D., Bradley, J., Paul, D. and Catcheside, P. G. (2010), 'Changes in lung volume and diaphragm muscle activity at sleep onset in obese obstructive sleep apnea patients vs. healthy-weight controls', *Journal of Applied Physiology* **109**(4), 1027–1036.

Stadler, D. L., McEvoy, R. D., Sprecher, K. E., Thomson, K. J., Ryan, M. K., Thompson, C. C. and Catcheside, P. G. (2009), 'Abdominal compression increases upper airway collapsibility during sleep in obese male obstructive sleep apnea patients', *Sleep* **32**(12), 1579–1587.

Stoohs, R. A., Blum, H.-C., Knaack, L., Butsch-von-der Heydt, B. and Guilleminault, C. (2005), 'Comparison of pleural pressure and transcutaneous diaphragmatic electromyogram in obstructive sleep apnea syndrome', *Sleep* **28**(3), 321–329.

Strohl, K. P., Hensley, M. J., Hallett, M., Saunders, N. A. and Ingram, R. H., J. (1980), 'Activation of upper airway muscles before onset of inspiration in normal humans', *J Appl Physiol Respir Environ Exerc Physiol* **49**(4), 638–42.

Strollo Jr, P. J., Soose, R. J., Maurer, J. T., de Vries, N., Cornelius, J., Froymovich, O., Hanson, R. D., Padhya, T. A., Steward, D. L. and Gillespie, M. B. (2014), 'Upper-airway stimulation for obstructive sleep apnea', *New England Journal of Medicine* **370**(2), 139–149.

Sullivan, C., Berthon-Jones, M., Issa, F. and Eves, L. (1981), 'Reversal of obstructive sleep apnoea by continuous positive airway pressure applied through the nares', *The Lancet* **317**(8225), 862–865.

Sutherland, K. and Cistulli, P. (2011), 'Mandibular advancement splints for the treatment of sleep apnea syndrome', *Swiss medical weekly* **141**(3940).

Taranto-Montemurro, L., Messineo, L., Sands, S. A., Azarbarzin, A., Marques, M., Edwards, B. A., Eckert, D. J., White, D. P. and Wellman, A. (2019), 'The combination of atomoxetine and oxybutynin greatly reduces obstructive sleep apnea severity. a randomized, placebo-controlled, double-blind crossover trial', *American Journal of Respiratory and Critical Care Medicine* **199**(10), 1267–1276.

Taranto-Montemurro, L., Sands, S. A., Grace, K. P., Azarbarzin, A., Messineo, L., Salant, R., White, D. P. and Wellman, D. A. (2018), 'Neural memory of the genioglossus muscle during sleep is stage-dependent in healthy subjects and obstructive sleep apnoea patients', *J Physiol* **596**(21), 5163–5173.

Terrill, P. I., Edwards, B. A., Nemati, S., Butler, J. P., Owens, R. L., Eckert, D. J., White, D. P., Malhotra, A., Wellman, A. and Sands, S. A. (2015), 'Quantifying the ventilatory control contribution to sleep apnoea using polysomnography', *Eur Respir J* **45**(2), 408–18.

Tregear, S., Reston, J., Schoelles, K. and Phillips, B. (2009), 'Obstructive sleep apnea and risk of motor vehicle crash: systematic review and meta-analysis', *Journal of clinical sleep medicine* **5**(06), 573–581.

Trinder, J. and Jordan, A. S. (2011), 'Activation of the upper airway dilator muscle genioglossus during sleep is largely dependent on an interaction between chemical drive and mechanoreceptor feedback', *Sleep* **34**(8), 983–4.

van Lunteren, E., Van de Graaff, W. B., Parker, D. M., Mitra, J., Haxhiu, M. A., Strohl, K. P. and Cherniack, N. S. (1984), 'Nasal and laryngeal reflex responses to negative upper airway pressure', *Journal of Applied Physiology* **56**(3), 746–752.

Vandenbussche, N. L., Overeem, S., van Dijk, J. P., Simons, P. J. and Pevernagie, D. A. (2015), 'Assessment of respiratory effort during sleep: esophageal pressure versus non-invasive monitoring techniques', *Sleep medicine reviews* **24**, 28–36.

Vincken, W., Guilleminault, C., Silvestri, L., Cosio, M. and Grassino, A. (1987), 'Inspiratory muscle activity as a trigger causing the airways to open in obstructive sleep apnea', *American Review of Respiratory Disease* **135**(2), 372–377.

Weaver, T. E. and Grunstein, R. R. (2008), 'Adherence to continuous positive airway pressure therapy: the challenge to effective treatment', *Proceedings of the American Thoracic Society* **5**(2), 173–178.

Wellman, A., Edwards, B. A., Sands, S. A., Owens, R. L., Nemati, S., Butler, J., Passaglia, C. L., Jackson, A. C., Malhotra, A. and White, D. P. (2013), 'A simplified method for determining phenotypic traits in patients with obstructive sleep apnea', *Journal of applied physiology* **114**(7), 911–922.

Wellman, A., Genta, P. R., Owens, R. L., Edwards, B. A., Sands, S. A., Loring, S. H., White, D. P., Jackson, A. C., Pedersen, O. F. and Butler, J. P. (2014), 'Test of the starling resistor model in the human upper airway during sleep', *J Appl Physiol (1985)* **117**(12), 1478–85.

Wheatley, J. R., Mezzanotte, W. S., Tangel, D. J. and White, D. P. (1993), 'Influence of sleep on genioglossus muscle activation by negative pressure in normal men', *Am Rev Respir Dis* **148**(3), 597–605.

White, D. P. and Younes, M. K. (2012), 'Obstructive sleep apnea', *Compr Physiol* **2**(4), 2541–94.

Widrow, B., Glover, J. R., McCool, J. M., Kaunitz, J., Williams, C. S., Hearn, R. H., Zeidler, J. R., Dong, J. E. and Goodlin, R. C. (1975), 'Adaptive noise cancelling: Principles and applications', *Proceedings of the IEEE* **63**(12), 1692–1716.

Wiegand, L., Zwillich, C. W. and White, D. P. (1989), 'Collapsibility of the human upper airway during normal sleep', *J Appl Physiol (1985)* **66**(4), 1800–8.

Wilcox, P. G., Pare, P. D., Road, J. D. and Fleetham, J. A. (1990), 'Respiratory muscle function during obstructive sleep apnea', *Am Rev Respir Dis* **142**(3), 533–9.

Wilkinson, V., Malhotra, A., Nicholas, C. L., Worsnop, C., Jordan, A. S., Butler, J. E., Saboisky, J. P., Gandevia, S. C., White, D. P. and Trinder, J. (2008), 'Discharge patterns of human genioglossus motor units during sleep onset', *Sleep* **31**(4), 525–533.

Wu, F.-Y., Tong, F. and Yang, Z. (2016), 'Emgdi signal enhancement based on ica decomposition and wavelet transform', *Applied Soft Computing* **43**, 561–571.

Xiao, S. C., He, B. T., Steier, J., Moxham, J., Polkey, M. I. and Luo, Y. M. (2015), 'Neural respiratory drive and arousal in patients with obstructive sleep apnea hypopnea', *Sleep* **38**(6), 941–9.

Younes, M. (2003), 'Contributions of upper airway mechanics and control mechanisms to severity of obstructive apnea', *Am J Respir Crit Care Med* **168**(6), 645–58.

Younes, M. (2004), 'Role of arousals in the pathogenesis of obstructive sleep apnea', *Am J Respir Crit Care Med* **169**(5), 623–33.

Younes, M. (2008), 'Role of respiratory control mechanisms in the pathogenesis of obstructive sleep disorders', *J Appl Physiol (1985)* **105**(5), 1389–405.

Younes, M., Loewen, A. H., Ostrowski, M., Laprairie, J., Maturino, F. and Hanly, P. J. (2012), 'Genioglossus activity available via non-arousal mechanisms vs. that required for opening the airway in obstructive apnea patients', *J Appl Physiol (1985)* **112**(2), 249–58.

Younes, M., Ostrowski, M., Atkar, R., Laprairie, J., Siemens, A. and Hanly, P. (2007), 'Mechanisms of breathing instability in patients with obstructive sleep apnea', *J Appl Physiol (1985)* **103**(6), 1929–41.

Younes, M. and Riddle, W. (1981), 'A model for the relation between respiratory neural and mechanical outputs. i. theory', *Journal of Applied Physiology* **51**(4), 963–978.

Younes, M., Riddle, W. and Polacheck, J. (1981), 'A model for the relation between respiratory neural and mechanical outputs. iii. validation', *Journal of Applied Physiology* **51**(4), 990–1001.

Young, T., Peppard, P. E. and Gottlieb, D. J. (2002), 'Epidemiology of obstructive sleep apnea: a population health perspective', *American journal of respiratory and critical care medicine* **165**(9), 1217–1239.

Önal, E., Lopata, M. and O'Connor, T. (1982), 'Pathogenesis of apneas in hypersomnia-sleep apnea syndrome', *American Review of Respiratory Disease* **125**(2), 167–174.

Önal, E., Lopata, M. and O'Connor, T. D. (1981), 'Diaphragmatic and genioglossal electromyogram responses to isocapnic hypoxia in humans', *American Review of Respiratory Disease* **124**(3), 215–217.

Appendix A

Matlab GUI for analysis

A complex challenge in the analysis of sleep signals is ensuring that the process is streamlined and at least partially automated so that it can be easily repeated for multiple subjects, whilst accounting for the fact individuals vary significantly and artefacts are common. Any automated analysis therefore likely requires some manual review. This led to the development of a custom GUI to facilitate the analysis in this project. Tools needed to be adaptable and easy to use at the front end by research staff across a multidisciplinary team to ensure future applicability. This appendix describes the design, layout, functionality and capabilities of the analysis interface. The GUI was developed using MATLAB Version 2017b (Mathworks, Natick, MA, USA).

A.1 GUI Requirements

There were four main areas of functionality developed and implemented in the analysis tool for the work discussed in this thesis, which are displayed in Figure A.1. Raw data are first imported and then calibrated, filtered and processed as required. Then, the novel metric of attempted ventilation is modelled. Obstruction and effort are then determined on a breath by breath basis using this new measure. These signals are displayed for review by the user. The tool also allows for event analysis, either reading timepoints from an event list (e.g. sleep-scored data) or using a threshold derived flow or obstruction parameter to determine events. In Chapters 6 and 7, a flow threshold was used to identify periods of airway collapse, and these events are displayed and reviewed. Finally, breath by breath calculations are performed on the selected events, matching parameters from achieved

and attempted ventilation. Each of these requirements is summarised in the schematic in Figure A.1.

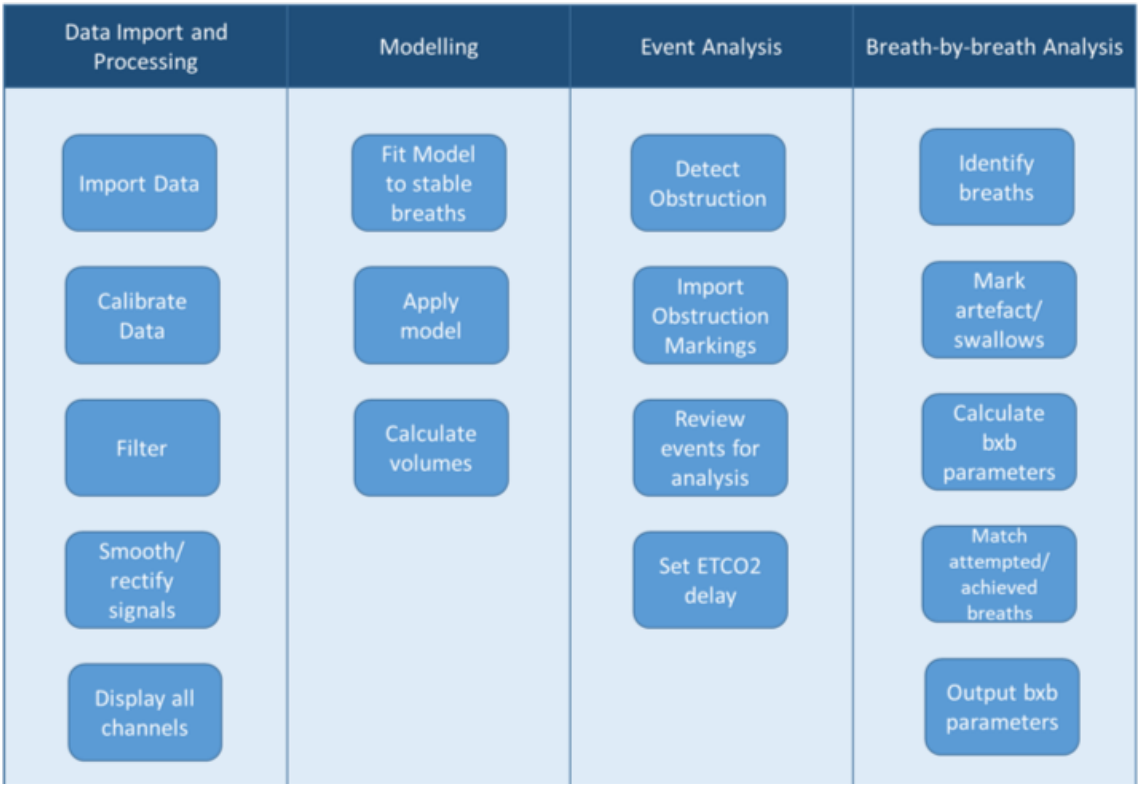

Figure A.1: Requirements for GUI analysis tool

A.2 User Interface

The Graphical User Interface (GUI) was built with a series of displays so that the user can view and review different aspects of the data files from a sleep recording. Tabs allow each of the displays to be selected. Figure A.2 shows the initial user interface for the analysis tool. The user is first asked to select a file to read. Data are loaded and the initial screen displays flow, oesophageal pressure, gastric pressure and smoothed rectified EMGdi and EMGgg. Once parameters Pmus and attempted ventilation have been calculated they are also displayed. Scored events and arousals and sleep staging can be imported and regions displayed to the user as highlighted regions on the plots. Cursors allow the user to scroll through the whole night recording and zoom in and out of regions of interest.

In a separate tab, breath-by-breath analysis can be performed on subsets of data. Breath start and end timings are defined from flow crossings and a volume threshold, and then other respiratory parameters such as inspiratory and expiratory duration, volume, minute

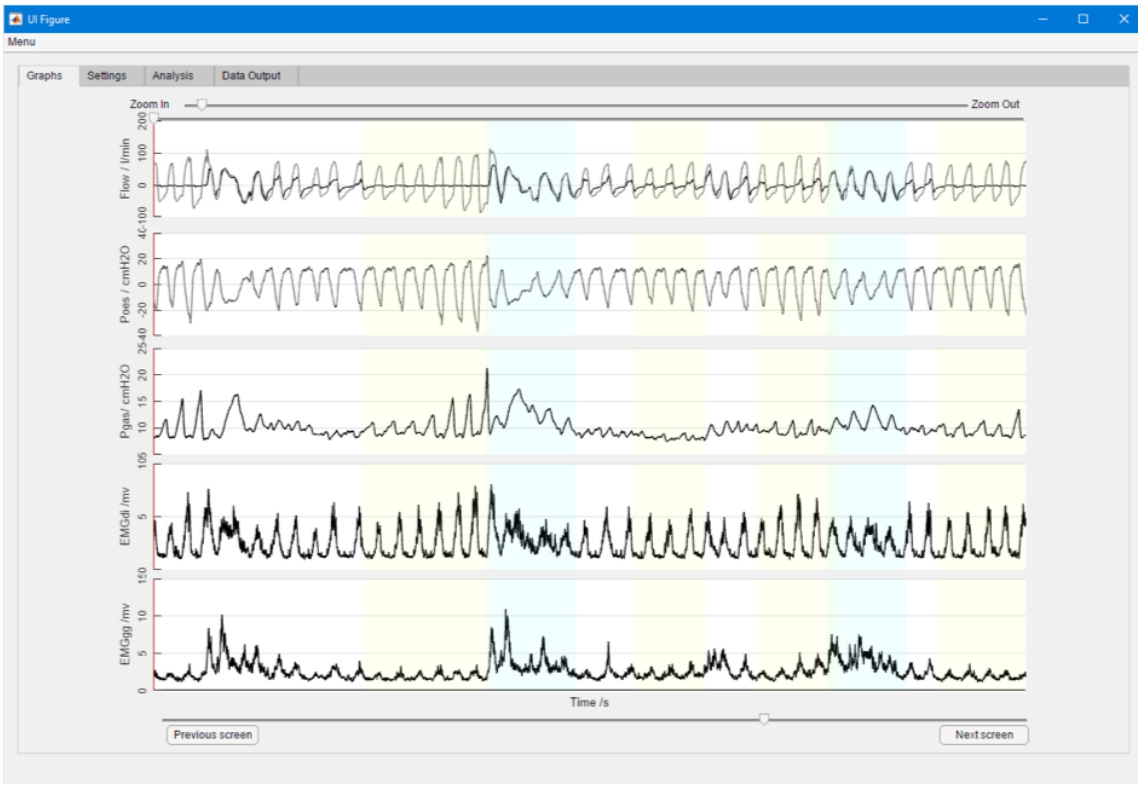

Figure A.2: Initial signal display screen on GUI

ventilation, peak and tonic flow, pressure and EMG values are calculated. The final window displays output data to allow review if needed. A drop down menu provides the user with the ability to select a series of analysis steps. More details on each of the aspects of this analysis is given in the following section.

A.3 Analysis Stages

A.3.1 Data Import and Processing

Sleep recording data were acquired using a WinDaq acquisition system (DataQ Instruments, Ohio, USA), and stored in CODAS data storage format. For standard application, software is provided with the WinDaq system to view signals, however these packages do not provide the capability required for analysis. A script was created in MATLAB to read the raw sleep data. A CODAS-format data file contains three sections: a data file header, the acquired data, followed by a data file trailer. Depending on the acquisition set up and hardware used, the exact data file architecture can change.

Some existing code in the public domain (author: Tobias Moser, University of Zurich,

2015) has been written to read the data file header and data section. However, it is not equipped to read from files in which multiple sample rates are acquired and data stored according to acquisition time. It also does not read the file trailer. A script was written to read information about channel numbers and sample rates from the header to determine data structure. Raw data are read as 16-bit integers then indexed according to channel and segmented into individual signals. Calibration and scaling factors are read from the header, and signals adjusted accordingly. In the datasets used for Chapters 4 – 7, respiratory signals were generally acquired at 200 Hz and electromyography (EMG) and electroencephalography (EEG) signals at 1 kHz.

The data file trailer contains event markers and channel labels. Event markers are 32-bit integers corresponding to time from start of acquisition and channel labels in a character string. Pointers from the header are used to identify data sections and assign labels to data channels.

Scored event data (for example sleep staging, arousals and obstruction) are stored in Microsoft Excel format so these data can be read directly, with all timings converted to WinDaq acquisition time using event markers simultaneously recorded in both systems.

Where required, signals are either low pass or band pass filtered to remove extraneous noise before analysis. Cardiogenic artefact is removed from oesophageal pressure using custom template identification and subtraction methods discussed in Chapter 3. Diaphragm EMG is filtered using the ICA-wavelet based technique to minimise ECG noise. In addition to raw format, EMG channels are rectified and smoothed with a moving time average window of 100ms to allow analysis of peak and tonic signals.

The ETCO2 signal has an inbuilt circulatory delay of approximately 1-2 seconds. To ensure values are appropriately assigned on a breath by breath basis, manual review of delay time is required. Using the GUI, the user can mark the start of a breath on the flow trace (baseline crossing) and ETCO2 trace (drop in CO_2). A script then calculates the delay time between the two marked points and applies the correction to calculations on ETCO2 signal.

Pressure calibrations are read from values stored in the acquisition data files. The flow channel required calibration from syringe manoeuvres at the start of the recording that corresponded to a known volume of 1 litre. The user is asked to identify the start and end of the calibration period, then the area under the curve is calculated and averaged to derive the flow channel scale factor, which is then applied to data throughout the rest of the recording. An example of this procedure is shown in Figure A.3.

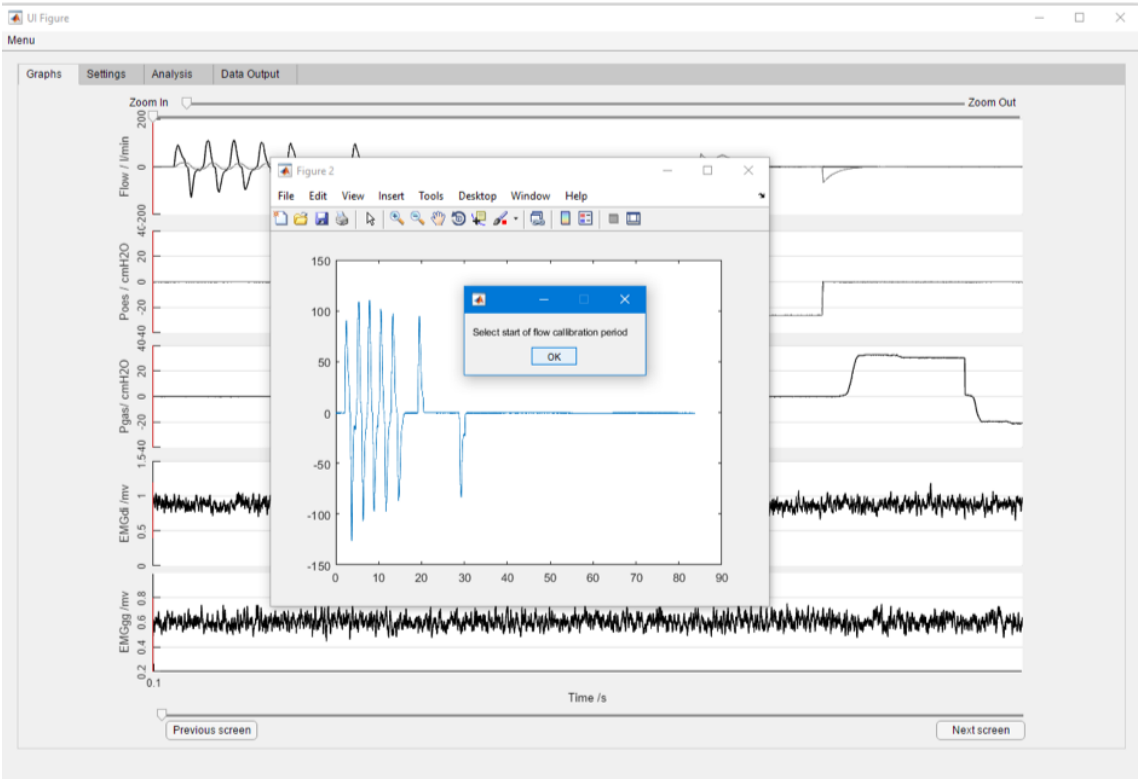

Figure A.3: Calibration for flow channel. The user selects the region of calibration syringe manoeuvres, which are then detected and calibrated to a fixed volume

A.3.2 Modelling

In the modelling section of the software, a Pmus signal is derived from Poes by calculating the continuous volume from the flow signal and applying a volume-based chest wall correction using average values of chest wall compliance 0.1l/cmH2O. This is assigned to a new channel. The user then can select a period of wake or stable breathing in sleep to fit the attempted ventilation model parameters, as discussed in Chapter 5. Flow crossings are used to mark start and end points of breaths. The classic respiratory mechanics equation is fitted to Pmus and volume/flow to derive constants Ers and Rrs using multiple regression. Fits are produced on a breath-by-breath basis, and a threshold R^2 value is used to remove breaths with poor fits, likely due to artefact, then an average taken. This threshold can be amended as required, depending on signal quality. The model is then applied to Pmus for the remainder of the data to derive an attempted ventilation signal. This is displayed on the ventilation plot so that achieved and attempted ventilation can be compared. Baseline crossings are used to define inspiration onset and offset for both the measured flow and the attempted flow derived from effort. This allows for analysis of all efforts, irrespective of the patency of the airway.

A.3.3 Event Analysis

The user can decide whether obstruction events are either defined from imported scored data or from a ratio of the effort-to-flow metrics from the model. Once identified, a separate window allows users to review each event. The analysis window containing data 30 seconds prior to and 30 seconds following an event is displayed on the screen for review, and the user can zoom in or out over the event as required. The UI is shown in Figure A.4. Achieved and attempted ventilation are displayed on the top trace. The user can edit the marked start and end of the event using cursors. This is important for the work in Chapters 6 and 7 to allow for accurate determination of the point of event start and airflow recovery. Events can be excluded entirely if on review they have been incorrectly identified as an obstructed period, for example if the mask was removed, or if there is significant artefact. Short periods of artefact (e.g. swallows) can be scored by the user using two start and end cursors. Any breaths that fall within this period will be marked in the output so that they can be later excluded from analysis if required. Time to nearest scored arousal is determined for each event, as well as time to next scored or identified obstruction.

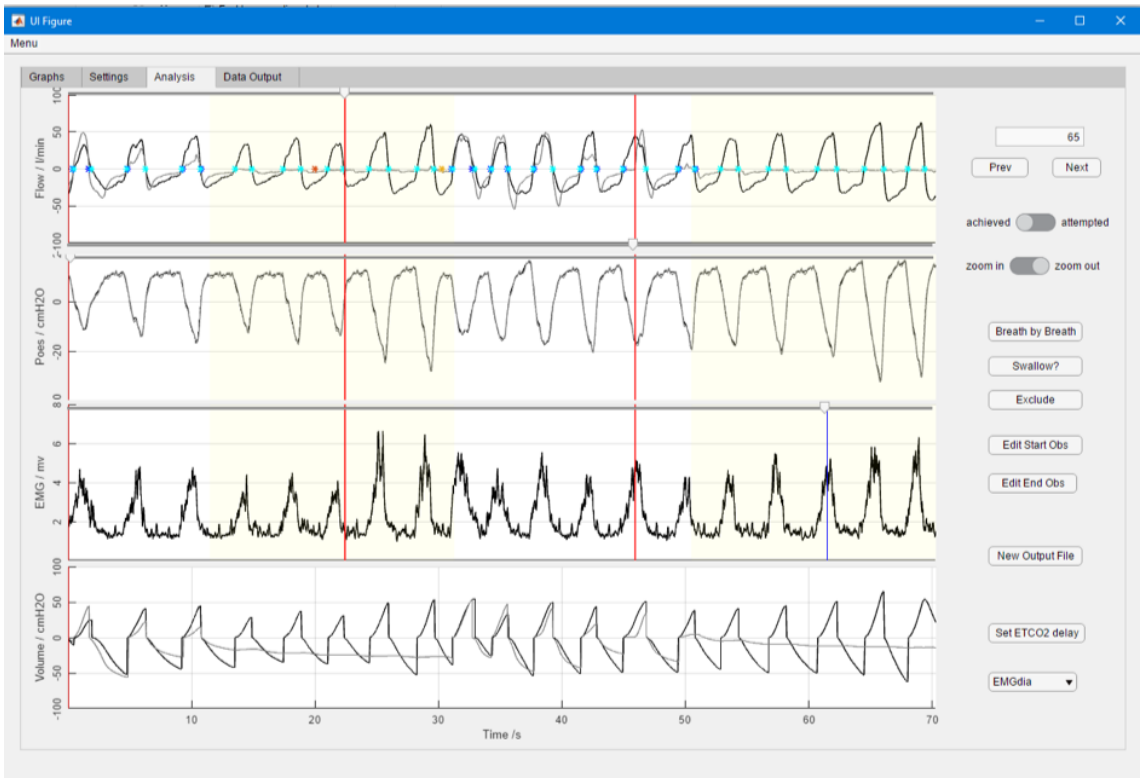

Figure A.4: User interface for event review and scoring

A.3.4 Breath-by-breath Analysis

Once the user has completed the event selection and has identified start/end time of events, they can calculate all breath by breath parameters and export the data by pressing the 'Breath by Breath' button. This function calculates breath by breath parameters for both the achieved and attempted signals, including ventilation (inspiratory and expiratory time, volume, minute ventilation, total breath time, breathing frequency, ETCO2) and muscle activity (peak, tonic and average area under the curve for smoothed rectified EMGdi and EMGgg). This is done for both achieved and attempted ventilation signals independently, then breaths are matched where there is overlap. If there is no equivalent breath in the measured flow (for example during apnoea), measured ventilation parameters are zero. The output is exported to both Excel and Matlab files for further analysis. Sleep stage, epoch and posture information is identified for each breath from scored times where available. Events are numbered, and individual breaths are further labelled relative to event start, event end and arousal if present. A long format file output is produced containing the output for each breath so that statistical group analysis can be performed later.

Appendix B

Matlab code for method implementation

B.1 Code to fit E and R

```
function [arrayE,arrayR,Residual]=fitER(dt,flow,poes,breathTimes
    )

%continous volume calculation from flow integration breathTimes
    in an array of start and end times of individual breaths
%User can select whether to fit to inspiratory period only or
    total breath time

Volume=cumsum(flow)*dt;

for i=2:length(breathTimes)

    t1=breathTimes(i,1);
    t2=breathTimes(i,2);

%calculate continous volume,flow and pressure for each breath

V=Volume(t1:t2)-Volume(t1);
```

```
F=flow(t1:t2);
P=poes(t1:t2);

%fit parameters for each breath to output array of coefficients
   E, R and the residual from the fitting for each breath input

tbl=table(P, F, V,...
      'VariableNames',{'Poes','Flow','Vol'});
 lm=fitlm(tbl,'Poes~Flow+Vol');
 arrayR(i-1)=(lm.Coefficients.Estimate(2));
 arrayE(i-1)=(lm.Coefficients.Estimate(3));
 Residual(i-1)=(lm.Rsquared.Adjusted);

 % Can define a threshold fitting residual from which to average
     parameters E and R

 ResidualThreshold=0.8          %can change this value
 arrayR=arrayR(Residual>ResidualThreshold);
 arrayE=arrayE(Residual>ResidualThreshold);

 R=mean(arrayR);
 E=mean(arrayE);
end
```

B.2 Code to implement method

```
function [Vdot_intended, V_intended]=applyMethod(Time, Pmus,Flow, E,
        R, startIdx,segmentLength)

dt=(Time(end)-Time(1))/length(Time);
endIdx=startIdx+segmentLength/dt;

%Initialise arrays
V_intended=zeros(round(segmentLength/dt),1);
Vdot_intended=zeros(round(segmentLength/dt),1);
```

```
%Implement method
for i=2:(segmentLength/dt)
    Vdot_intended(i) = (-(-Pmus(startIdx+i))-(E*V_intended(i)))/R;

    V_intended(i+1) = V_intended(i) + Vdot_intended(i)*dt;
end
```

Appendix C

Additional figures for Chapter 6

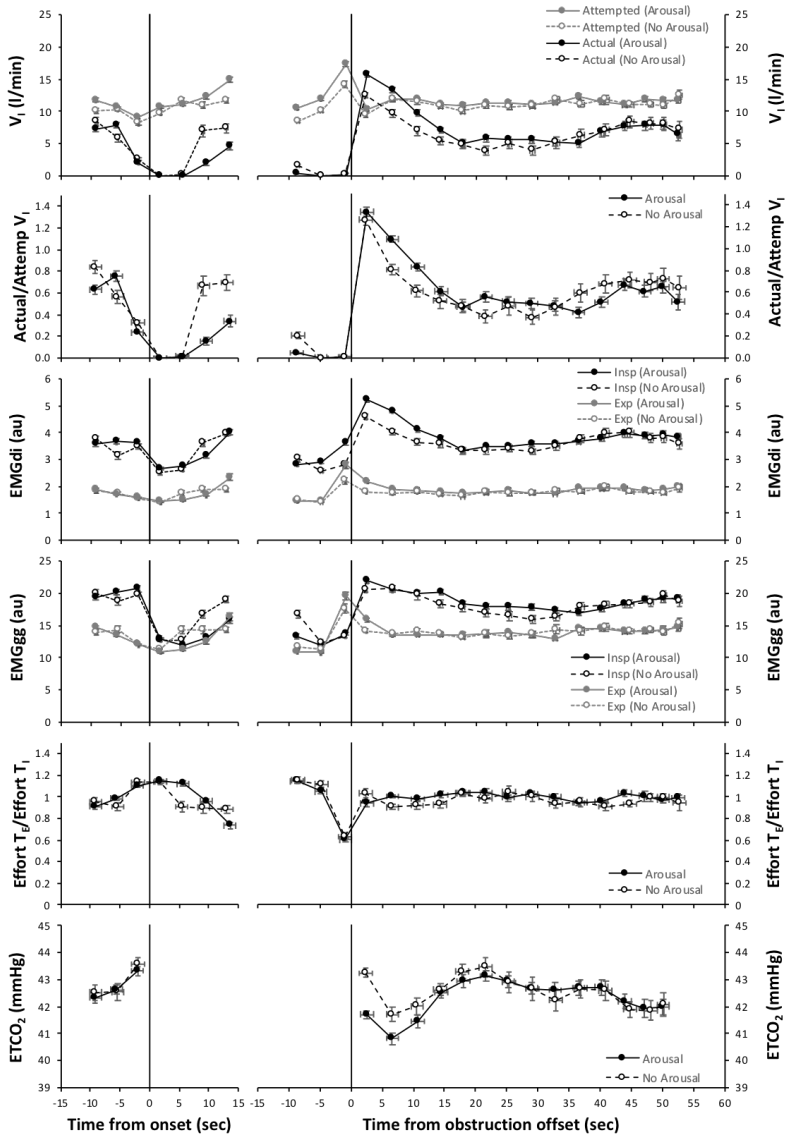

Figure C.1: Subject 1. Breath-by-breath physiological measures with arousal (black) or no arousal (grey). Measured minute ventilation, attempted minute ventilation as derived from oe- sophageal pressure, inspiratory and expiratory EMGdi and EMGgg, e ort duty cycle and ETCO2 plotted for the three breaths prior to and three breaths following obstruction onset, and three breaths prior to and eight breaths following airway re-opening. Data are plotted at mean time relative to obstruction onset and offset respectively.

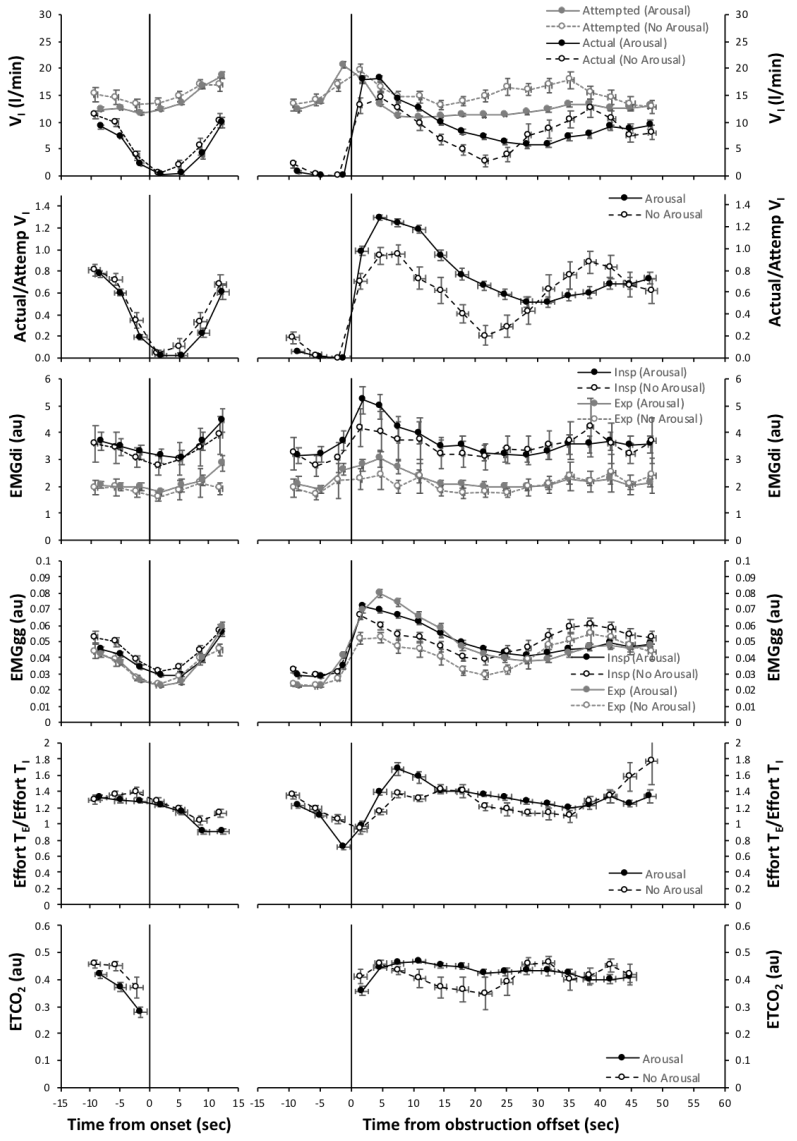

Figure C.2: Subject 2. Breath-by-breath physiological measures with arousal (black) or no arousal (grey). Measured minute ventilation, attempted minute ventilation as derived from oe- sophageal pressure, inspiratory and expiratory EMGdi and EMGgg, e ort duty cycle and ETCO2 plotted for the three breaths prior to and three breaths following obstruction onset, and three breaths prior to and eight breaths following airway re-opening. Data are plotted at mean time relative to obstruction onset and offset respectively.

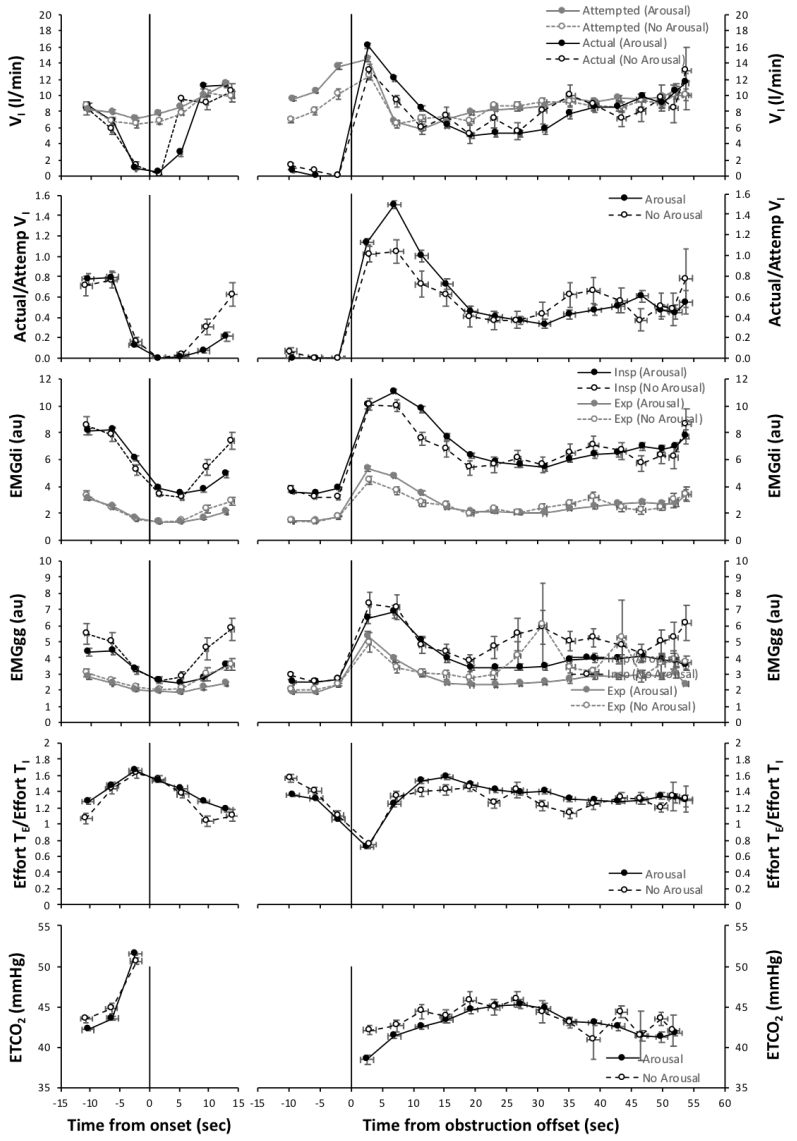

Figure C.3: Subject 3. Breath-by-breath physiological measures with arousal (black) or no arousal (grey). Measured minute ventilation, attempted minute ventilation as derived from oe- sophageal pressure, inspiratory and expiratory EMGdi and EMGgg, e ort duty cycle and ETCO2 plotted for the three breaths prior to and three breaths following obstruction onset, and three breaths prior to and eight breaths following airway re-opening. Data are plotted at mean time relative to obstruction onset and offset respectively.

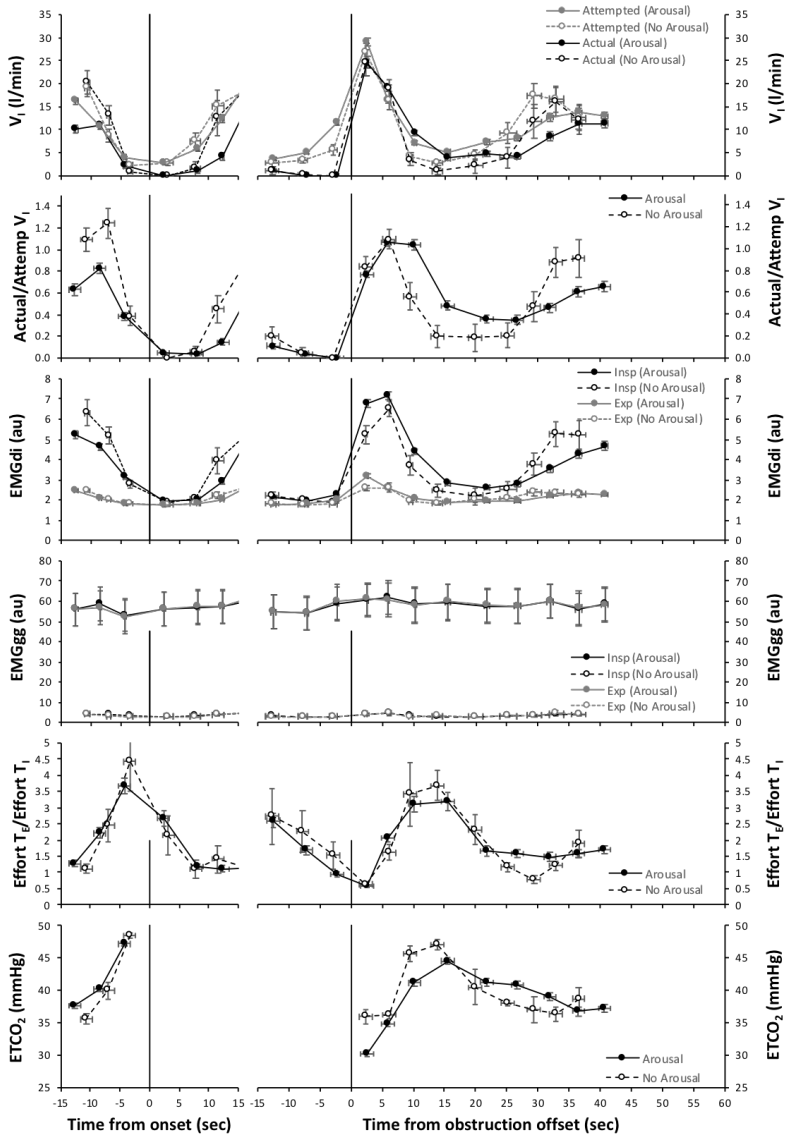

Figure C.4: Subject 4. Breath-by-breath physiological measures with arousal (black) or no arousal (grey). Measured minute ventilation, attempted minute ventilation as derived from oe- sophageal pressure, inspiratory and expiratory EMGdi and EMGgg, e ort duty cycle and ETCO2 plotted for the three breaths prior to and three breaths following obstruction onset, and three breaths prior to and eight breaths following airway re-opening. Data are plotted at mean time relative to obstruction onset and offset respectively.

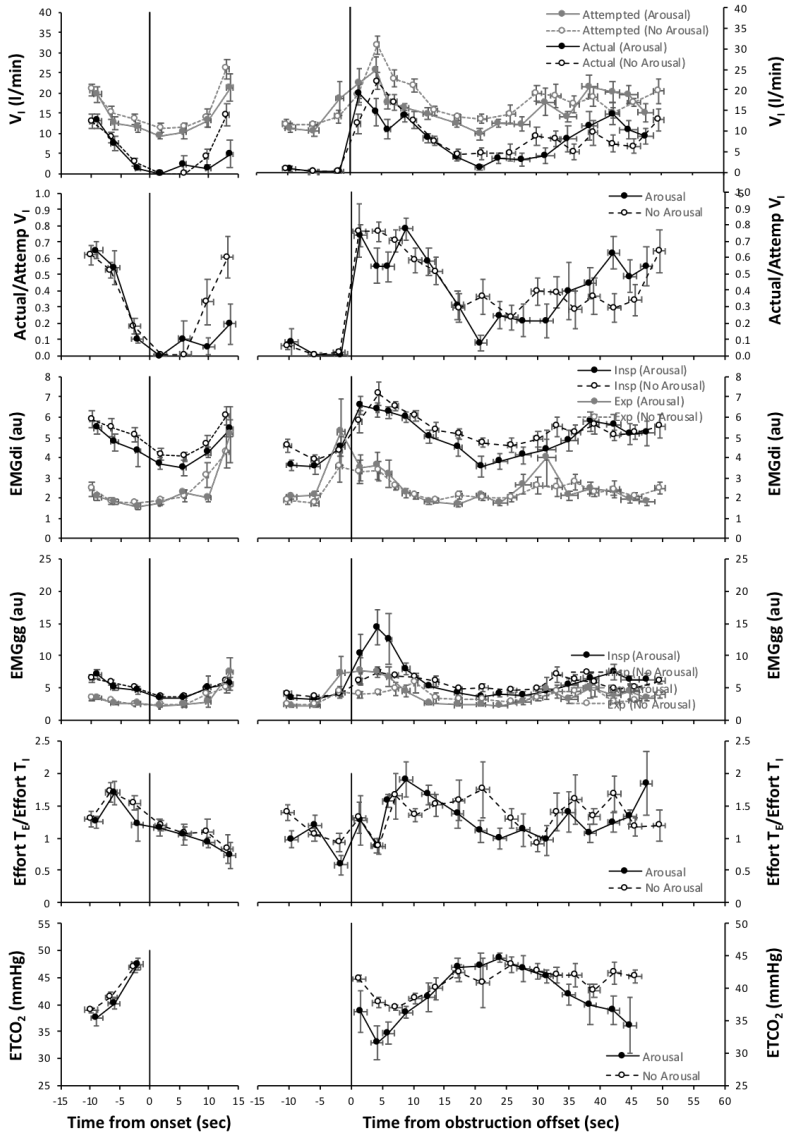

Figure C.5: Subject 5. Breath-by-breath physiological measures with arousal (black) or no arousal (grey). Measured minute ventilation, attempted minute ventilation as derived from oe- sophageal pressure, inspiratory and expiratory EMGdi and EMGgg, e ort duty cycle and ETCO2 plotted for the three breaths prior to and three breaths following obstruction onset, and three breaths prior to and eight breaths following airway re-opening. Data are plotted at mean time relative to obstruction onset and offset respectively.

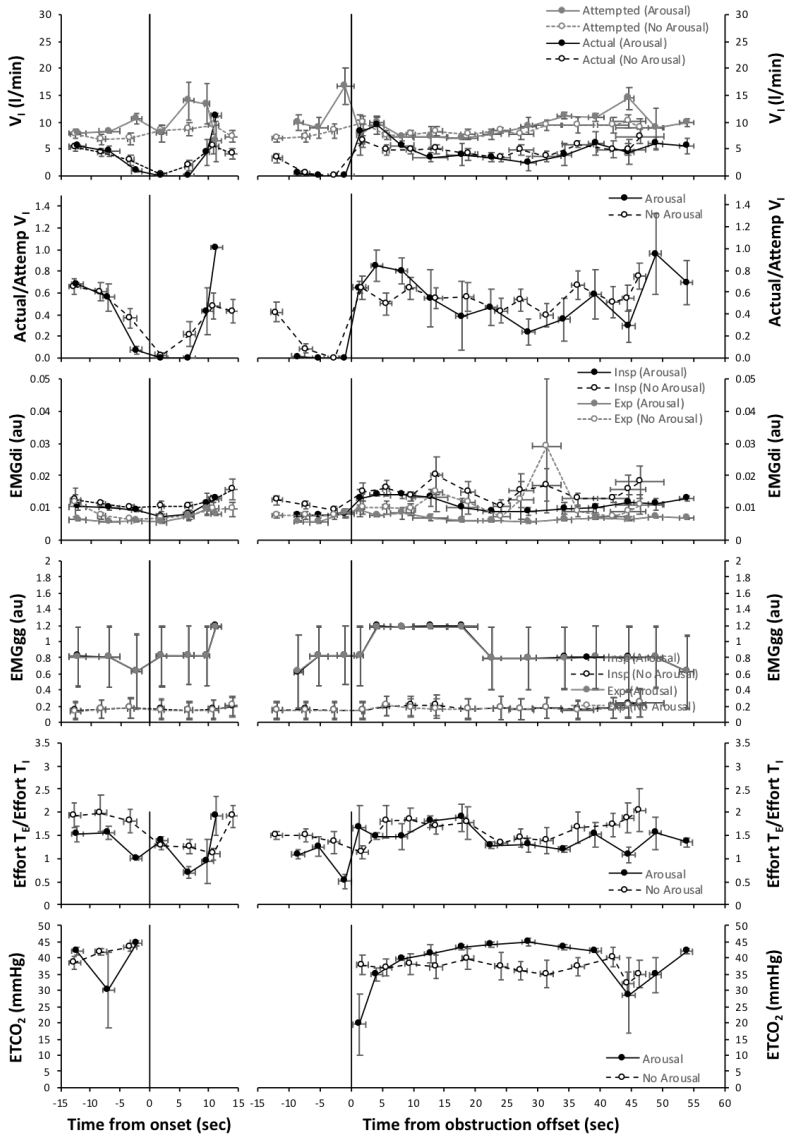

Figure C.6: Subject 6. Breath-by-breath physiological measures with arousal (black) or no arousal (grey). Measured minute ventilation, attempted minute ventilation as derived from oe- sophageal pressure, inspiratory and expiratory EMGdi and EMGgg, e ort duty cycle and ETCO2 plotted for the three breaths prior to and three breaths following obstruction onset, and three breaths prior to and eight breaths following airway re-opening. Data are plotted at mean time relative to obstruction onset and offset respectively.

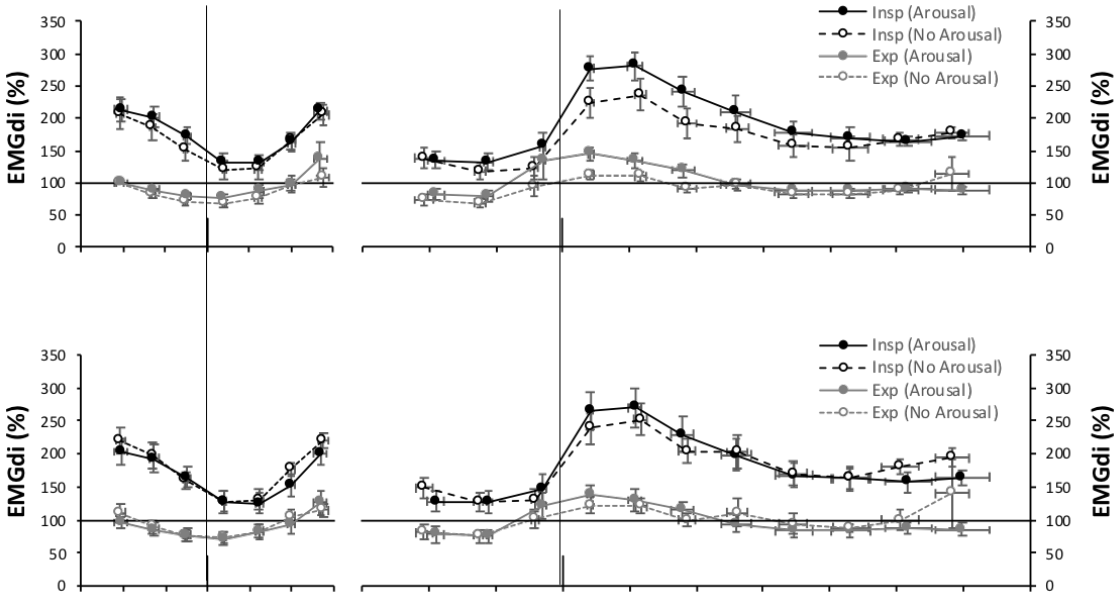

Figure C.7: EMGdi breath-by-breath group average results as scaled relative to pre event baseline value (breath -3 from obstruction onset) (top figure) and by mean tonic activity during a period of stable wake (bottom figure).

Appendix D

Additional figures for Chapter 7

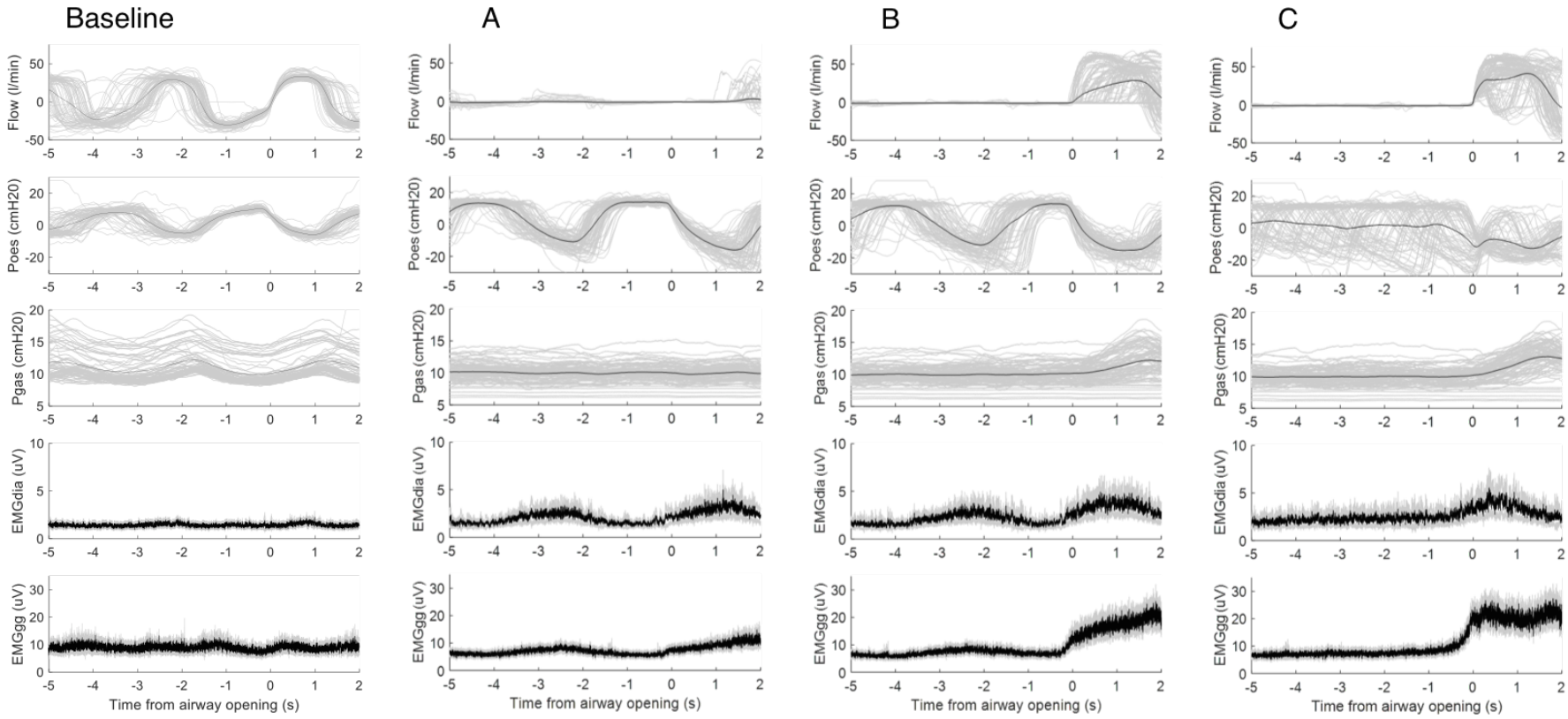

Figure D.1: Responses at all four breath timing points from participant 2 (Baseline events N=100, A,B,C events N=121). Baseline shows responses averaged with time zero aligned with inspiratory flow onset during wake along with one preceding breath, A) with time zero aligned with inspiratory effort onset of the first occluded breath, B) with time zero aligned with inspiratory effort onset on the breath associated with airflow recovery and C) with time zero aligned with airflow recovery.

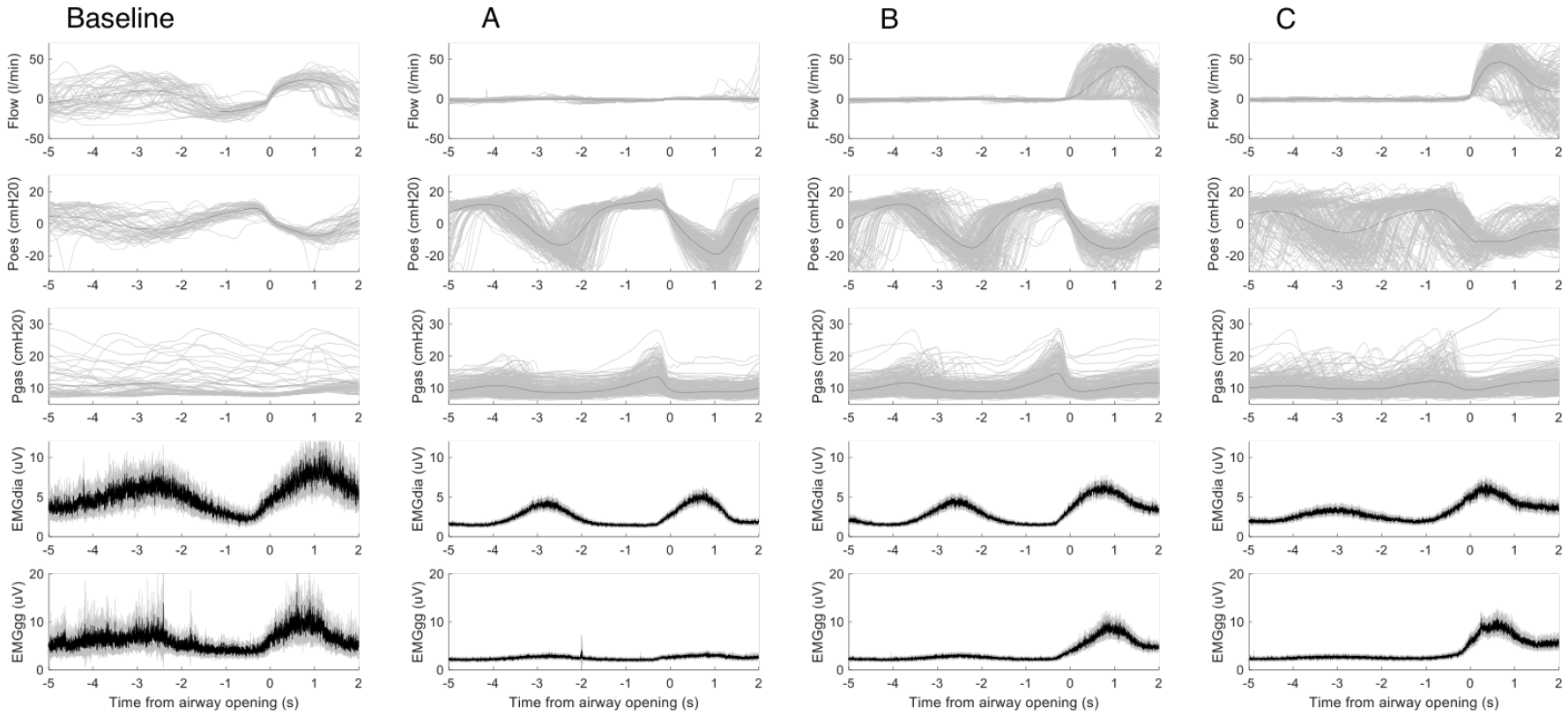

Figure D.2: Responses at all four breath timing points from participant 3 (Baseline events N=100, A,B,C events N=252). Baseline shows responses averaged with time zero aligned with inspiratory flow onset during wake along with one preceding breath, A) with time zero aligned with inspiratory effort onset of the first occluded breath, B) with time zero aligned with inspiratory effort onset on the breath associated with airflow recovery and C) with time zero aligned with airflow recovery.

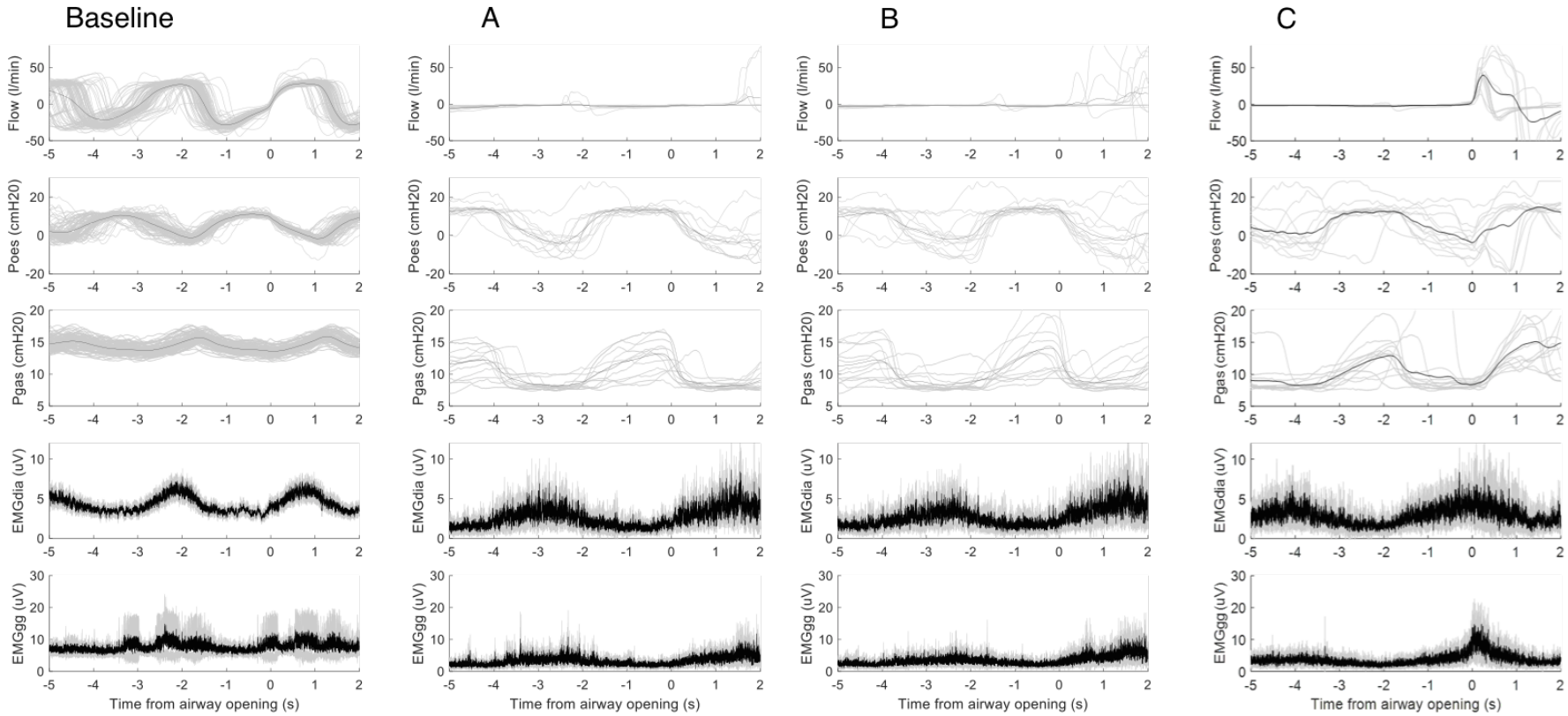

Figure D.3: Responses at all four breath timing points from participant 4 (Baseline events N=100, A,B,C events N=133). Baseline shows responses averaged with time zero aligned with inspiratory flow onset during wake along with one preceding breath, A) with time zero aligned with inspiratory effort onset of the first occluded breath, B) with time zero aligned with inspiratory effort onset on the breath associated with airflow recovery and C) with time zero aligned with airflow recovery.

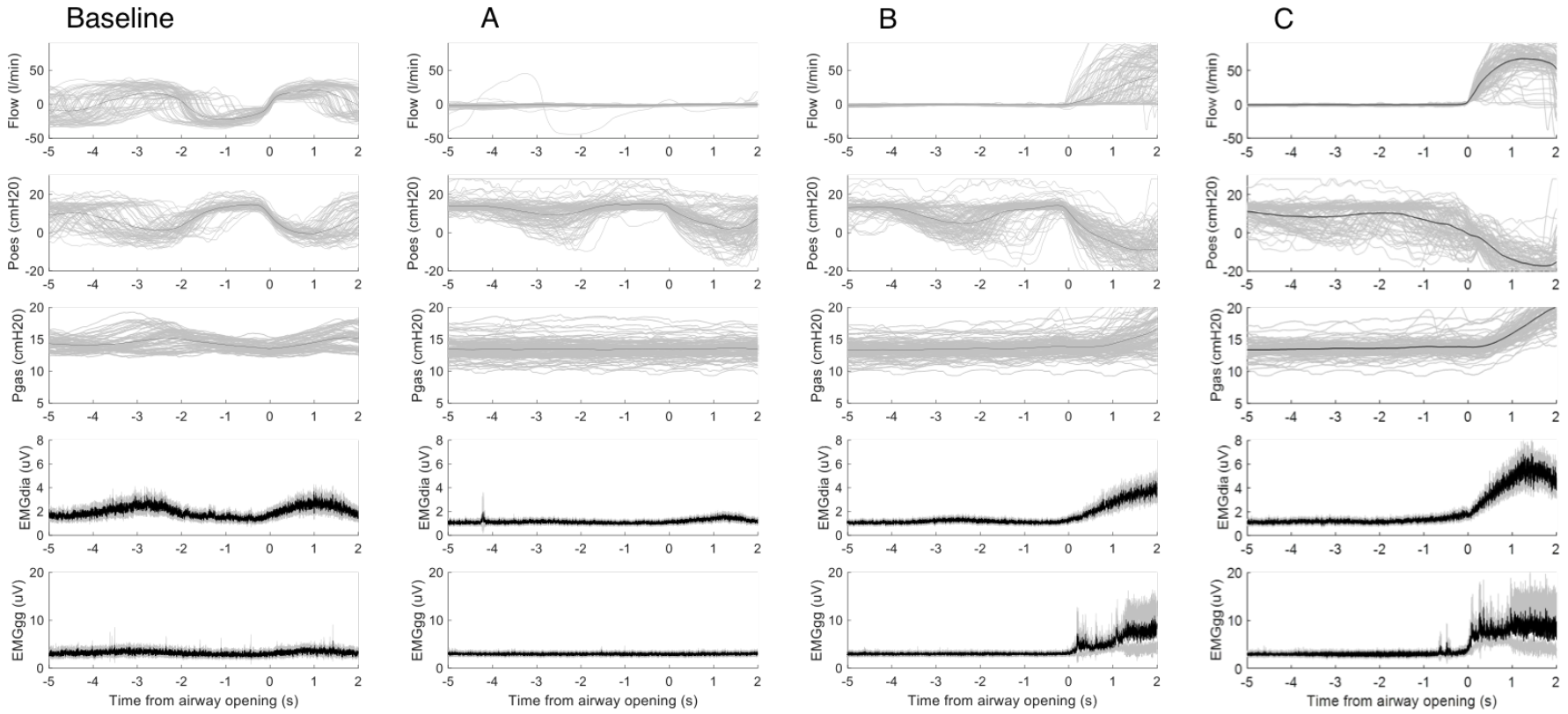

Figure D.4: Responses at all four breath timing points from participant 5 (Baseline events N=100, A,B,C events N=23). Baseline shows responses averaged with time zero aligned with inspiratory flow onset during wake along with one preceding breath, A) with time zero aligned with inspiratory effort onset of the first occluded breath, B) with time zero aligned with inspiratory effort onset on the breath associated with airflow recovery and C) with time zero aligned with airflow recovery.

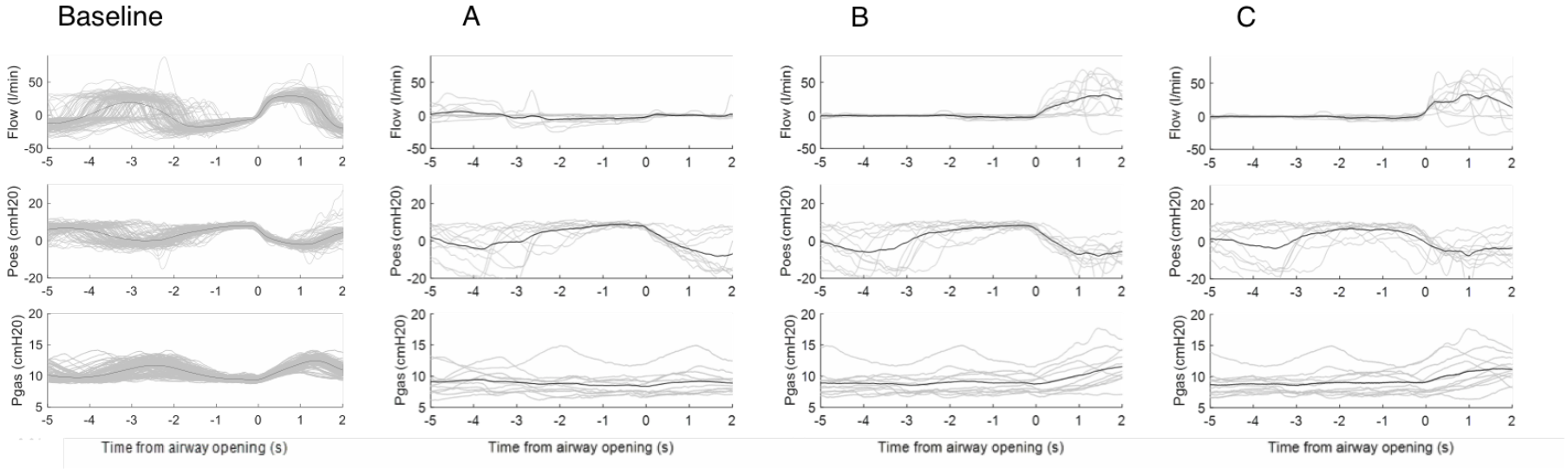

Figure D.5: Responses at all four breath timing points from participant 6 (Baseline events N=100, A,B,C events N=14). This participant lost EMGgg wires and gain changes so EMGgg and EMGdi were excluded from averaging. Baseline shows responses averaged with time zero aligned with inspiratory flow onset during wake along with one preceding breath, A) with time zero aligned with inspiratory effort onset of the first occluded breath, B) with time zero aligned with inspiratory effort onset on the breath associated with airflow recovery and C) with time zero aligned with airflow recovery.